Final Technical Report

Grant No. NSG 1307

AIRCRAFT NOISE PROPAGATION

AIRCRAFT NOISE PROPAGATION Final Technical Report (Georgia Inst. of Tech.) 128 p HC A07/MF A01 CSCL 20A
N78-26879
Unclas
G3/71 23551

By

W. James Hadden and Allan D. Pierce
Principal Investigators

Prepared for

National Aeronautics and Space Administration
Langley Research Center
Hampton, Virginia

June 1978

GEORGIA INSTITUTE OF TECHNOLOGY
SCHOOL OF MECHANICAL ENGINEERING
ATLANTA, GEORGIA 30332

1978

GEORGIA INSTITUTE OF TECHNOLOGY
School of Mechanical Engineering
Atlanta, Georgia

AIRCRAFT NOISE PROPAGATION

Final Technical Report
Grant No. NSG 1307
June 1978

By

W. James Hadden and Allan D. Pierce
Principal Investigators

for the

National Aeronautics and Space Administration
Langley Research Center
Hampton, Virginia

AIRCRAFT NOISE PROPAGATION

W. James Hadden, Jr. and Allan D. Pierce
Principal Investigators

Final Technical Report
June 1978
Grant No. NSG 1307

National Aeronautics and Space Administration
Langley Research Center
Hampton, Virginia

AIRCRAFT NOISE PROPAGATION

W. James Hadden, Jr. and Allan D. Pierce
Principal Investigators

Final Technical Report
June 1978
Grant No. NSG 1307

National Aeronautics and Space Administration
Langley Research Center
Hampton, Virginia

W. James Hadden, Jr.
Principal Investigator

Allan D. Pierce
Principal Investigator

S. Peter Kezios, Director
School of Mechanical Engineering

TABLE OF CONTENTS

Page

Chapter 1

INTRODUCTION

During the period June 1974 to the present, research relative to the understanding and alleviation of aircraft noise has been carried out by the investigators with grant support from the National Aeronautics and Space Administration. This report summarizes the principal results from this research.

Among the activities during the grant period were laboratory experiments and theoretical studies on the diffraction of sound by surfaces with the intention of providing basic information relevant to the understanding of the acoustical implications of the engine over wing configuration. That the presence of the wing below the engine may partially shield listeners on the ground from engine noise during flyovers has been the topic of a number of previous reports and papers[1-5] and has been the subject of investigation by Hellstrom[6], by von Glahn, Goodykoontz and Wagner[7], by Conticelli, Di Blasi and O'Keefe[8], by Jeffery and Holbeche[9], and by Sears.[10] A principal objective is the attainment of a rational method for quantitatively estimating just how much noise reduction would be achieved by a given design. Such a method would serve as a guide in the design of future EOW aircraft and would enable one to make quantitative comparisons of alternative designs.

In order to gain some quantitative insight into the nature of sound diffraction by wings and to provide a data base for the assessment of various theoretical approaches to the overall problem, a series of experiments were conducted at NASA Langley Research Center during the summer of 1976. These were carried out by Allan D. Pierce and Robin Vidimos in collaboration with John S. Priesser and other NASA personnel; the reduction of the data was carried out under the direction of W. James Hadden, Jr. In Chapter 2, a summary is given of the nature of these experiments and of the results.

One of the theoretical problems presented by the overall topic of aircraft engine noise diffraction by wings is that the source of the sound is not a large number of wavelengths away from the diffracting surface (although in cases of interest the listener is). Virtually all existing computational techniques for sound diffraction by bodies are based on the assumption that both distances are large, so some analytical development was necessary to revise existing theories such that they would be amenable to rapid computation and would give quantitative insight for cases corresponding to the topic of wing shielding of engine noise. The details of this analytical study are given in Chapter 3.

Another topic considered during the period of the grant was the effect of variable ground impedance on aircraft noise propagation. A pertinent question is to what extent the sound received on the ground is characteristic of the local impedance near the listener and to what extent the impedance at distant points affects the local reception. Chapter 3, prepared by Dr. Hadden, gives a theory for the scattering of spherical waves by a rectangular area whose acoustic impedance differs from that of the surrounding plane. Results of experiments (performed during summer 1975 at NASA Langley Research Center by W. James Hadden, Jr., Robin A. Vidimos, and Philip Sencil) concerning reflection from rectangular patches are also described in Chapter 4.

A topic related to both the variable ground impedance problem and that of the diffraction of noise by wings is that of the effects of finite surface impedance on diffraction. Chapter 5 is comprised of a paper by the authors written during the grant period which summarizes the principal results of an analytical study concerned with this topic.

Chapter 6 gives a theory developed during the grant period for the diffraction of sound from a point source by a thin rigid screen in the absence of ambient flow. The work described there is a simple extension of work reported by S. Candel on the plane wave diffraction problem. (See Chapter 6 for a listing of relevant references.) Analysis given here shows that a simple transformation will reduce the point source problem in the presence of ambient flow to one in which there is no flow. The solution so derived should allow some insight into the influence of forward motion effects on aircraft noise diffraction by wings.

REFERENCES

1. M. Reshotko, W. A. Olsen and R. G. Dorsch, "Preliminary Noise Tests of the Engine-over-the-Wing Concept. I: 30°-60° Flap Position," NASA-TM-X-68032, March 1972.

2. M. Reshotko, W. A. Olsen and R. G. Dorsch, "Preliminary Noise Tests of the Engine-over-the-Wing Concept. II: 10°-20° Flap Position," NASA-TM-X-68104, June 1972.

3. R. G. Dorsch and M. Reshotko, "EBF Noise Tests with Engine Under-the-Wing and Over-the-Wing Configurations," NASA SP-320, 1973, pp. 455-473.

4. D. Chestnutt, D. J. Maglieri, and R. E. Hayden, "Flap Noise Generation and Control," NASA SP-320 (1973), pp. 413-426.

5. R. G. Dorsch, P. L. Lasagna, D. J. Maglieri and W. A. Olsen, "Flap Noise," NASA SP-311 (1972), pp. 259-290.

6. G. Hellström, "Noise Shielding Aircraft Configurations, Comparison between Predicted and Experimental Results," ICAS paper 74-58, 1974.

7. U. von Glann, Goodykoontz and J. Wagner, "Nozzle Geometry and Forward Velocity Effects on Noise for CTOL Engine-over-the-Wing Concept," NASA-TM-X-71453, November 1973, N73-33742.

8. V. M. Conticelli, A. Di Blasi and J. V. O'Keefe, "Noise Shielding Effects for Engine-over-the-Wing Installations," AIAA paper 75-474, 1975.

9. R. W. Jeffery and T. A. Holbeche, "An Experimental Investigation of Noise-Shielding Effects for a Delta-winged Aircraft in Flight, Wind Tunnel and Anechoic Room," AIAA paper 75-513, 1975.

10. F. H. Sears, "The Acoustic Shielding of Noise by a Jet Wing," M.S. Thesis, MIT (1975).

Chapter 2

LABORATORY EXPERIMENTS ON SOUND DIFFRACTION

The experiments performed in connection with the study of wing-shielding of noise were divided into three parts. In the first experiment (Fig. 1), the obstacle used was a thin screen, the source was an acoustically small driver through which selected pure tones were projected, the source being located close to the barrier. Narrow-band sound pressure levels were measured on a circular arc far from the edge of the screen and also at several locations close to the screen but well inside its acoustic shadow. In the second experiment the previously described barrier and receiver configuration was used, the pure-tone source being replaced by a 1 inch diameter jet. The third experimental configuration (Fig. 2) consisted of the acoustic driver, a thick straight-sided barrier with a cylindrical cap, and receiver and arc centered on the junction of the cap and the straight side of the barrier which was nearer to the driver.

The source-obstacle-receiver configuration for the first experiment is sketched in Fig. 3. Narrow-band pressure levels were recorded at the microphone positions shown. Results for pure tone exciation of the driver at 490, 900 and 2050 Hz with the driver in positions 2 (level with the top of the screen) and 4 (9 inches below the top of the screen) are presonted in

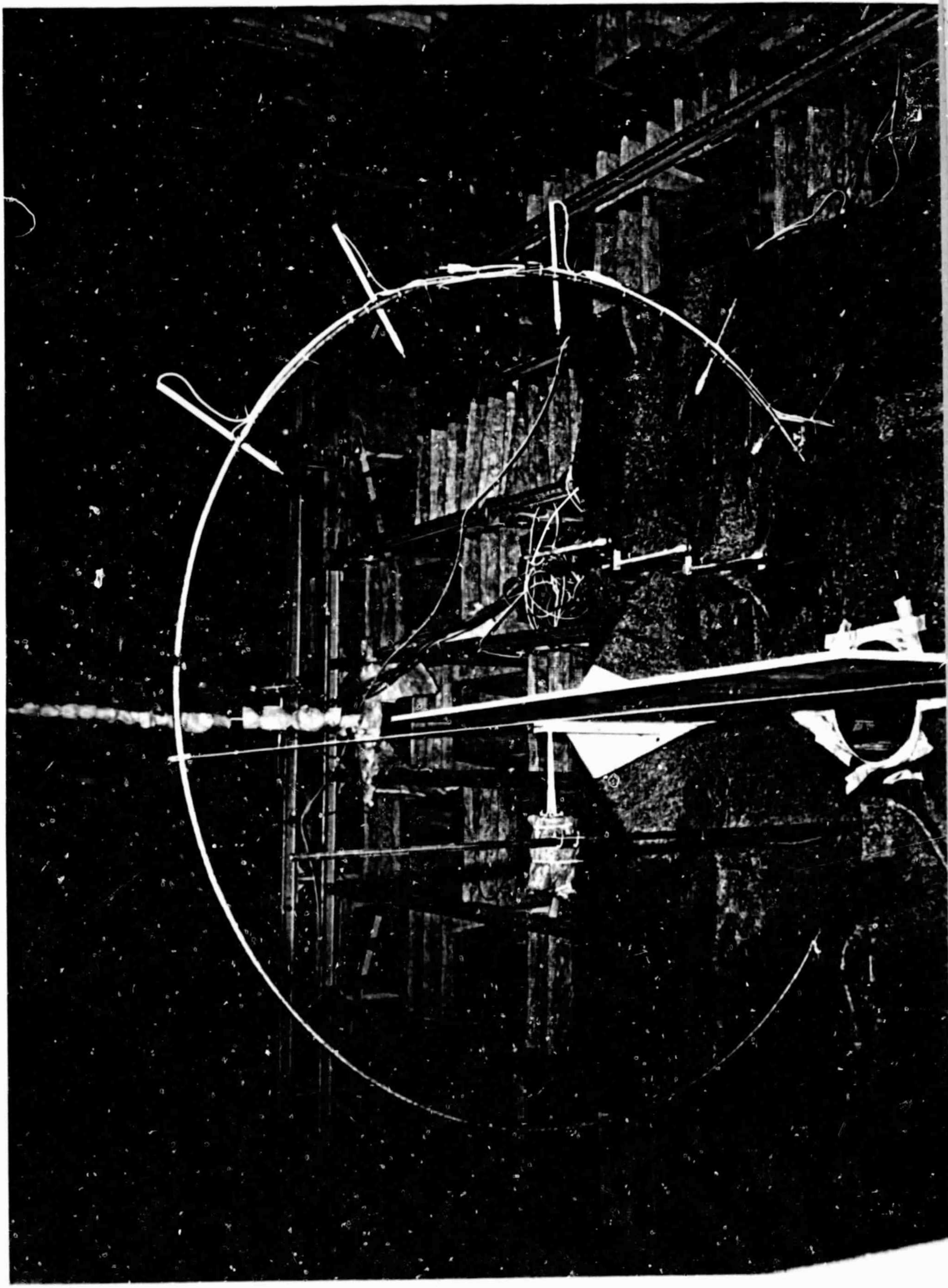

Fig. 1. Photograph of experimental apparatus for first experiment.

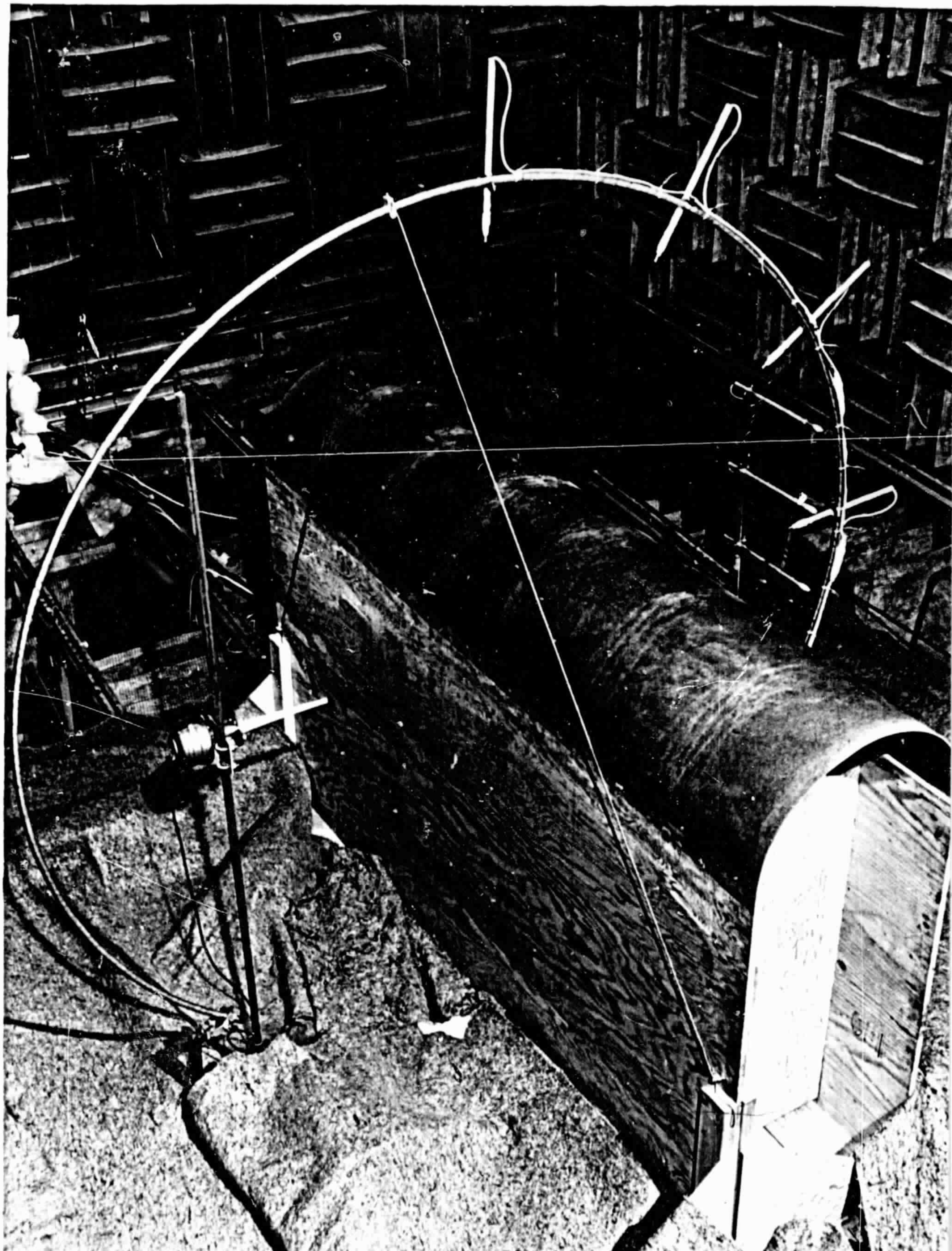

Fig. 2. Photograph of experimental apparatus for third experiment.

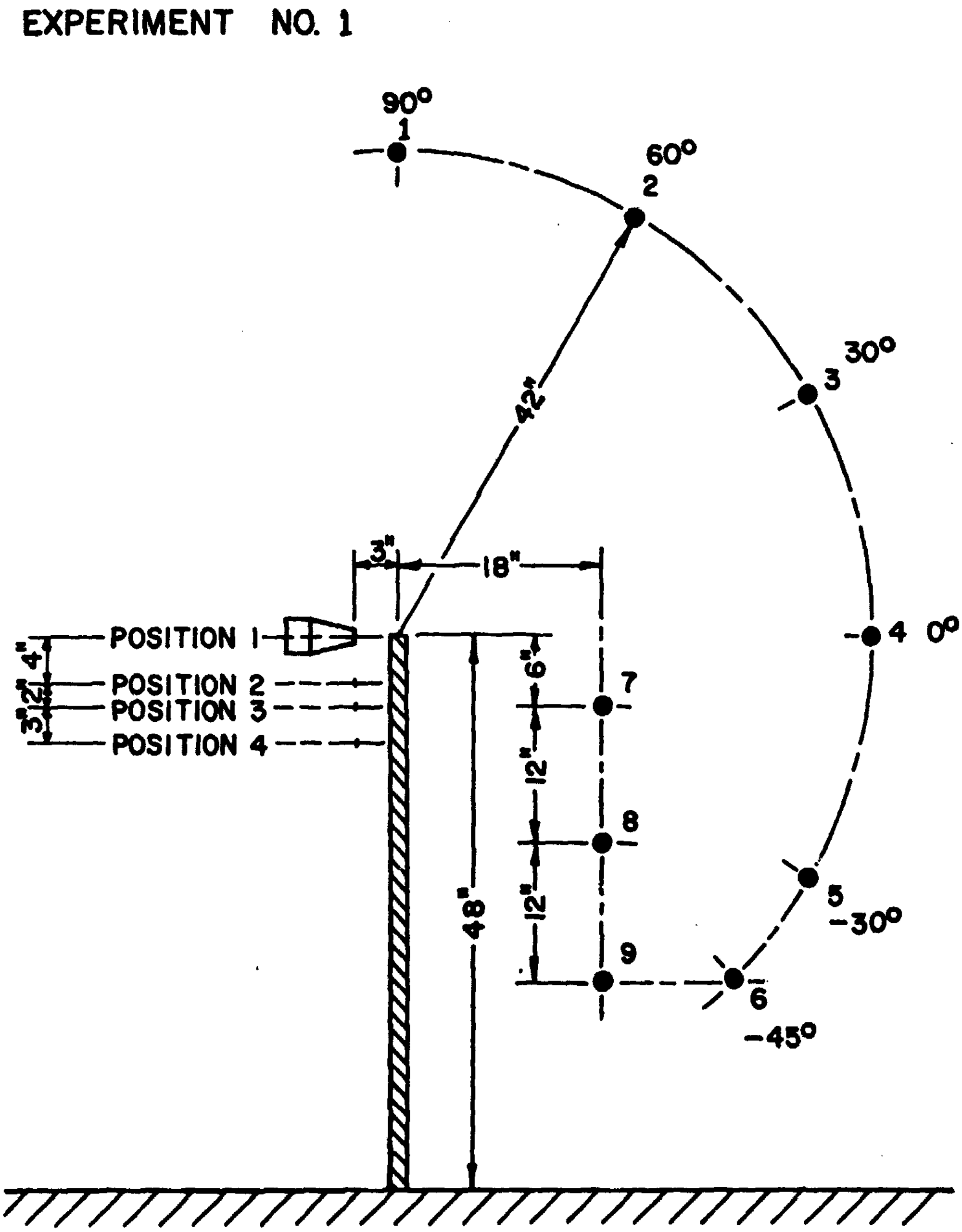

Fig. 3. Sketch of source-receiver-screen configuration for first experiment (see also Fig. 1).

Figs. 4-6. The pressure levels for microphone positions 1, 7, and 8, shown in Fig. 3, are presented in Table I. Although the pressure levels measured at a fixed distance from the edge of the screen show the expected trends of increased shadowing effect on the screen as the frequency increases and as the source height decreases, we strongly suspect that these data were affected by transmission through the plywood screen. A brief calculation indicates that the coincidence frequency for such a panel is approximately 800 Hz. Thus, the measurements at the lower two frequencies mentioned above may be significantly contaminated by sound transmission through the screen.

The geometric arrangement for the second experiment is shown in Figs. 7 and 8. The one-inch diameter jet was operated at pressures of 2.8 and 5 psi; one-third octave band levels were recorded at the microphone positions indicated in Fig. 7, for center frequencies 500, 1000, 2000, and 4000 Hz. The measured 1/3-octave band levels for the reference condition (Fig. 7) and in the presence of the screen (Fig. 8) are compared in Figs. 9-11. It should be noted that the results for 1000 Hz in Fig. 9 and for 4000 Hz in Fig. 10 have been shifted upward by 10 dB for convenience in presentation. Similarly, the results for 2000 Hz in Fig. 12 have been shifted downward by 10 dB. As in the first experiment, it is likely that transmission through the plywood screen is a contaminating artifact of the measurements in the bands centered at 500 and 1000 Hz. The measured 1/3-octave band levels for microphone

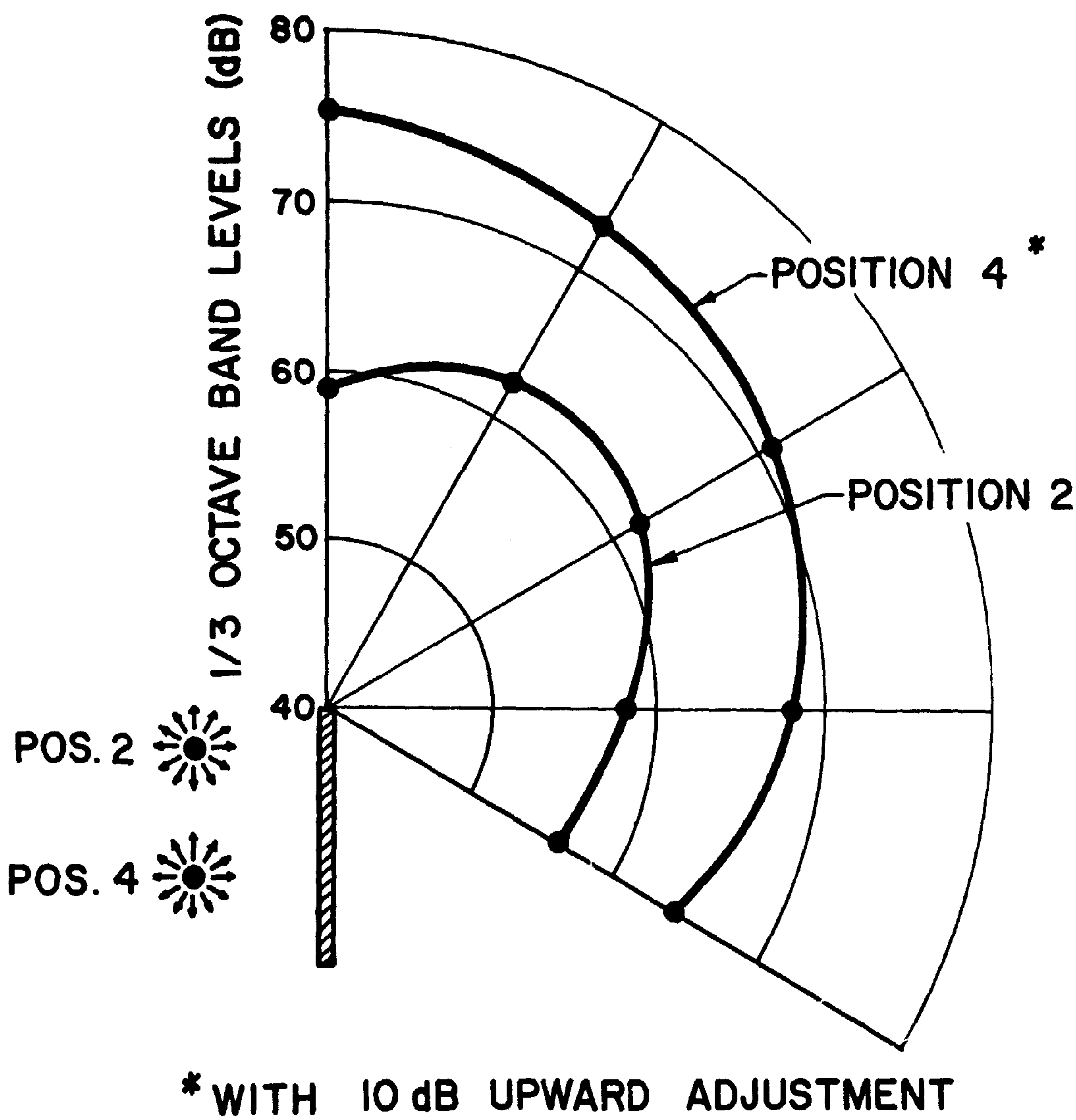

Fig. 4. Measured narrow-band pressure levels 3.5 ft. from top of screen at 490 Hz for two souce positions (see Fig. 1).

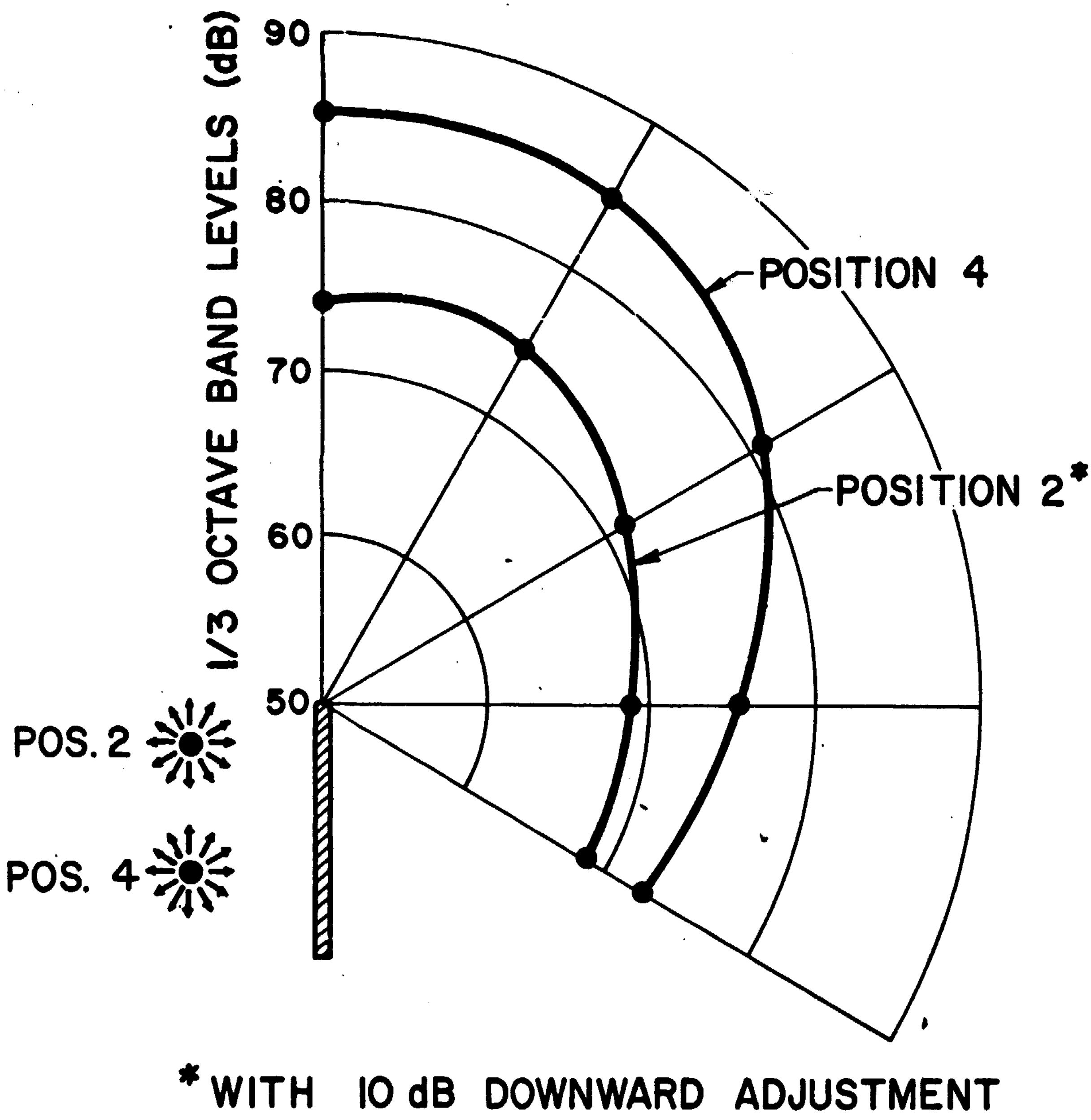

Fig. 5. Measured narrow-band pressure levels 3.5 ft. from top of screen at 900 Hz for two source positions (see Fig. 1).

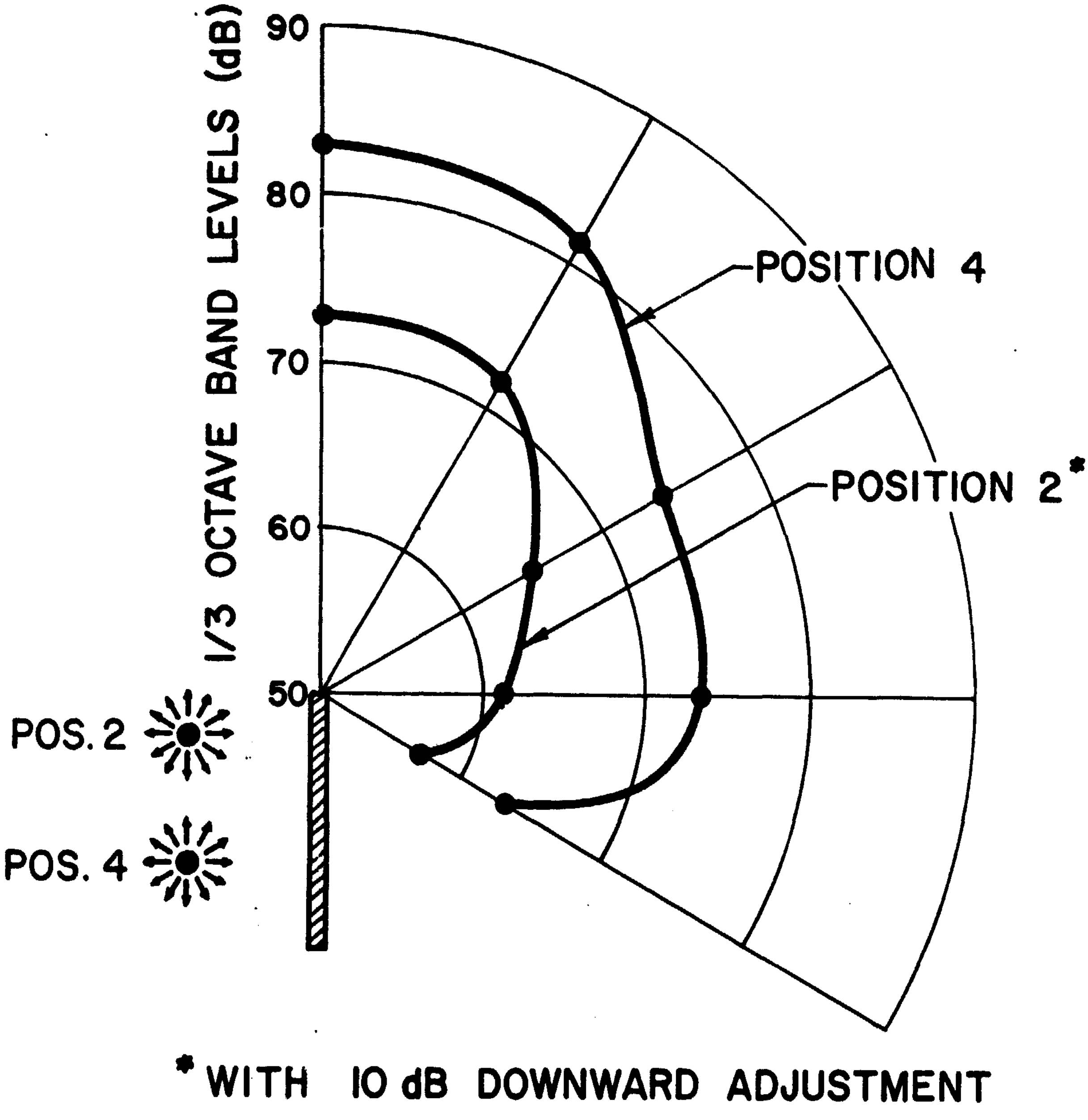

Fig. 6. Measured narrow-band pressure levels 3.5 ft. from top of screen at 2050 Hz for two source positions (see Fig. 1).

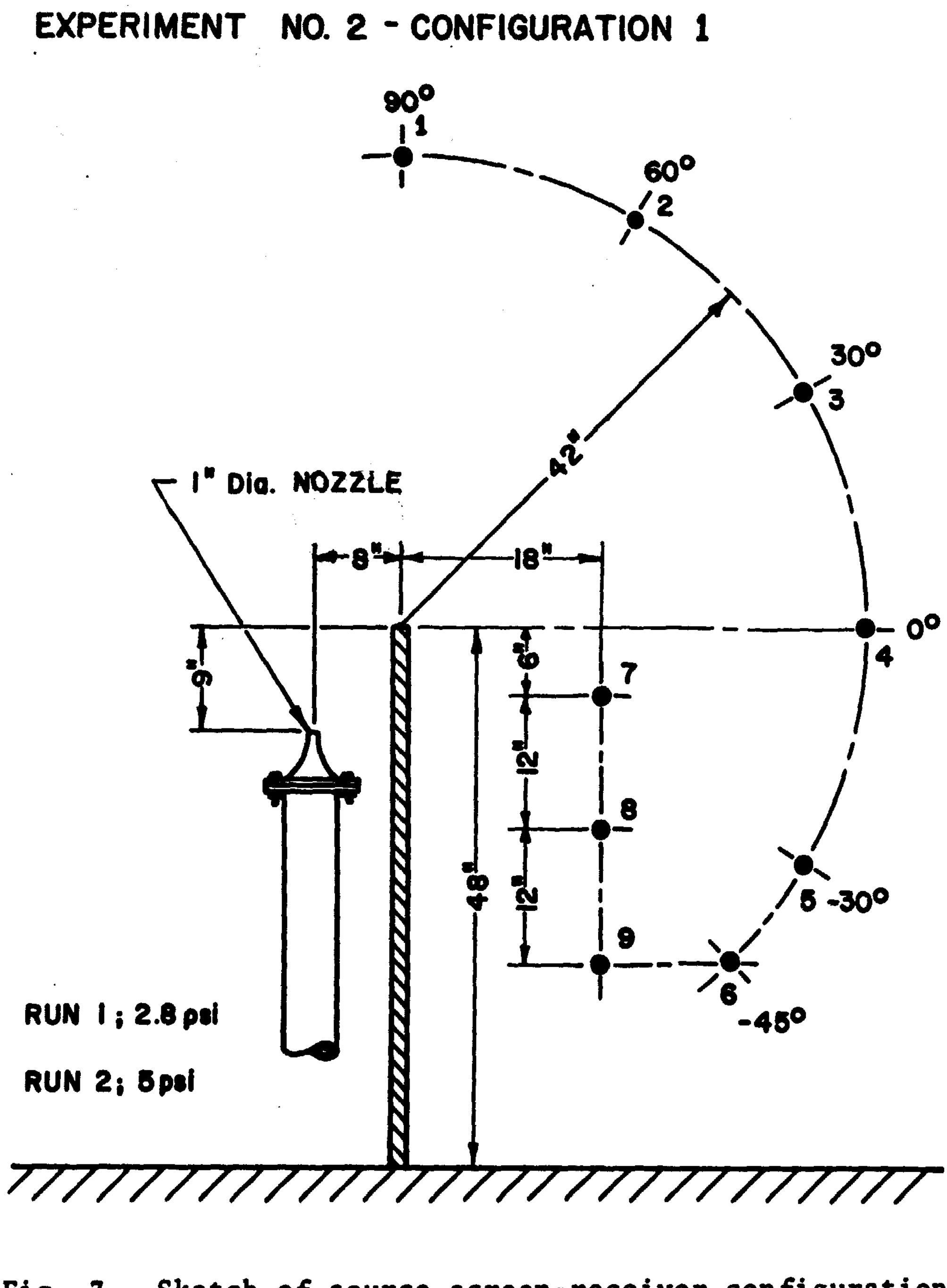

Fig. 7. Sketch of source-screen-receiver configuration for sound experiment.

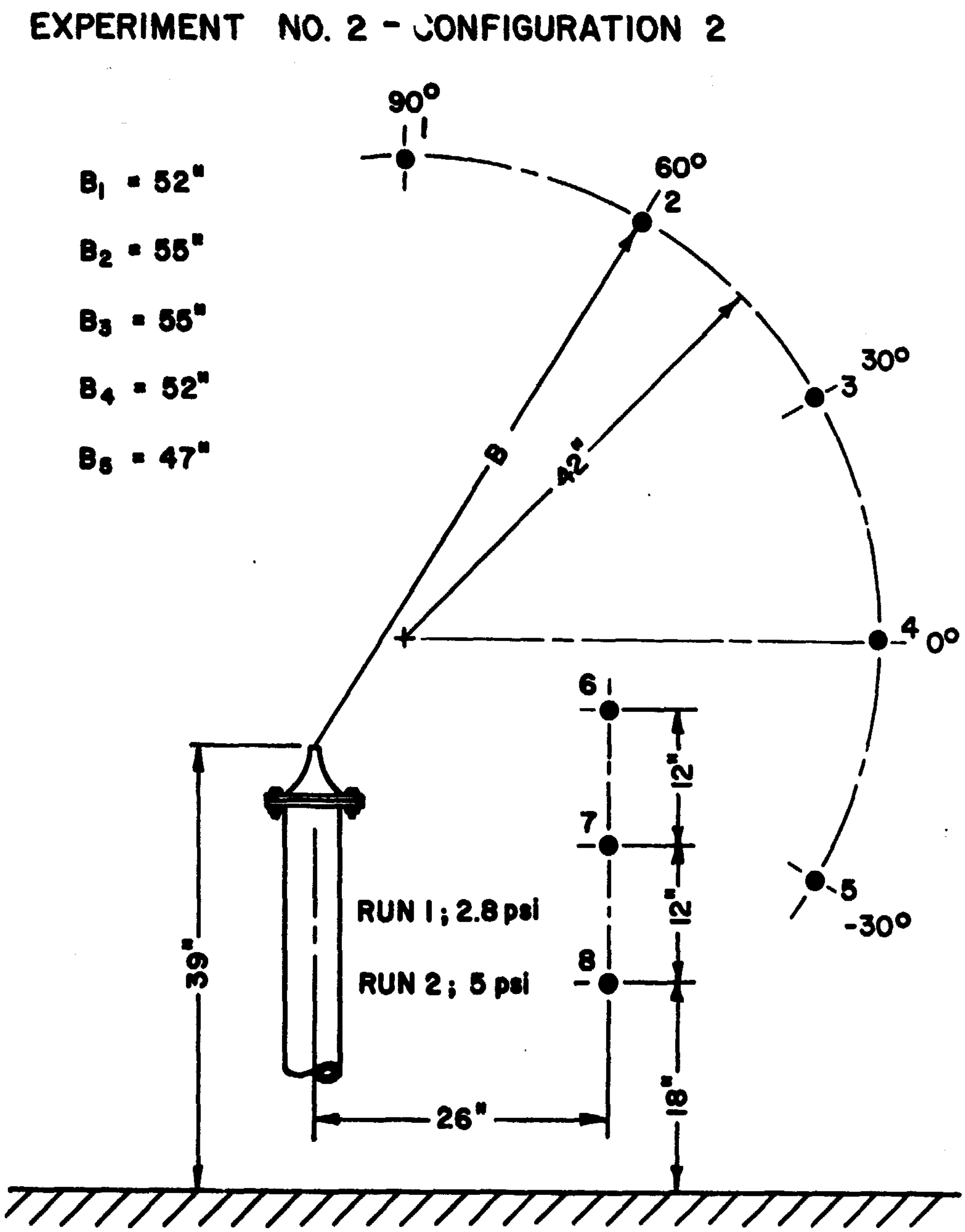

Fig. 8. Sketch of source-receiver geometry for second experiment: jet noise directivity measurements.

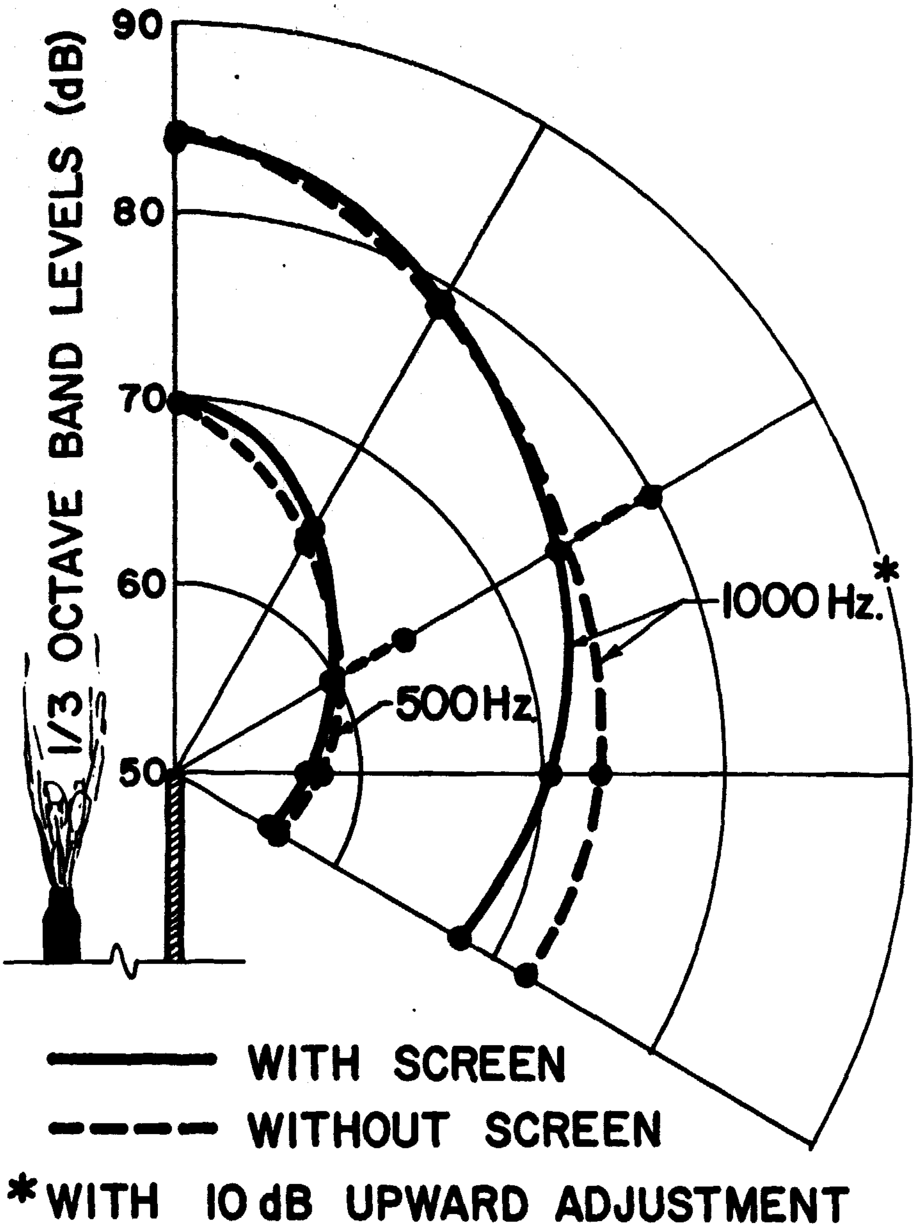

Fig. 9. Measured 1/3-octave band levels at outer frequencies shown for jet noise: jet pressure, 2.8 psi; distance from top of screen, 3.5 ft. (see Figs. 7 and 8).

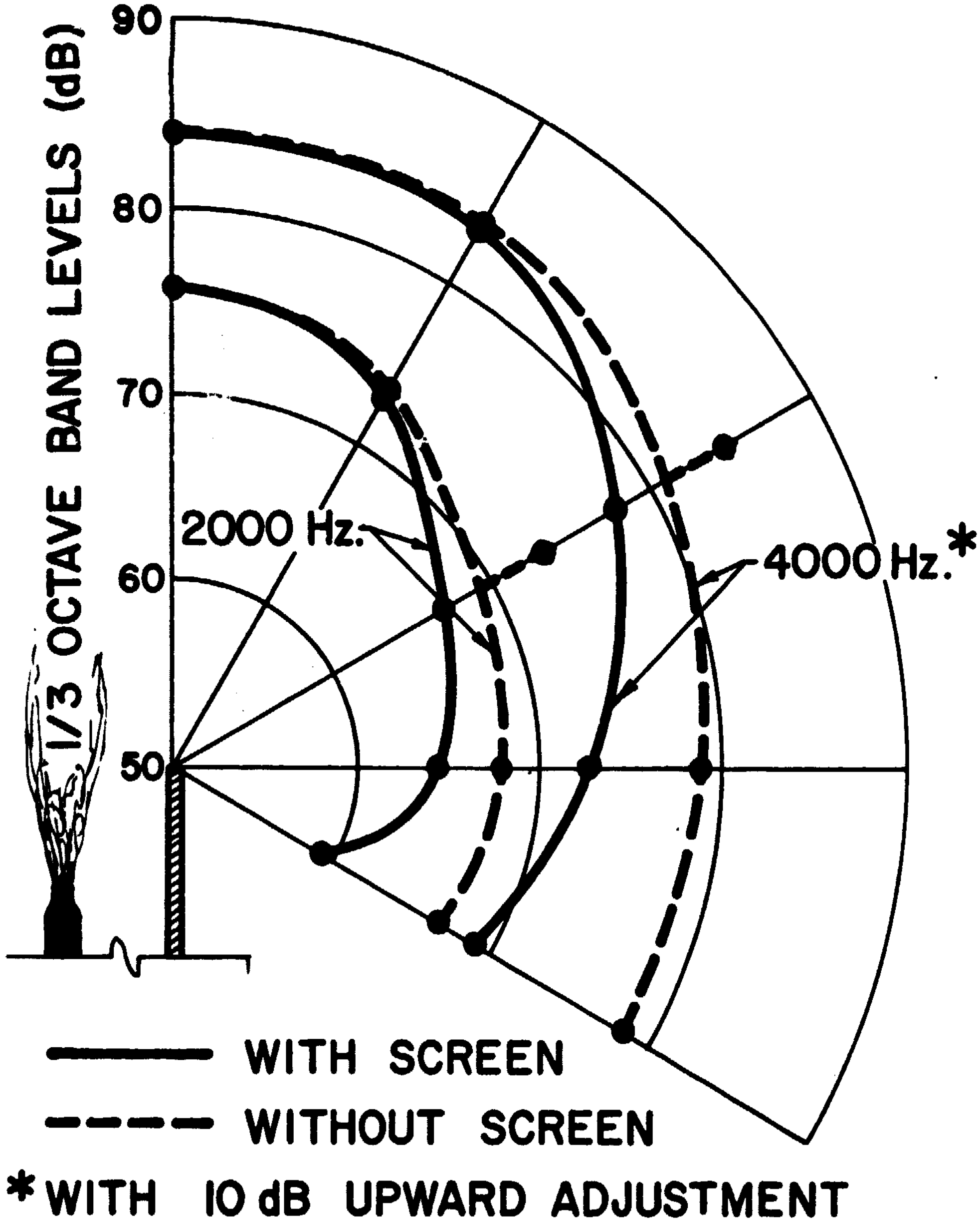

Fig. 10. Measured 1/3-octave band levels at outer frequencies shown for jet noise; jet pressure, 2.8 psi; distance from top of screen, 3.5 ft. (see Figs. 7 and 8).

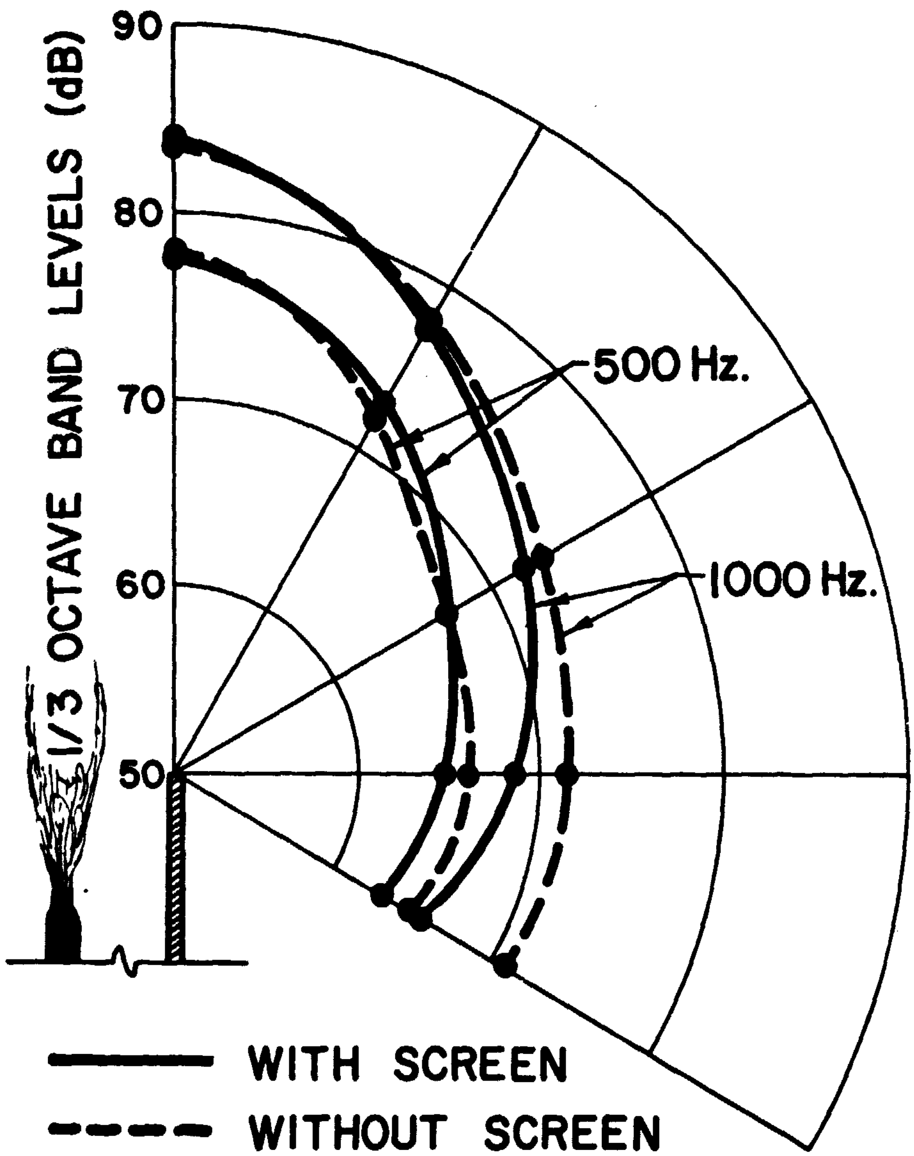

Fig. 11. Measured 1/3-octave band levels at outer frequencies shown for jet noise: jet pressure, 5.0 psi; distance from top of screen, 3.5 ft. (see Figs. 7 and 8).

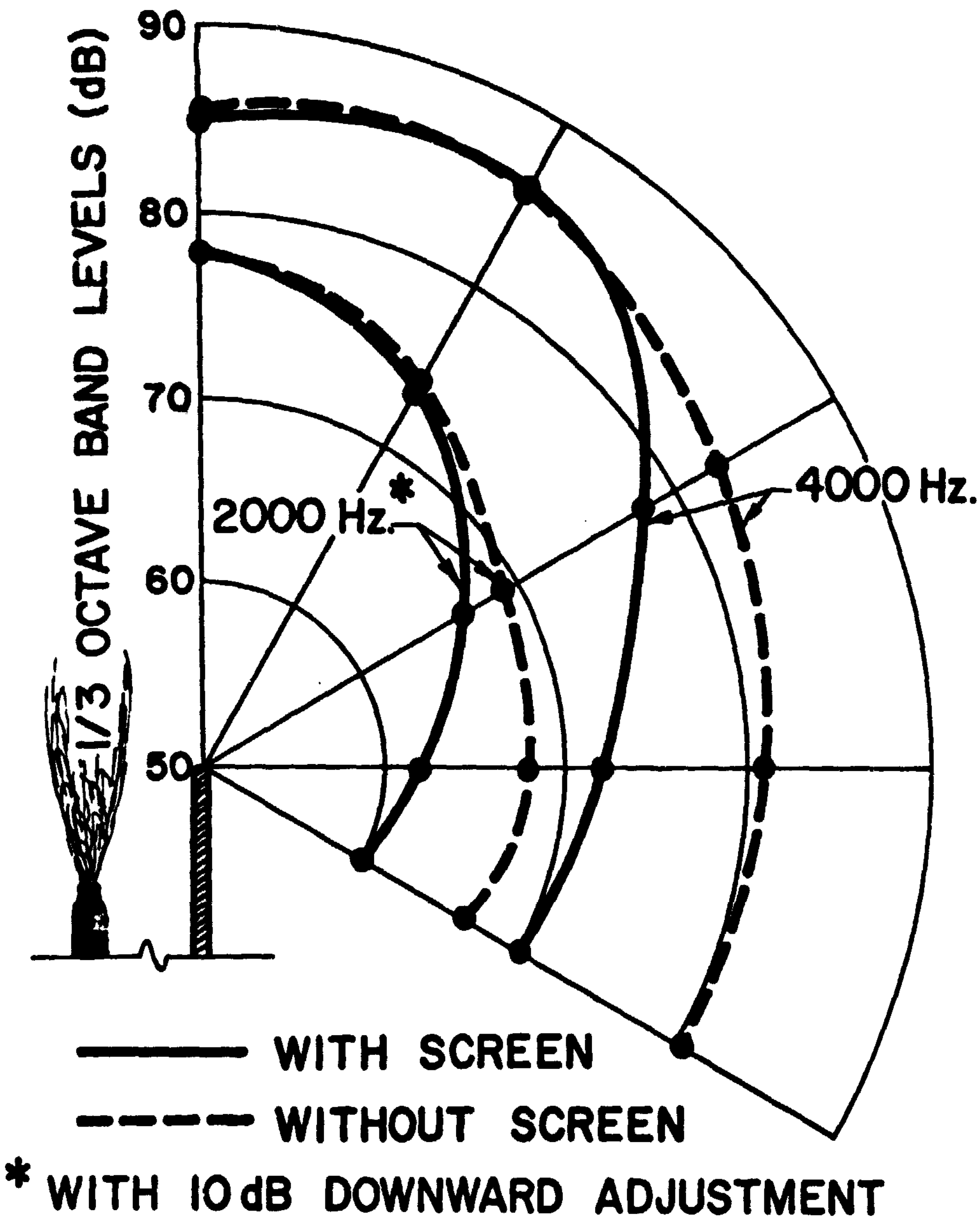

Fig. 12. Measured 1/3-octave band levels at outer frequencies shown for jet noise: jet pressure, 5.0 psi; distance from top of screen, 3.5 ft. (see Figs 7 and 8).

Table I. Narrow-band Pressure Levels Close to the Screen in the Acoustic Shadow of a Point Source

Frequency	490 Hz		900 Hz		2050 Hz		4050 Hz	
	Driver		Driver		Driver		Driver	
Microphone Location[a]	Position 2	Position 4	Position 2	Position 4	Position 2	Position 4	Position 2	Position 4
1	59.0 dB	65.3 dB	84.0 dB	85.3 dB	82.8 dB	83.0 dB	88.3 dB	86.3 dB
7	69.5	66.0	89.8	84.0	82.8	84.0	76.5	80.0
8	58.8	56.3	81.5	71.0	82.8	81.3	76.0	73.0

[a]Refer to Figure 1 for microphone positions.

positions 1, 7, 8, and 9 are presented in Table II.

The third experiment was intended to supply information as to the effects of a thick barrier and a curved diffracting surface. The source-barrier-receiver geometry for this experiment is sketched in Fig. 13. The sides of the barrier were sheets of 1" plywood. The cap was also constructed of 1" plywood formed so as to produce a half-cylinder with a radius of 12 inches. As in the first experiment, pure-tone excitation was applied to an acoustically small source. The source was located close (in terms of acoustic wavelengths) to one side of the obstacle. Several source heights relative to the highest point on the barrier were used. Narrow-band sound pressure levels were measured on an arc at a fixed distance from a point near the junction between the straight and curved portions of the barrier. Additional sound level measurements were made in a vertical plane in the acoustical shadow of the barrier at a horizontal distance of 88 inches from the source. The measured pressure levels for several source heights are presented in Tables III-V. These measurements show the expected increase of the shadowing effect with frequency and, in the main, the expected increase of the shadowing effect with difference between the source heights and the highest point o the obstacle. In some cases the variation in pressure level with angle is not a uniform decrease from the position almost directly above the source to that well inside the shadow of the barrier: the deviations which arise are no doubt due to

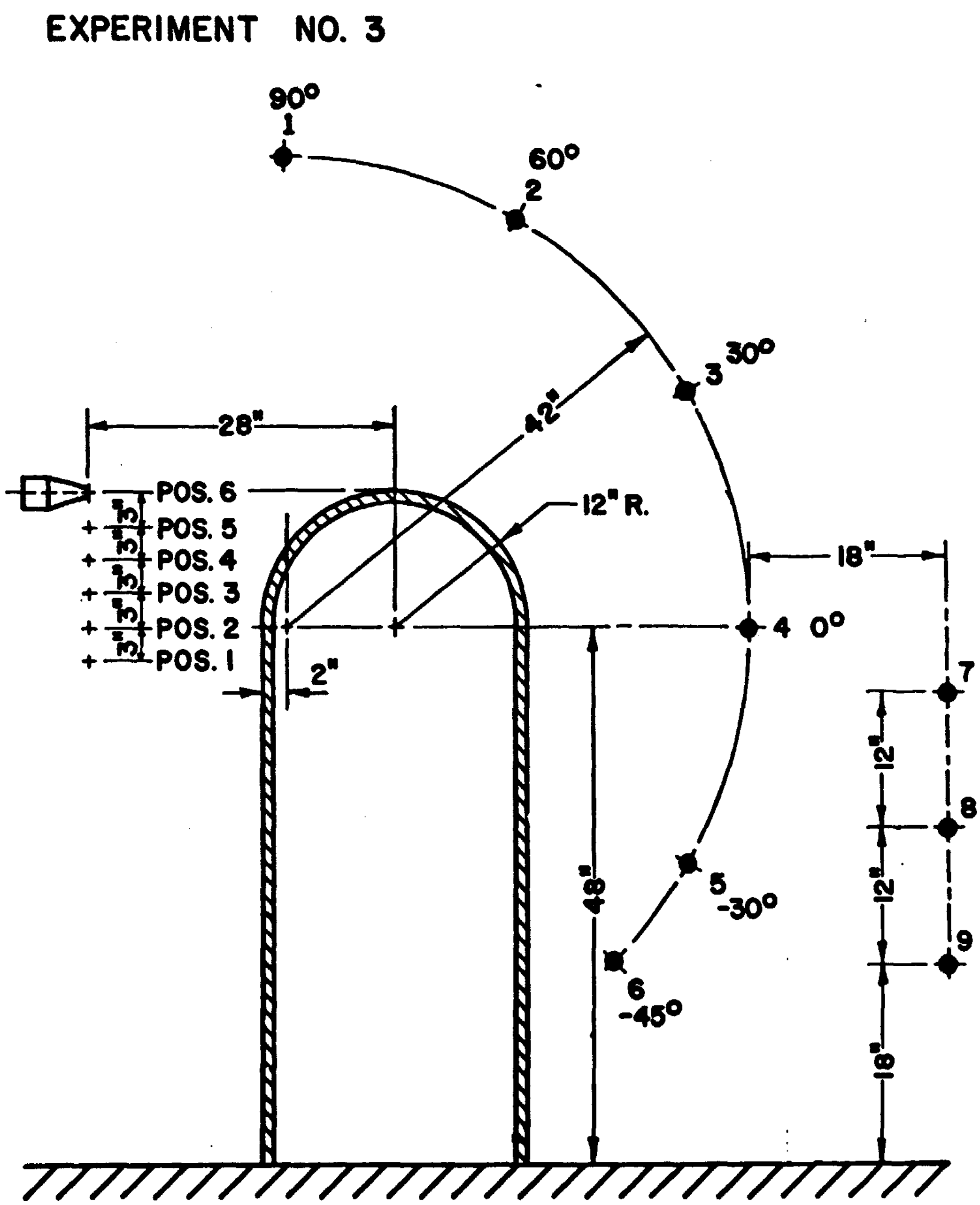

Fig. 13. Sketch of source-barrier-receiver geometry for third experiment (see also Fig. 2).

Table II. One-third Octave Band Levels Close to the Screen in the Acoustic Shadow of a 1-inch Jet

Frequency	500 Hz		1000 Hz		2000 Hz		4000 Hz	
Microphone Location[a]	Screen Absent	Screen Present	Screen Absent	Screen Present	Screen Absent	Screen Present	Screen Absent	Screen Present
Pressure: 2.8 psi								
1	69.8 dB	70.0 dB	74.2 dB	74.0 dB	76.0 dB	75.6 dB	74.2 dB	74.0 dB
7	64.5	62.6	68.6	64.0	72.0	65.0	73.5	63.6
8	62.8	60.8	65.5	60.2	70.0	60.2	72.2	59.2
9	61.0	58.2	63.0	56.0	66.0	57.8	69.5	56.5
Pressure: 5.0 psi								
1	78.0	77.5	83.5	84.0	87.8	88.0	85.5	85.0
7	71.0	70.5	77.0	72.0	83.0	75.0	85.0	74.2
8	69.0	67.5	73.8	68.0	80.0	70.5	83.5	70.0
9	57.6	66.0	61.2	63.8	66.6	68.2	70.8	67.0

[a] Refer to Figs. 7 and 8 for microphone positions.

Table III. Narrow-band Pressure Levels for Diffraction of Sound by a Cylindrically Capped Barrier: Source 12" Below Highest Point on Barrier.

Microphone Location[a]	Frequency			
	490 Hz	900 Hz	2050 Hz	4050 Hz
1	64.5 dB	86.8 dB	81.5 dB	91.5 dB
2	64.0	88.0	83.5	90.3
3	59.0	82.0	79.8	82.5
4	55.5	80.3	66.3	66.8
5	52.3	68.5	60.5	66.5
7	50.5	74.5	69.5	62.0
8	39.5	71.5	58.8	64.5
9	51.5	70.0	47.8	70.3

[a]Refer to Fig. 13 for microphone positions.

Table IV. Narrow-band Pressure Levels for Diffraction of Sound by a Cylindrically Capped Barrier: Source 6" Below Highest Point on Barrier.

Microphone Location[a]	Frequency			
	490 Hz	900 Hz	2050 Hz	4050 Hz
1	66.0 dB	91.0 dB	89.0 dB	95.0 dB
2	63.8	86.8	83.3	87.5
3	59.3	84.5	77.0	87.5
4	58.0	78.3	69.5	75.8
5	53.8	68.3	65.0	70.5
7	49.5	73.5	68.0	67.5
8	45.0	75.3	67.5	69.8
9	51.3	74.8	65.3	61.3

[a]Refer to Fig. 13 for microphone positions.

Table V. Narrow-band Pressure Levels for Diffraction of Sound by a Cylindrically Capped Barrier: Source at Height of Highest Point on Barrier.

Microphone Location[a]	Frequency			
	490 Hz	900 Hz	2050 Hz	4050 Hz
1	66.3 dB	91.3 dB	87.3 dB	85.8 dB
2	64.5	84.5	86.3	89.5
3	61.8	86.8	81.5	86.8
4	56.0	75.8	68.5	78.8
5	55.0	71.5	68.3	69.8
7	49.3	75.3	72.3	74.8
8	47.5	77.0	66.3	61.0
9	51.0	71.3	63.3	65.0

[a]Refer to Fig. 13 for microphone positions.

constructive interference between waves transmitted directly to the receiver and those reflected from the cylindrical cap.

Chapter 3

THEORY OF SOUND DIFFRACTION AROUND SCREENS AND WEDGES

INTRODUCTION

Solutions corresponding to constant frequency sound diffraction by a rigid wedge or a rigid screen (a limiting case of a wedge) are well known.[1,2] In particular, the exact solution for the case of a point source in the vicinity of such a wedge or screen appears in various places in the literature as a contour integral in the complex plane with an integrand of moderate complexity involving elementary transcendental functions.[3,4] This integral is not directly expressible in a closed form, but its value when both source and listener distances from the edge are large compared to a wavelength can be expressed to a uniform asymptotic approximation in terms of Fresnel integrals[5,6] or related functions[7]. Expansions have also been derived which are appropriate to the case when either source or listener is close (relative to a wavelength) to the edge.[8]

For those situations in which one of the distances involved is neither large nor small compared to a wavelength, it may be necessary to perform a numerical integration of the contour integral (or of other integrals which would appear in equivalent expressions) or to sum a large number of terms of the expansion appropriate to the length being small compared to a wavelength. Such numerical integration or summation, however, may be slowly convergent and may be difficult to perform even with the aid of a large digital computer. Although direct computations of this sort have been performed by Ambaud and Bergassoli[9], the method they describe, while leading to accurate values which agree well with their experiments, is intrinsically limited in application to source-listener geometries in which neither location is at an extremely large number of wavelengths from the edge. Further, the method is such that severe computational difficulties would be encountered were the listener arbitrarily close to the shadow zone boundary. While one might expect such calculations to meld with calculations using the results of a uniform asymptotic approximation, the match would be evident only from a direct numerical comparison.

The present chapter is prompted by the problem of estimating aircraft noise shielding by wings (engine-over-wing configuration), one of the features of which is that the sound sources are neither very close or very far (relative to all wavelengths of interest) from the wing trailing edge. Research on this topic should be aided by the availability of a convenient general purpose method for the calculation of the acoustic pressure (i.e., the Green's function) at an arbitrary listener location caused by the presence of a unit strength point source near a rigid wedge or screen. Ideally, the method should be based on a formulation which reduces directly (without excessively intricate manipulations) to know limiting cases (i.e., source on edge or source and listener both far from edge).

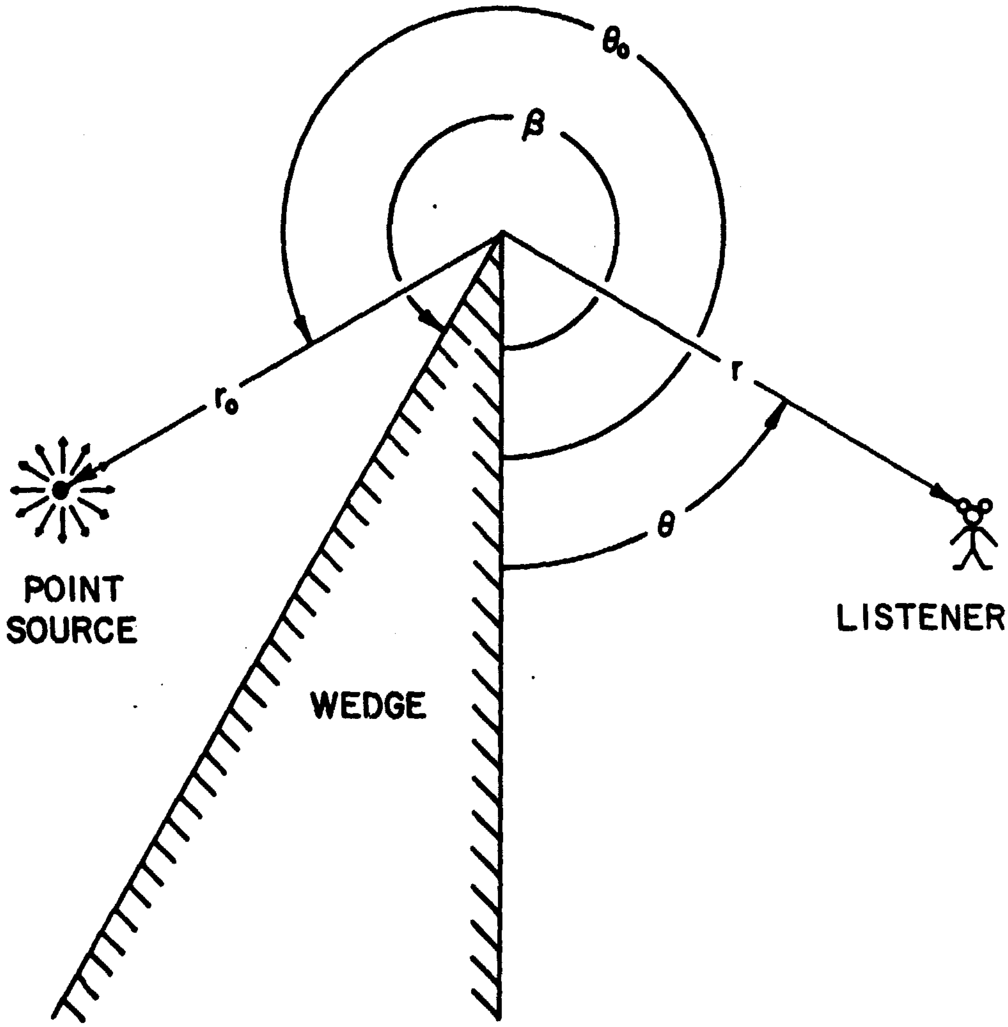

Fig. 1. Geometry used to describe diffraction of sound waves from a point source by a wedge.

Such a formulation, with accompanying numerical examples, is presented here. Furthermore, the plots included here should enable one, without further need of a digital computer, to estimate the sound field and the sound reduction for the important limiting case when the listener is many wavelengths away from the edge and much further than is the source ($kL>>1, rr_o/L^2<<1$ in the notation explained below). Discussion is also given of the accuracy of approximations commonly made in acoustical studies.

I. GEOMETRY AND FORMAL SOLUTION

The geometry appropriate to the problem under consideration is that of a rigid wedge whose edge lies along the z-axis (Fig. 1) in a cylindrical coordinate system (r,θ,z), with the two faces taken as the $\theta = 0$ and $\theta = \beta$ planes, such that the region exterior to the wedge extends from $\theta = 0$ to $\theta = \beta$ (with $\beta>\pi$). A thin screen corresponds to $\beta = 2\pi$. (Here we use the same notation as was used in a previous paper[7] by one of the authors.)

The source of sound is a single harmonic point source (angular frequency ω, wavenumber $k = \omega/c$) located at a point $(r_o,\theta_o z_o)$ and of strength such that the acoustic pressure field p in the source's immediate vicinity is given by e^{ikR}/R plus bounded terms when R, the net distance from the source, is substantially less than the distance of source from edge. Here a customary time dependent factor of $e^{-i\omega t}$ is understood but omitted for simplicity. The acoustic pressure field dependence thus corresponds to a Green's function $G(\underset{\sim}{x}|\underset{\sim}{x}_o)$ which satisfies the scalar Helmholtz equation with the customary source term $-4\pi\delta(\underset{\sim}{x}-\underset{\sim}{x}_o)$ on the right hand side. Boundary conditions corresponding to the rigid wedge are that $\partial G/\partial\theta = 0$ at $\theta = 0$ and $\theta = \beta$, respectively.

For present purposes, it is convenient to take the solution to the problem just posed in the form (but in the present notation) utilized by Ambaud and Bergassoli[9]. This, with some paraphrasing of notation, can be written

$$G(\underset{\sim}{x}|\underset{\sim}{x}_o) = \sum_{i=1}^{4}\left[G(\zeta_i)U(\pi-\zeta_i) + V(\zeta_i)\right] \tag{1}$$

where

$$\zeta_1 = |\theta-\theta_o| \tag{2a}$$

$$\zeta_2 = 2\beta - |\theta-\theta_o| \tag{2b}$$

$$\zeta_3 = \theta + \theta_o' \tag{2c}$$

$$\zeta_4 = 2\beta - (\theta+\theta_o) \tag{2d}$$

Here $U(\zeta)$ is the Heaviside unit step function. The $G(\zeta_i)U(\pi-\zeta_i)$ terms for $i = 1,3,4$ correspond to waves inferred from purely geometrical acoustical considerations, i.e., $(i=1)$ a direct wave, $(i=3)$ a wave reflected from the $\theta = 0$ face, and $(i=4)$ a wave reflected from the $\theta = \beta$ face. (The term $G(\zeta_2)U(\pi-\zeta_2)$ is always zero, since ζ_2 is always greater than π, but is included to preserve the symmetry of the expression.) The term $G(\zeta)$ represents a radially symmetric spherically spreading wave, generically denoted by e^{ikR}/R, where (arbitrary argument ζ)

$$R = [r^2 + r_o^2 + (z-z_o)^2 - 2rr_o \cos \zeta]^{\frac{1}{2}} \tag{3}$$

This distance, for the four particular values of ζ listed above, may be interpreted as: (i=1) distance from source; (i=2) distance from an image-image point; $(r_o, 2(\beta-\pi) + \theta_o, z_o)$ if $\theta > \theta_o$; (i=3) distance from image of source reflected through $\theta = 0$ plane; and (i=4) distance from image of source reflected through $\theta = \beta$ plane. (While the geometrical interpretation of ζ_2 may seem irrelevant since $U(\pi-\zeta_2)$ is always zero, the interpretation is germane to the interpretation of $V(\zeta_2)$ in the limiting case, termed the Fresnel number approximation, below. The image-image is formed either by reflecting the source through the $\theta = 0$ plane, then reflecting this image through the $\theta = \beta$ plane or by carrying out the reflections in inverse order. The construction is indicated in Fig. 2.) In the cases i = 1,3,4, the presence of the Heaviside unit step functions as factors in the geometrical acoustics terms insures that: (i=1) the direct wave is zero unless the source may be "seen" by the listener; (i=3) there is no contribution from a wave reflected from the $\theta = 0$ face unless one can construct a specularly reflected ray going from source to face to listener; and (i=4) there should be an analogous ray reflected from the $\theta = \beta$ face connecting source and listener if the corresponding geometrical acoustics term can contribute to the field.

The sum of the terms $V(\zeta_i)$ in Eq. (1) may be interpreted as the diffracted wave. Each may be written in a similar fashion as a definite integral, which, in the form taken by Ambaud and Bergassoli, is

$$V(\zeta) = -(1/\pi)\int_0^\infty G(\pi+iw)\, Q(w,\nu,\zeta)\, dw \tag{4}$$

with

$$Q(w,\nu,\zeta) = \frac{(\nu/2)\sin[\nu(\pi-\zeta)]}{\cosh(\nu w) - \cos[\nu(\pi-\zeta)]} \tag{5}$$

the index ν being π/β ($\nu = 1/2$ for the thin screen, 2/3 for a right angled wedge). Here $G(\pi+iw)$ represents the wave function e^{ikR}/R, R being given by Eq. (3), with ζ replaced by $\pi+iw$, or, equivalently, with $\cos\zeta$ replaced by $-\cosh w$. The quantity R^2 is real and positive, R being understood to be the positive square root of R^2, throughout the integration over w.

II. REFORMULATION OF DIFFRACTION INTEGRAL

Direct numerical evaluation of $V(\zeta)$, while possible, is unwieldy because of (1) the infinite limits, (2) the oscillatory nature of the integrand and the attendant slow convergence in many cases of interest, and (3) the fact that Q is unbounded near $w = 0$ as $\zeta \to \pi$. To avoid such difficulties we change the variable of integration and the path of integration. To this purpose, we note that $Q = d\psi/dw$ where ψ is such that

$$\tan \psi \quad = \quad \tan[A(\zeta)]\tanh[(\nu/2)w]$$

and where A is $(\nu/2)(-\beta-\pi+\zeta)$ plus any multiple of π. If we refine the definition of $A(\zeta)$ and ψ such that ψ varies from 0 to A as w varies from 0 to ∞, the proper choice for A is (given $0<\zeta<2\beta$)

$$A(\zeta) = (\nu/2)(-\beta-\pi+\zeta) \quad + \quad \pi U(\pi-\zeta) \tag{6}$$

The value of ψ corresponding to its tangent as given above is understood to lie between $-\pi$ and π and to have the same sign as A. One may note that $A(\zeta)$ is discontinuous at $\zeta = \pi$: $A(\zeta)$ increases from a positive value $(\nu/2)(\beta-\pi)$ at $\zeta = 0$ up to $\pi/2$ at $\zeta = \pi^-$, then drops abruptly to $-\pi/2$ at $\zeta = \pi^+$ and subsequently increases linearly, passing through 0 at $\zeta = \beta+\pi$, up to the original value $(\nu/2)(\beta-\pi)$ when $\zeta = 2\beta$.

Some indication of the variation of values of the $A(\zeta_i)$ [abbreviated A_i here] with the source and listener coordinates θ_o and θ may be obtained if one considers the specific case (typically of greatest interest) in which the source is on the far side of the wedge, $\beta > \theta_o > \pi$, the listener is in the shadow zone, $0 < \theta < \theta_o - \pi$ (See Figure 3). In this case all the A_i are negative and between $-\pi/2$ and 0, the magnitudes

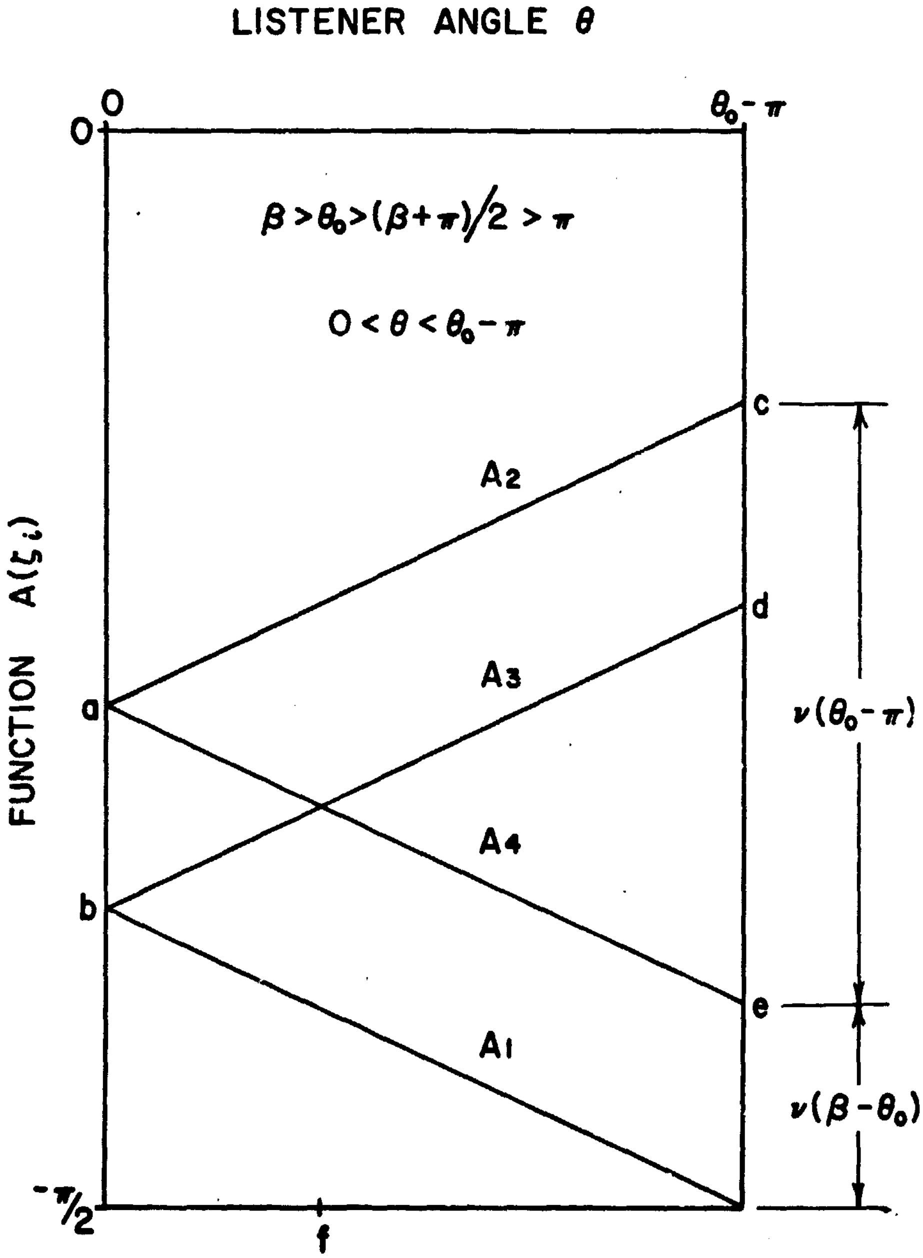

Fig. 3. The functions $A(\zeta_i)$ for $i=1,2,3,4$ (where ζ_i is a function of the wedge angle and the source and listener angles).

$|A_1|$ and $|A_4|$ increasing with increasing θ and conversely for $|A_3|$ and $|A_2|$. At $\theta = 0$, $A_1 = A_3$ and $A_2 = A_4$; in general one has $|A_1| > |A_3| > |A_2|$ and $|A_1| > |A_4| > |A_2|$. One may note that the line, A_1 versus θ equals $-\pi/2$ at the shadow zone boundary. The lines A_3 and A_4 cross only if $\theta_o > (\beta+\pi)/2$ and, when they do, they cross at $\theta = \beta - \theta_o$ with the mutual value $A_3 = A_4 = -\pi/2 + (\nu/2)(\beta-\pi) = -\pi\nu/2$.

If we now change the variable of integration to $q = \psi/A$, then $Q\,dw = A\,dq$ and q varies from 0 to 1. The remainder of the integrand can also, after some algebra, be expressed in terms of q rather than w. The pertinent intermediate result is

$$R = [L^2 + rr_o(Y - Y^{-1})^2]^{1/2} \tag{7}$$

where we abbreviate

$$L = [(r + r_o)^2 + (z - z_o)^2]^{1/2} \tag{8}$$

$$Y = \left\{ \frac{\tan(A) + \tan(qA)}{\tan(A) - \tan(qA)} \right\}^{1/(2\nu)} \tag{9}$$

The quantity Y, and therefore the spherical wave factor, is independent of the sign of A. Thus we may rewrite the integral in Eq. (4) as

$$V(\zeta) = -(1/\pi)\,A(\zeta)(e^{ikL}/L)\,F_\nu(|A|,\alpha,\varepsilon) \tag{10}$$

where

$$F_\nu(|A|,\alpha,\varepsilon) = \int_0^1 I(q)\,dq \tag{11a}$$

$$\alpha = k\, rr_o/L;\ \varepsilon = rr_o/L^2$$

$$I(q) = (L/R)\, e^{ik(R-L)} \tag{11b}$$

with L and R as given above.

The set of arguments of F_ν is readily seen from the above equations to be complete. The forms chosen for the parameters ε and α are particularly convenient in the consideration of limiting cases. From geometrical considerations, ε is always less than 1/4. The parameter α, which has the appearance of a Fresnel wave parameter, may in principle have any value. The quantity L has the important geometrical interpretation of being the length of the shortest two segment path which goes from source to edge and then to listener (i.e., L is the length of a diffracted ray path).

III. THE DEFORMED CONTOUR

The variable q is now considered as a complex variable and the integral over I(q) in the definition of F_ν above is interpreted as a contour integral in the complex q plane. Rather than integrate directly along the real axis, we choose a path C which (1) goes from 0 to 1, (2) has finite length, (3) is such that $\mathrm{Re}(R-L) = 0$ at every point on the path, and (4) is such that, for nonzero α, $e^{ik(R-L)}$ decreases monotonically from 1 to 0 as q travels the path C from q = 0 to q = 1. That a path with these properties exists is supported by the mathematical foundations of the method of steepest descents and is substantiated by the construction given below.

The evaluation of the integral along the contour C is facilitated by a reformulation of the function I(q), Eq. (12).

The restriction $\mathrm{Re}(R-L) = 0$ along the path implies that we may introduce a real parameter K such that, at any point on the path, R is related to K by

$$R = L[1 + i\varepsilon K^2] \tag{13}$$

Here K ranges from 0 through positive values when q ranges from 0 through successive points on the path. The relationship between q and K may be determined by equating the squares of Eqs. (7) and (13), then inserting the expression (9) for Y, and solving for q. In this manner one finds

$$q = \frac{1}{|A|} \tan^{-1} [\tanh \frac{\nu X}{2} \tan |A|] \tag{14a}$$

with

$$\sinh X = K[i/2 - \varepsilon K^2/4]^{1/2} \tag{14b}$$

The several ambiguities in the definitions of the square root and of the implied inverse trigonometric functions are resolved by the requirement that q vary continuously from 0 to 1 (although not on the real axis) as K varies from 0 to ∞. To accomplish this, one defines the square root in Eq. (14b) to be such that its phase is between $\pi/4$ and $\pi/2$, then defines X to be such that $\mathrm{Re}(X) > 0$, $0 < \mathrm{Im}(X) \leq \pi/2$, and q to be such that it lies in the first quadrant.

The computation of q_R and q_I for given values of K is generally facilitated by reducing Eqs. (14) to explicit equations involving only elementary functions of real variables. Such a reduction yields, for example

$$\tan(2|A|q_R) = \frac{\sin(2|A|)\sinh a}{\cos b + \cosh a \cos(2|A|)} \tag{15a}$$

in which

$$\begin{matrix}\sinh(a/\nu) \\ \sin(b/\nu)\end{matrix} = K[(1 + Q^2)^{1/2} \pm Q]^{1/2} \tag{15b}$$

with

$$Q = \frac{1}{2} K^2 [1 - \varepsilon + \frac{1}{4} \varepsilon^2 K^4] \tag{15c}$$

The expression for tanh $(2|A|q_I)$ is similar to Eq. (16a): sinh a, cosh a and cos b should be replaced by sin b, cos b, and cosh a, respectively. The restrictions mentioned above concerning phases and branches imply that b/ν is between 0 and $\pi/2$ for $K < (2/\varepsilon)^{1/4}$ and is between $\pi/2$ and π for $K > (2/\varepsilon)^{1/4}$. The restrictions further imply that $2|A|q_R$ lies between 0 and π.

Some computed plots of the deformed contour C in the complex q plane and of the corresponding variation of K along the contour are shown in Figs. 4 and 5. Analysis of the equations given above indicates that such contours always proceed from $q = 0$ obliquely upward at an angle of 45° with the real axis and this is confirmed by the computations. The terminal point $q = 1$, is approached from above and to the right, making an angle $(1-\nu)\pi$ with the real axis to the right of $q = 1$ for non-zero ε. In the limiting case of a screen, $\nu = ½$, the contour terminates at a right angle with the real axis. In the limit

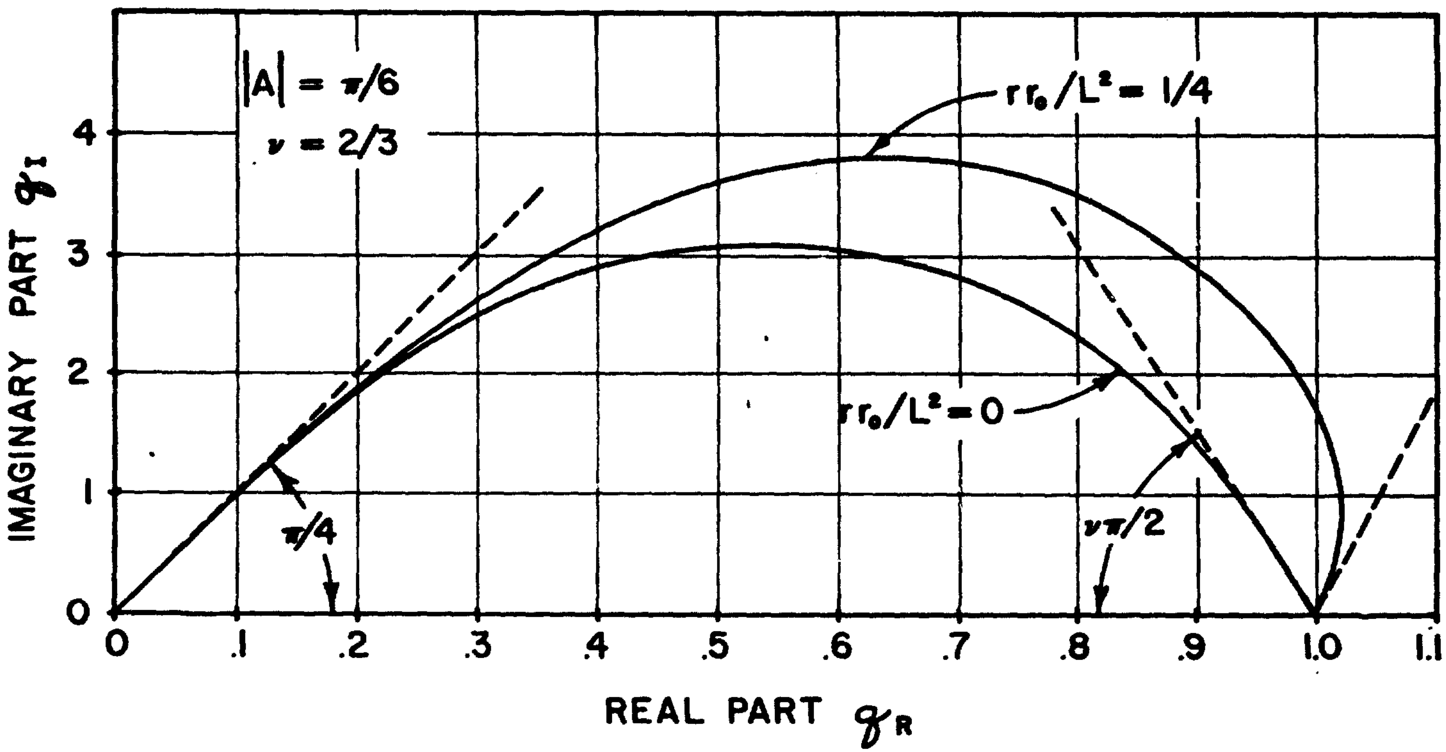

Fig. 4. Typical deformed contours in the complex q-plane which correspond to paths of steepest descent for a factor in the exponential in the integrals described in the text.

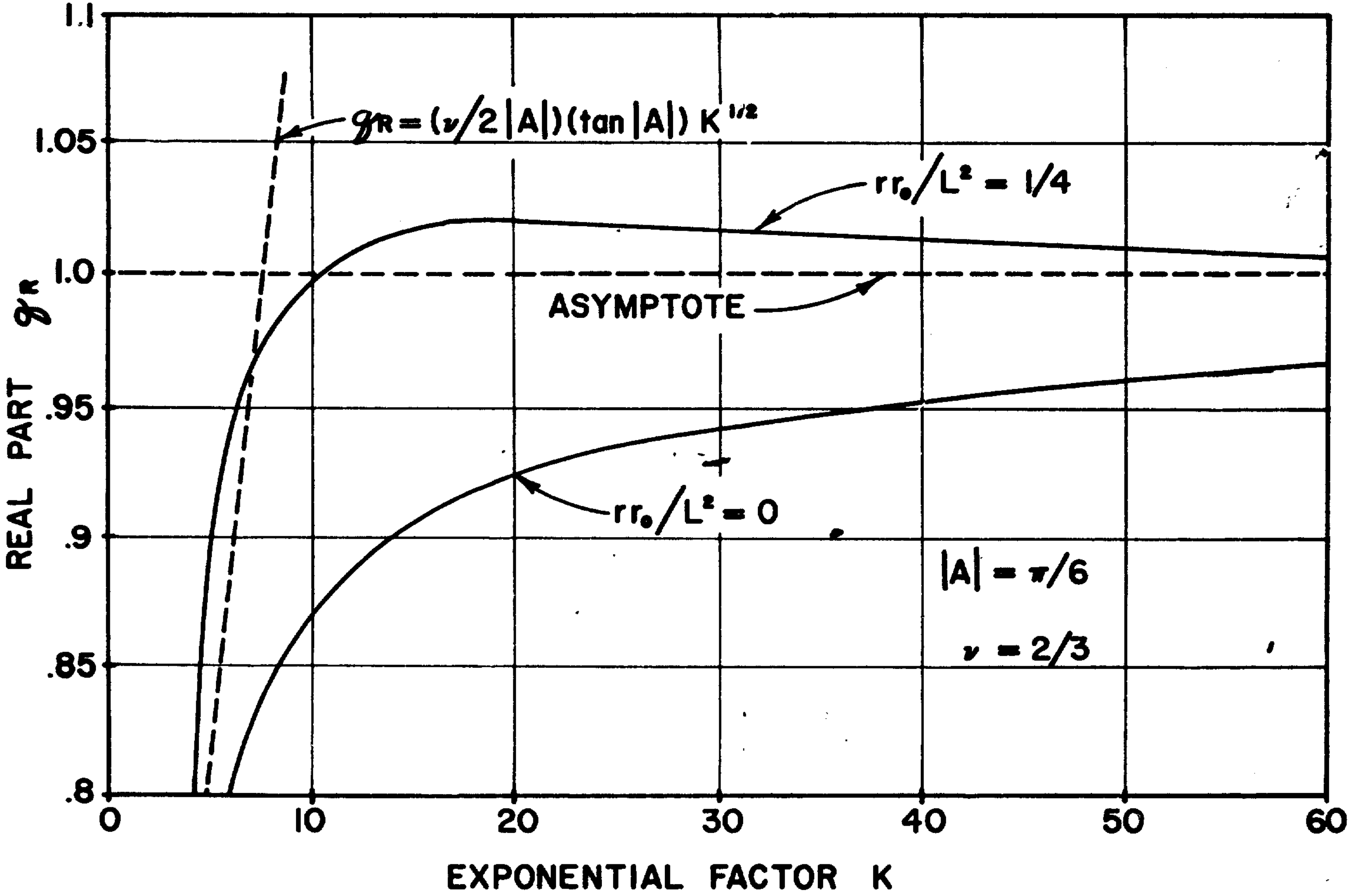

Fig. 5. Relationship between real part of the complex variable q and the factor K occurring in the exponent of the integrand. (These in conjunction with the curves in Fig. 4 give an indication of the manner in which K varies along the integration contour.)

of vanishingly small ε, the contour C approaches a limiting form which approaches $q = 1$ obliquely downward from the left, making an angle of $\nu\pi/2$ with the real axis. The principal modification of this limiting form caused by nonzero ε is a small "kink" near $q = 1$ in which q_R overshoots $q_R = 1$ slightly (except for $\nu = \frac{1}{2}$), the contour then bending back and approaching $q = 1$ obliquely downward from the right. The quantity K always increases monotonically from 0 to ∞ along the contour, except for the limiting case where $|A|$ is identically $\pi/2$. If $|A|$ is slightly less than this upper limit, K remains virtually zero along the major bulk of the contour but increases rapidly to ∞ near the very end of the path.

At this point, we may note that the reformulation of the diffraction integral as represented by Eqs. (10-12), with C taken as the integration contour, has removed all the difficulties pointed out at the beginning of this section. The limits of integration are now finite, the modulus of the integrand $I(q)$ is bounded by 1, and the integration along C removes the problem of the oscillatory nature of the integrand.

IV. LIMITING CASES

The formulation as presented leads either directly or with minor mathematical manipulation to a number of important limiting expressions for the Green's function and for the various terms which contribute to it.

1. Source or listener on edge. This case is characterized by $\epsilon = 0$ and $R = L$ for all values of q, so we have

$$F_\nu(|A|,0,0) = 1 \tag{19a}$$

and the total Green's function reduces to

$$G(x|x_0) = 2\nu L^{-1}e^{ikL} = (2\pi/\beta)L^{-1}e^{ikL} \tag{19b}$$

where, in this instance, L is simply the distance from source to listener. The above pressure field, except for the limiting case of a thin screen (where $\beta = 2\pi$), is always larger than what would be expected were the wedge not present. The Green's function for source or receiver on the edge could also be derived from simple symmetry arguments (the field must exhibit spherical symmetry for source on edge, the total volume velocity of the source must be the same as in the absence of the wedge, but the volume velocity per unit solid angle increases by a factor of $4\pi/2\beta$, where 2β is the solid angle external to the wedge about a point on the edge) without the necessity of the general solution.

2. The limit $|A| \to \pi/2$ or $\zeta \to \pi$. In this case the approximation $R \approx L$ is valid over most of the length of the contour C, the contribution from portions of the contour where this approximation does not hold becoming increasingly negligible as $|A|$ becomes progressively closer to $\pi/2$. Thus, we obtain

$$F_\nu(\pi/2,\alpha,\varepsilon) \approx 1 \tag{16a}$$

so the sum of the corresponding geometrical wave $G(\zeta)U(\pi-\zeta)$ and the appropriate diffracted wave term $V(\zeta)$ should have the limit

$$\lim_{\zeta\to\pi} \{G(\zeta)U(\pi - \zeta) + V(\zeta)\} = (1/2)e^{ikL}/L \tag{16b}$$

regardless of from which side the limit is approached. Thus, the total field, as expected, is continuous.

3. The uniform asymptotic limit, where $krr_0/L \gg 1$, $|A|$ is arbitrary. This corresponds to both kr and kr_0 being large and $|z - z_0|$ being less than or comparable to $(r^2 + r_0^2)^{\frac{1}{2}}$. Equivalently, both source and listener are far from the edge and the angle between the edge and the broken ray from source to edge to listener is not close to 0.

In the evaluation of this asymptotic limit, it is convenient to regard K as the variable of integration. The derivative dq/dK may be evaluated by implicit differentiation of Eqs. (15b) such that dq/dK is a function of a and b times the derivative d(a+ib)/dK. Since krro/L is large we may expect the dominant contribution to the integral to come from small values of K. However in the limit $K \to 0$, dq/dK is inversely proportional to $\cos(2|A|)$ and is singular when $|A| \to \pi/2$. To cover this contingency one expands the denominator in the function just mentioned to the next order nonvanishing term (which turns out to be second order) in K. The remainder of the factors (except for the exponential) are approximated by their limits as $K \to 0$. In particular, one may note from Eqs. (15) that $d(a+ib)/dK$ is just $\nu(1+i)$ in this limit. The variable of integration is next changed to $u = \alpha^{1/2}K$, then the resulting integral is recognized as a constant times the integral

$$A_D(X) = (X/\pi^{\frac{1}{2}}) \int_0^\infty \frac{e^{-u^2}\, du}{[(\pi/2)X^2 + i\, u^2]} \tag{17}$$

$$= f(X) - i\, g(X) \qquad (X > 0)$$

where

$$X = [4\alpha/\pi]^{\frac{1}{2}}\, (1/\nu)\, \cos(|A|) \tag{18}$$

Here F(X) and g(X) are the auxiliary Fresnel functions discussed in a previous paper[7] by one of the authors and which are tabulated on pages 323-324 of the NBS Handbook of Mathematical Functions.[11] The mathematical manipulations as outlined above then lead to the expression

$$F_\nu \approx (\pi/\sqrt{2})\, e^{i\pi/4}\, [(\sin|A|)/|A|][f(X) - i\, g(X)] \tag{19}$$

for $krr_o/L >> 1$. One may note that, although the coefficient of $\cos(|A|)$ in Eq. (18) is presumed large, it cannot necessarily be assumed that X is large since $\cos(|A|)$ would be very small were $|A|$ close to $\pi/2$.

In the limit of large X, the quantity $f - ig$ approaches $1/(\pi X)$ and thus F_ν decreases asymptotically as the inverse square root of α for nonzero value of $\cos(|A|)$. When $|A|$ approaches $\pi/2$, both f(X) and g(X) approach the value 1/2, the limiting values for $X \to 0$. In this limit F_ν goes to 1, just as indicated by Eq. (16a). It should also be noted that in this approximation F_ν is independent of the parameter ε for a fixed value of α.

4. <u>The Fresnel number approximation</u>.[12] If, in addi[illegible]n to $krr_o/L >> 1$, it is true that $\cos(|A|)$ is substantially less than ν, the parameter X in Eq. (18) may be interpreted as $X = (2N)^{1/2}$ where N is a Fresnel number given by

$$N = (L - R_A)/(\lambda/2) \tag{20}$$

which represents the excess of the diffracted path length L beyond some direct path length R_A in units of half wavelengths. The appropriate identification of R_A is

$$R_A = [r^2 + r_o^2 + (z-z_o)^2 - 2rr_o\cos(B_\nu)]^{1/2} \tag{21}$$

with $B_\nu(|A|)$ taken as

$$B_\nu(|A|) = \pm\{\pi - (2/\nu)(\pi/2 - |A|)\} + 2n\pi \tag{22}$$

with n being an integer (0, positive, or negative) and with any choice of the two signs. With the purpose of giving a meaningful geometrical interpretation of B_ν, one may show with some effort that it is possible to choose the sign and the integer n such that

$$\theta + B_\nu = \theta_o \qquad (\zeta = |\theta - \theta_o|) \tag{23a}$$

$$= \theta_o + 2(\beta-\pi) \qquad (\zeta = 2\beta-|\theta - \theta_o|,\ \theta > \theta_o) \tag{23b}$$

$$= \theta_o - 2(\beta-\pi) \qquad (\zeta = 2\beta-|\theta - \theta_o|,\ \theta_o > \theta) \tag{23c}$$

$$= -\theta_o \qquad (\zeta = \theta + \theta_o) \tag{23d}$$

$$= 2\beta - \theta_o \qquad (\zeta = 2\beta - \theta - \theta_o) \tag{23e}$$

Thus, with reference to the discussion following Eq. (3), R_A is the direct distance of listener from (i = 1) the source; (i = 2) the image of the image; (i = 3) the image formed by reflection through the $\theta = 0$ plane; or (i = 4) the image formed by reflection through $\theta = \beta$ plane.

That X is approximately $(2N)^{\frac{1}{2}}$ where N is as defined above in the limits $\cos(|A|) \ll \nu$, α, follows from the general expresion (22), from the (consistent) approximation $\sin[(1/\nu)(\pi/2 - |A|)] \approx (1/\nu)\cos(|A|)$, from the fact that ε is always less or equal to 1/4, from the definition (8) of L, and from an appropriate binomial expansion of R_A.

When the Fresnel number approximation is valid, $|A|$ should be close to $\pi/2$, so it is consistent to approximate the $\sin(|A|)/|A|$ factor in Eq. (19) by $2/\pi$ and the resulting expression for F_ν becomes

$$F_\nu \simeq (\sqrt{2})\, e^{i\pi/4} \{f([2N]^{\frac{1}{2}}) - i\, g([2N]^{\frac{1}{2}})\} \tag{24}$$

This represents a considerable simplification in that the right side depends on one and only one parameter N of relatively simple geometrical interpretation. There is no explicit ν, $|A|$, α, or ε dependence, other than the manner in which these enter into the determination of N. The expression above also has the virtue of never giving a magnitude of F_ν greater than 1.

The corresponding expression for $V(\zeta)$ in the Fresnel number approximation may be obtained from Eq. (10) with $A(\zeta)$ replaced by $(\pi/2)\sin(\pi - \zeta)$. This is in accordance with Eq. (6) and the fact that $|A|$ should be close to $\pi/2$. Consequently, Eq. (24) should be multiplied by $\sin(\zeta - \pi)(2L)^{-1}e^{ikL}$ to obtain $V(\zeta)$.

5. <u>The case when</u> kL <u>is large but</u> krr_0/L <u>is finite or</u> $\varepsilon \ll 1$, α <u>finite</u>. The two statements are equivalent since $kL \to \infty$ with krr_0/L fixed implies $rr_0/L^2 \to 0$. This limiting case is of interest in those problems where the source is at finite or small distance relative to a wavelength from the edge but the listener is at a large number of wavelengths from the edge, much further than is the source. Conversely, because the solution conforms to reciprocity

(interchange of source and listener), the corresponding limiting solution corresponds to the pressure field in the vicinity of the edge when the source is a large distance away. In this reciprocal problem the incident wave near the edge is very nearly planar, so the limit can be obtained from the solution of the related problem of plane waves incident on a rigid wedge. The limiting case, source near edge, listener far from edge, is of principle interest in aircraft noise problems where the source is in the vicinity of a wing but the listener is on the ground at a large distance away.

The limiting value of the diffraction integral F_ν as $rr_o/L^2 \to 0$ may be simply denoted as $F_\nu(|A|,\alpha,0)$. The limit exists and may be readily obtained from the formulation given in the previous section by (1) replacing the factor L/R in the integrand by 1 and (2) setting $\varepsilon = 0$ in Eqs. (14) and (15). This yields $\sin(b/\nu) = \tanh(a/\nu)$ and Eq. (15b) gives $K^2 = \sinh^2(a/\nu)/\cosh(a/\nu)$. The integrand $I(q)$ reduces to $e^{-\alpha K^2}$ along the contour C.

The value of the integral $F_\nu(|A|,\alpha,0)$ for $|A| = \pi/2$, or for $\alpha = 0$, or for $\alpha >> 1$ may be inferred from the cases 1-3 discussed above. Thus F_ν is 1 for $|A| = \pi/2$ or for $\alpha = 0$ and is given by Eq. (19) for $\alpha >> 1$. Also, the Fresnel number approximation, Eq. (24), should be applicable in the double limit $\alpha >> 1$ and $\cos A << \nu$, the appropriate identification for the Fresnel number N in the limit $\varepsilon \to 0$ being

$$N = 4[rr_o/(\lambda L)]\cos^2(B_\nu/2) \qquad (25)$$

As regards the behavior of $F_\nu(|A|,\alpha,0)$ for $\alpha << 1$, one can derive an expansion of the contour integral in noninteger powers of α, the starting point being

$$F_\nu(|A|,\alpha,0) = 1 - \int_0^\infty (1 - e^{-\alpha K})(dq/da)da \tag{26}$$

In view of the restriction $krr_0/L << 1$, the first factor in integrand above is small unless a is relatively large. Thus, if we seek just the leading term and anticipate that this, for sufficiently small values of the expansion parameter, is larger than any given constant times this parameter, it is sufficient to adopt the approximations $K^2 \simeq (1/2)e^{a/\nu}$, $dq/da \simeq |A|^{-1}\sin(2|A|)e^{i\nu\pi/2}\, e^{-a}$, i.e. asymptotic limits for $\varepsilon = 0$, a large. Then the variable of integration may be changed to $u = (1/2)\,\alpha e^{a/\nu}$ such that $(dq/da)da$ is a product of u-independent factors and $u^{-\nu-1}du$, one of these factors being $[\alpha/2]^\nu$. The lower limit on the u integration becomes $\alpha/2$, but, providing ν is not very close to 1 (i.e., we here exclude the case of highly obtuse wedges), this can be approximated by 0 insofar as we are only interested here in the lowest order (which is lower than first order) term in α. In this manner, one obtains

$$F_\nu(|A|,\alpha,0) \simeq 1 - |A|^{-1}\sin(2|A|)e^{-i\nu\pi/2}[\alpha/2]^\nu\Gamma(1-\nu) \tag{27}$$

Here we recognize (after integration by parts) that the integral over u of $\nu(1-e^{-u})u^{-\nu-1}$ is the gamma function with argument $1-\nu$.

The fact that ν is less than 1 implies that the magnitude of F_ν decreases sharply from 1 (the derivative of its magnitude with respect to the expansion parameter is negative and becomes singular when the parameter approaches zero) when α increases from zero. As discussed subsequently below, this implies that a modest amount of sound reduction in the shadow zone is achieved even when the source is only a slight distance from the edge.

In this same limit of $rr_o/L^2 \to 0$, $krr_o/L \ll 1$, the total Green's function (found by inserting the above into Eq. 1) becomes

$$G(\underset{\sim}{x}|\underset{\sim}{x}_o) = (2\pi/\beta)L^{-1}e^{ikL}\,\{1 + 2e^{-i\nu\pi/2}[1/\Gamma(1+\nu)][krr_o/(2L)]^\nu \cos(\nu\theta)\cos(\nu\theta_o)\} \tag{28}$$

where we make use of the identity

$$\sin(\nu\pi)\Gamma(1-\nu) = \nu\pi/\Gamma(1+\nu)$$

The above approximate Green's function is consistent with a more general expansion given by Tuzhilin.[8] One may note that, if the listener is in the shadow zone, $\cos(\nu\theta)$ and $\cos(\nu\theta_o)$ have opposite signs, so the second term in Eq. (28) would decrease the magnitude of the Green's function in such cases (as should be expected) from that represented by just the first term. The phase of the Green's function is predicted to be greater than kL. (The formulation in general requires the phase in the shadow zone to lie between kL and kL + $\pi/4$.)

6. The case of a thin screen ($\nu = 1/2$) for $\varepsilon \to 0$ with α finite. For the most part, it is conceptually simpler to consider each $V(\zeta_i)$ in Eq. (1) as being calculated individually, the sum being found subsequently. Although these occur in pairs, $V(\zeta)$ and $V(2\beta-\zeta)$, there appears in general to be no major analytical simplification obtained by considering such a pair as a unit. An important exception is the case of the thin screen ($\nu = 1/2$). The fact that some simplification should be possible in this limit should be evident from the fact that the geometry of source, images, and image-image in this limit is degenerate: the source and image-image coincide and the locations of the two images coincide. The analytical simplification is of minor computational advantage except in the limit $\varepsilon \to 0$. The simplification which results in this limit (which, as pointed out above, is equivalent to the problem of diffraction of plane waves by a thin screen) is that the Green's function and each of its two constituent pairs, $V(\zeta_1) + V(2\beta-\zeta_1)$ and $V(\zeta_3) + V(2\beta-\zeta_3)$, can be expressed rather simply in terms of Fresnel integrals. (Given the incident plane wave interpretation of this limit, this is a well known result.)

The manner in which the result may be obtained from the formulation presented here is first to change the integration over q to one over a. Then the sum $V(\zeta) + V(2\beta-\zeta)$, with $V(\zeta)$ as given by Eqs. (10-12), with the q integration along the contour

C, may be grouped as a single integral over a from 0 to ∞ which involves a factor

$$A(\zeta)\ dq(|A\ \zeta)|,a)/da + A(2\beta-\zeta)\ dq(|A\ 2\beta-\zeta)|,a)/da$$

One should note that q, considered as a function of A and a, will in general have different values if $|A|$ is taken as $|A(\zeta)|$ or $|A(2\beta-\zeta)|$. Evaluating this expression for $\nu = 1/2$, $\beta = 2\pi$, $\varepsilon = 0$, such that $\sin[2|A(\zeta)|] = |\cos(\zeta/2)|$, $\cos[2|A(\zeta)|] = -\sin(\zeta/2)$, $\tan b = \tanh a$, $K^2 = \sinh(2a)\tanh(2a)$, etc., it eventuates, after some lengthy algebra and application of various trigonometric identities, that this can be expressed rather simply as a function of K and $\cos(\zeta/2)$ times the derivative dK /da with no explicit dependence on a. Consequently, the variable of integration can readily be changed to $u = \alpha^{1/2}K$. Once this is done, the integral appears in the form of a constant times the diffraction integral $A_D(X)$ of Eq. (17) with the appropriate identification for X being

$$X = [4\alpha/\pi]^{1/2}|\cos(\zeta/2)| \tag{29}$$

In this manner, we obtain

$$\begin{aligned} &A(\zeta)F_{1/2}(|A(\zeta)|,\alpha,0) + A(2\beta-\zeta)F_{1/2}(|A(2\beta-\zeta)|,\alpha,0) \\ &= \mathrm{sign}\{\cos(\zeta/2)\}(\pi/2^{1/2})e^{i\pi/4}[f(X)-i\ g(X)] \end{aligned} \tag{30}$$

with X as given above. The corresponding expression for

$V(\zeta) + V(2\beta-\zeta)$ is just $-(1/\pi)L^{-1}e^{ikL}$ times Eq. (30). The total Green's function may then easily be written down from Eq. (1). In the case where the listener is in the shadow zone (diffracted field only), $\cos(\zeta/2)$ is negative both for $\zeta = |\theta-\theta_o|$ and for $\zeta = \theta+\theta_o$, so the field is

$$G(x|x_o) = 2^{-\frac{1}{2}}L^{-1}e^{ikL}e^{i\pi/4}\ \{[f(X) - i\ g(X)]_{\zeta\ =\ |\theta-\theta_o|} + [f(X) - i\ g(X)]_{\zeta\ =\ \theta+\theta_o}\} \tag{31}$$

in which the indicated values of ζ are to be used in Eq. (29) to compute the variable X.

V. NUMERICAL INTEGRATION SCHEME

We return now to the general problem of determining the integral F_ν. The integral over $I(q)$ along the curve C can be symbolically written

$$F_\nu = \int_C I(K,\varepsilon,\alpha)dq \tag{32}$$

where

$$I(K,\varepsilon,\alpha) = (1 + i\varepsilon K^2)^{-1}\ e^{-\alpha K^2} \tag{33}$$

The quantity K is that given implicitly by Eqs. (15) and may be considered a monotonically increasing real function of distance along the contour C.

The prototype integration scheme suggested is one in which: (1) the variable of integration is first changed to K; (2) the domain of K integration is broken into N + 1 intervals $(0, K_1)$, (K_1, K_2), ..., (K_N, ∞) where $N \geq 1$; (generally one takes $N = 1$) and (3) the integration over the first N intervals is transformed through an "integration by parts". Thus one has

$$F_\nu = \sum_{n=1}^{N} \int_{K_{n-1}}^{K_n} J(K, \varepsilon, \alpha, |A|)\, dK \tag{34}$$

$$+ I(K_N, \varepsilon, \alpha)\, q(K_N, \varepsilon) + \int_{K_N}^{\infty} (I)(dq/dK)dK$$

where

$$J(K) = -2\, I'(K)\, q(K)K$$

We also use the fact that $q(K) = 0$ if $K = 0$.

One may note that the real and imaginary parts of the function J(K) are bounded and continuously differentiable and that these component parts are certainly not oscillatory. Thus, one may expect that the first N integrals of the above will be amenable to any numerical integration scheme which, while utilizing values of the integrand at only a relatively limited number of points (less than, say, 10), achieves a high accuracy because of the "smoothness" of the integrand. Possible integration formulas (Chebyshev's equal weight, Gauss's, or Lobatto's, for example) are summarized in particular in Sec. 254 of the Handbook of Mathematical Functions[14]. (Our experience has been, in the present context, that 10 point Lobatto integration invariably gives at least eight digit accuracy.)

As regards the integral from K_N to ∞, the qualitity $|I(K_N)||1-q(K_N)|$ may for most practical purposes be considered as an upper bound to its magnitude. It may be presumed that one has chosen K_N sufficiently large, either that the magnitude of the integral is definitely negligible within the desired computational accuracy or else that the $e^{-\alpha K^2}$ factor in the integrand dominates its decay. In the former case the last term is discarded while in the latter case it is evaluated by (1) integrating by parts and (2) performing the integration over the resulting expression, which has the form (representing the sum of the last two terms in Eq. (34).

$$\int_{K_N}^{\infty} e^{-\alpha K^2} L(K)\, dK$$

(with an obvious identification for L(K)) by Hermite integration.[14] (Our experience is that an 8 point scheme is more than adequate).

The choice for the $K_1, \ldots, K_N$ as well as the parameter N should not be too critical. One could compare answers obtained with different choices of these parameters in order to assess whether or not some desired accuracy has been obtained. One could, for example, simply take N = 1 and $K_N = 1/\alpha$, unless α were extremely small compared to unity. (We have at present a somewhat elaborate scheme for chosing these parameters, but the details seem too arbitrary and unimportant to warrant their inclusion here.)

Computation time for a single value of F_ν may be considered as roughly directly proportional to the number of times which the function q(K) must be computed from Eq. (15) (which is a straight-forward evaluation requiring trigonometric and inverse trigonometric functions). This number is typically just 18 with the scheme as outlined above so the computation time should be of minor consequence, given the availability of a modern high speed digital computer.

Some sample calculations are presented in Figs. 6 and 7.

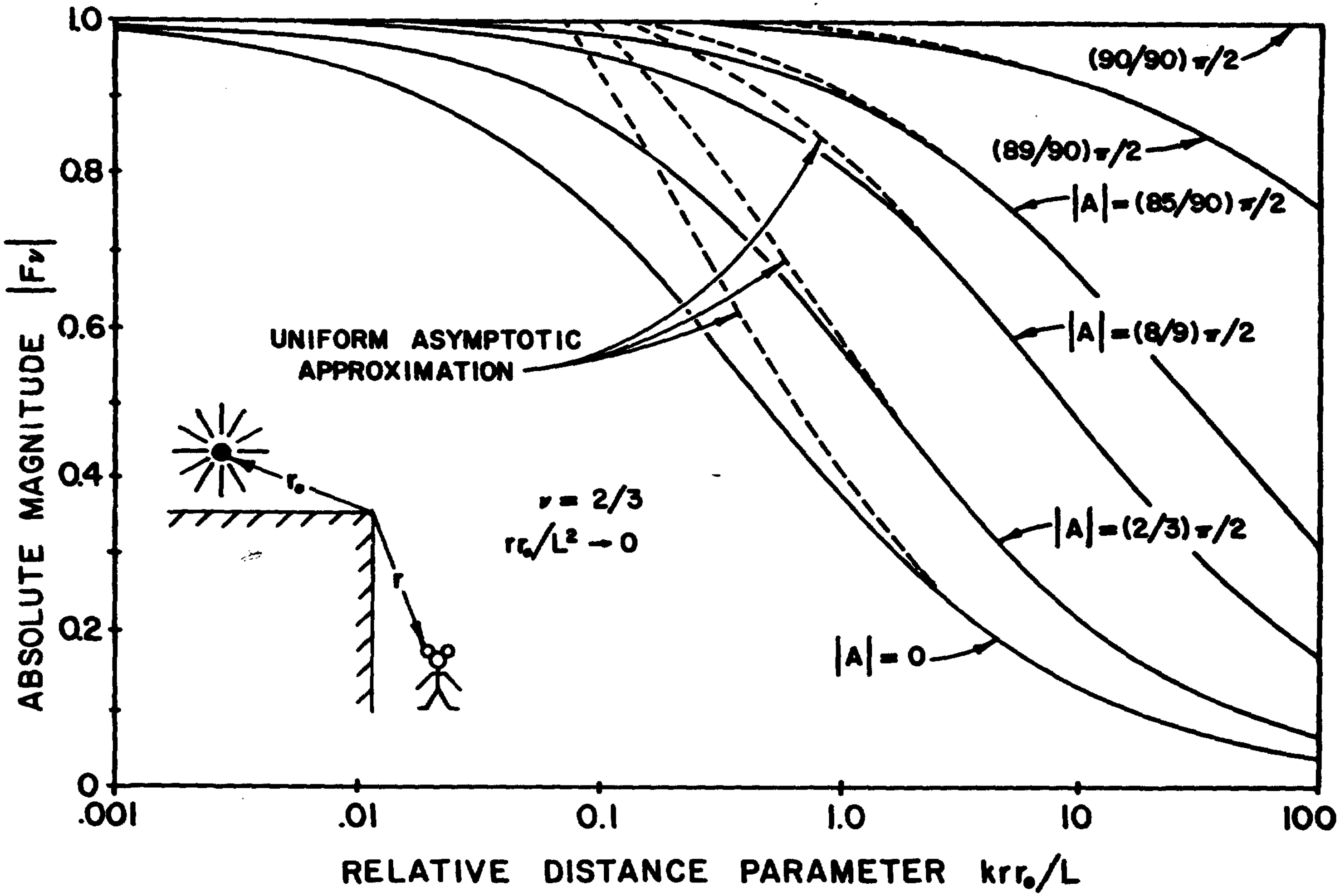

Fig. 6. Magnitude of diffraction function F_ν vs. relative distance parameter krr_o/L for the case $\nu = 2/3$ and for the limit $rr_o/L^2 \to 0$. The curves are shown for several values of the angular factor A. The results indicate that the uniform asymptotic approximation described in the text is valid for $krr_o/L > 1$.

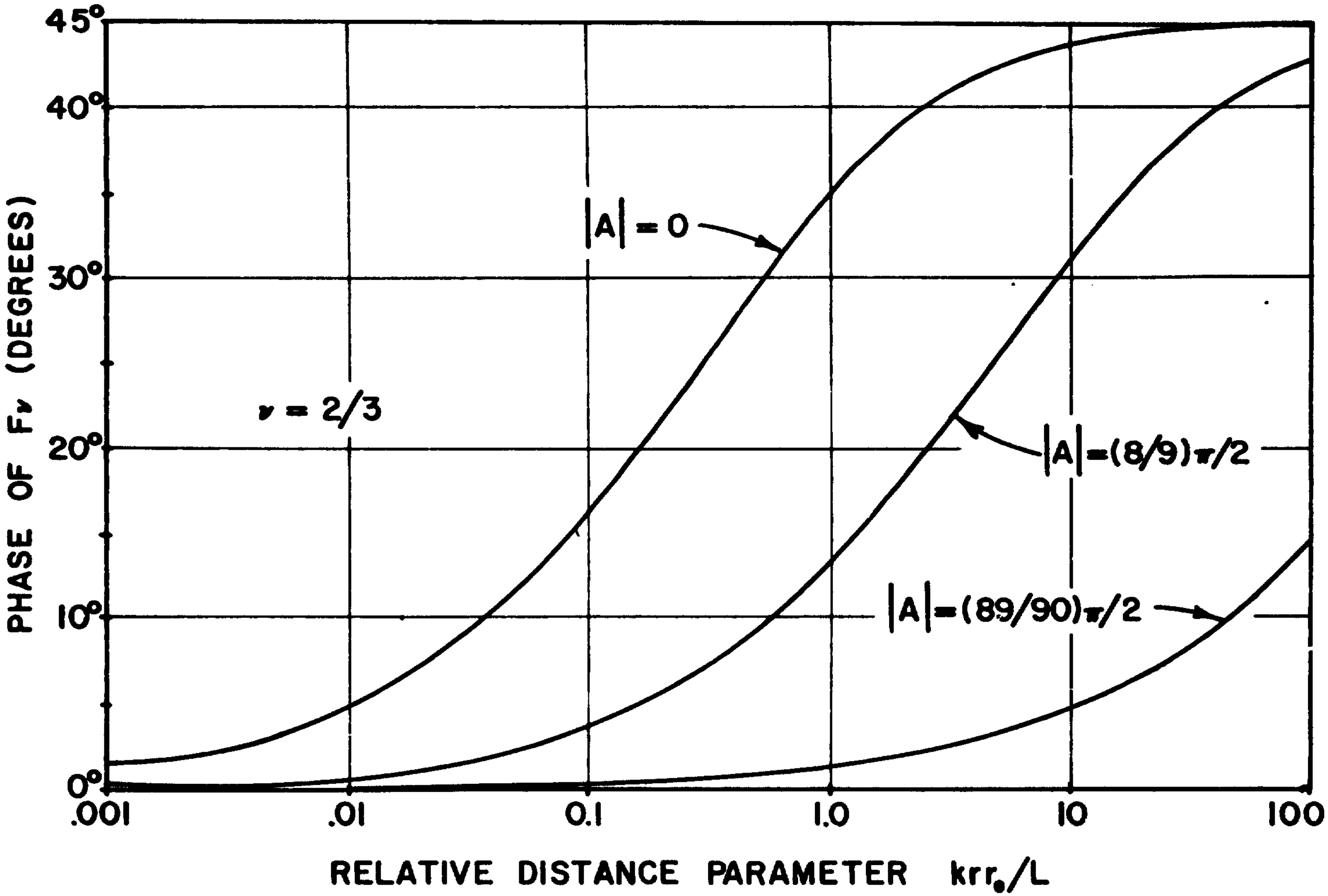

Fig. 7. Phase of the diffraction function F_ν vs. relative distance parameter krr_o/L for the case $\nu = 2/3$ and for the limit $rr_o/L^2 \to 0$, for various values of A. The figure indicates that the $A = 0$ curve is a good approximation except for $A = \pi/2$.

REFERENCES

1. An extensive bibliography of relevant earlier literature (including contributions by Poincare, Sommerfeld, and MacDonald) is given by H. G. Garnir, Bulletin de la Sociéte Royale des Sciences de Liège, 21, 207-231 (1952).

2. The standard "handbook" article for this subject is J. J. Bowman and T. B. A. Senior, "The Wedge," Chap. 6 in Electromagnetic and Acoustic Scattering by Simple Shapes, edited by J. J. Bowman, T. B. A. Senior, and P. L. E. Uslenghi [North-Holland, Amsterdam, 1969], pp. 252-283.

3. T. J. I'A. Bromwich, "Diffraction of Waves by a Wedge," Proc. Lond. Math. Soc. 14, 450-463 (1915).

4. H. S. Carslaw, "Diffraction of Waves by a Wedge of any Angle," Proc. Lond, Math. Soc. 18, 291-306 (1920).

5. F. J. W. Whipple, "Diffraction by a Wedge and Kindred Problems." Proc. Lond. Math. Soc. 16, 94-111 (1918) (See esp. p. 103).

6. F. Oberhettinger, "On Asymptotic Series for Functions occuring in the Theory of Diffraction of Waves by Wedges," J. Math. Phys. 34, 245-255 (1956). Journal of Mathematics and Physics (Cambridge, Mass.).

7. A. D. Pierce, "Diffraction of Sound around Corners and over Wide Barriers," J. Acoust. Soc. Amer. 55, 941-955 (1974).

8. A. A. Tuzhilin, "New Representation of Diffraction Fields in Wedge-Shaped Regions with Ideal Boundaries," Soviet Physics-Acoutics 9, No.2, 168-172 (1963).

9. P. Ambaud and A. Bergassoli, "Le problème du dièdre en acoustique" (The Problem of the Wedge in Acoustics), Acustica 27, 291-298 (1972).

10. The result is compatible with Rayleigh's conclusion (Sec. 280 in Theory of Sound) that mean square power radiated by a source with given volume velocity amplitude at a vertex of a cone should be inversely proportional to the solid angle of the cone, such that the pressure amplitude at given radial distance r is inversely proportional to the product of the cone's solid angle and r. That Rayleigh's analysis applies to the case of a source on a wedge's edge was pointed out by R. V. Waterhouse, "Diffraction Effects in a Random Sound Field," J. Acoust. Soc. Amer. 35, 1610-1620 (1963).

11. W. Gautschi, "Error Function and Fresnel Integrals," in Handbook of Mathematical Functions, edited by M. Abramowitz and I. A. Stegun (Dover, New York, 1965), pp. 295-329.

12. The term "Fresnel number" in the present paper is used in the same sense as in Z-i. Maekawa "Noise Reduction by Screens," Paper F13 in 5e Congrès International d'Acoustique, Vol. 1a, edited by D. E. Commins (Georges Thone, Liege, 1965). The result derived in the present paper is analogous to what Maekawa derives from the "Kirchhoff theory."

13. See, for example, M. Born and E. Wolf, Principles of Optics (Pergamon Press, Oxford, 4th Ed., 1970) pp. 568-569. The result is due to A. Sommerfield, Math. Ann. 47, 317-374 (1896).

14. P. J. Davis and I. Polonsky, "Numerical Interpolation, Differentiation, and Integration," in Handbook of Mathematical Functions, loc. cit., pp. 875-924. See esp. pp. 886-888, 890, 920, 924.

Chapter 4

SCATTERING OF SPHERICAL WAVES BY RECTANGULAR PATCHES

The body of this chapter consists of a copy of a paper prepared for submission to the *Journal of Sound and Vibration* by W. James Hadden, Jr., Robin A. Vidimos and Philip M. Sencil. [The experiments described in the paper were performed in an anechoic chamber at NASA Langley Research Center (Fig. i).]

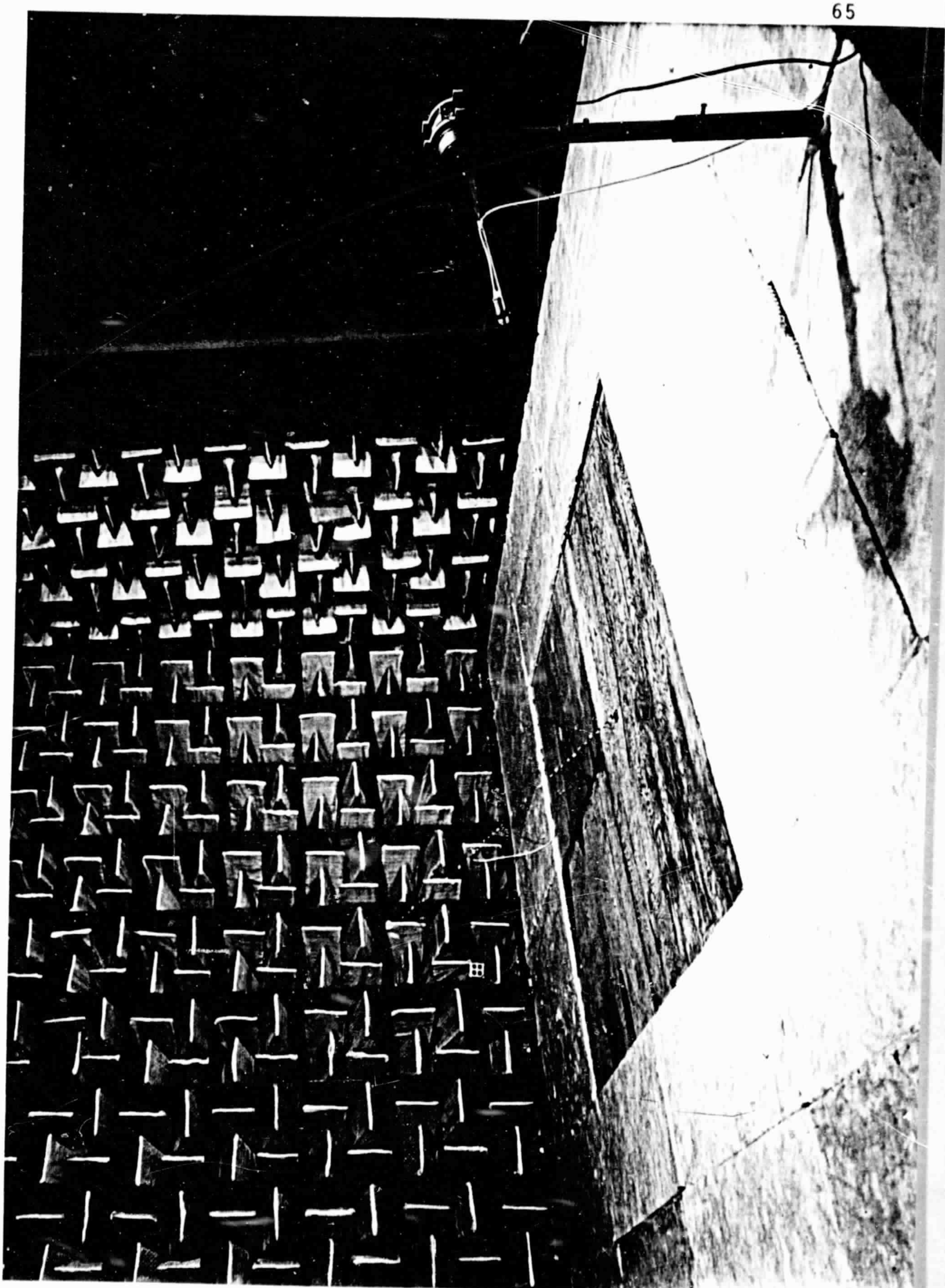

Fig. i. Photograph of experimental arrangement for scattering by patches.

Abstract

A theory is presented for the scattering of spherical waves by a rectangular area whose acoustic impedance differs from that of the surrounding plane. This theory extends previous analyses to include diffraction effects explicitly. Results of experiments concerning reflection from rectangular patches are also reported. Agreement between these results and predicted values is not uniformly good, although improvements could be achieved through alterations in the measurement procedure.

INTRODUCTION

The present paper is motivated by an interest in the effects of acoustical characteristics of the ground on sound originating in low-flying aircraft. As part of this study, analytical and laboratory investigations have been performed on the reflection of sound by plane surfaces of known acoustic impedance [1]. In analyses of the reflection of spherical waves by a plane surface on which a local-reaction impedance boundary condition is imposed, it is customary to employ the method of steepest descents in order to obtain an approximation for the reflected pressure [2,3]. The use of this approximation can be interpreted in terms of geometrical acoustics as neglecting the effect of waves scattered from regions of the surface outside a neighborhood of the shortest reflected ray path from the source to the receiver. The investigation with which the present paper is concerned sought to determine the size of the effective area near the vertex of the reflected ray. This information could be used in developing a simplified technique for predicting the received sound for moving sources near the surface.

In the interest of simplicity, experimental measurements were made in an anechoic chamber of sound pressure levels above rectangular patches of various areas. Pure tones were used to excite a small source. Sound pressure level measurements were made in the direction of the presumed reflected ray path. These experiments are described more fully in Section IV. In conjunction with the experimental work, a theoretical investigation of scattering by rectangular areas was undertaken in which diffraction effects due to the finite size of patches were included. This analysis is discussed in Sections I-III.

I. THEORETICAL EXPOSITION

The analytical development is roughly parallel to that of Morse and Ingard for plane wave incidence [4]. The surface $z = 0$ contains a rectangular patch with point impedance $\rho c \eta_A$; outside the patch the normalized impedance is taken as η. The geometry is illustrated in Figure 1: A point source is located at (r_s, θ_s, ϕ_s); the receiver coordinates are (r, θ, ϕ).

The received pressure may be expressed, employing Green's theorem, as

$$p(\underset{\sim}{r}) = p_o G(\underset{\sim}{r}|\underset{\sim}{r_s}) - \iint_S dS_o \Big[G(\underset{\sim}{r}|\underset{\sim}{r_o}) \frac{\partial p}{\partial z_o}(\underset{\sim}{r_o}) - p(\underset{\sim}{r_o}) \frac{\partial G}{\partial z_o}(\underset{\sim}{r}|\underset{\sim}{r_o}) \Big] \Bigg|_{z_o = o} \tag{1}$$

in which the Green's function $G(\underset{\sim}{r}|\underset{\sim}{r_o})$ is approximated by terms representing a source point $\underset{\sim}{r_o} = (r_o, \theta_o, \phi_o)$ and a single image point $\underset{\sim}{r_o'} = (r_o, \pi - \theta_o, \phi_o)$ with the image source strength (a modified plane-wave reflection coefficient) chosen such that the condition

$$G(\underset{\sim}{r}, \underset{\sim}{r_o}) - \frac{i\eta}{k} \frac{\partial G(\underset{\sim}{r}|\underset{\sim}{r_o})}{\partial z} = 0 \quad , \quad z = 0 \tag{2}$$

is satisfied to a better degree of approximation than could be obtained by using the plane-wave reflection coefficient. The approximation to the Green's function is

$$G(\underset{\sim}{r}|\underset{\sim}{r_o}) \simeq \frac{e^{ik|\underset{\sim}{r} - \underset{\sim}{r_o}|}}{4\pi|\underset{\sim}{r} - \underset{\sim}{r_o}|} + R' \frac{e^{ik|\underset{\sim}{r} - \underset{\sim}{r_o'}|}}{4\pi|\underset{\sim}{r} - \underset{\sim}{r_o'}|} \tag{3a}$$

$$R' = \frac{\eta\, B' \cos\theta_o' - 1}{\eta\, B' \cos\theta_o' + 1} \tag{3b}$$

$$B' = 1 + \frac{i}{k|\underset{\sim}{r} - \underset{\sim}{r_o}|} \tag{3c}$$

where θ_o' is the azimuthal angle between the source-to-receiver point line and a line parallel to the z axis, and the inclusion of the factor B' represents an attempt to account for the curvature of the wavefront.

The pressure terms in the integrand of equation (1) are approximated in a similar fashion as a combination of waves incident from a point source at $\underset{\sim}{r_s}$ and an image source at $\underset{\sim}{r_s'}$ below a plane characterized by the normalized impedance η_A. The appropriate form for this approximation for the pressure may be inferred readily from equations (3) with suitable modifications of parameters. Thus the "direct" pressure term in equation (1) is taken as

$$p_{Dir}(\underset{\sim}{r}) \approx p_o\left(\frac{e^{ik|\underset{\sim}{r} - \underset{\sim}{r_s}|}}{|\underset{\sim}{r} - \underset{\sim}{r_s}|} + R_s \frac{e^{ik|\underset{\sim}{r} - \underset{\sim}{r_s'}|}}{|\underset{\sim}{r} - \underset{\sim}{r_s'}|}\right) \tag{4}$$

in which R_s has the form of equation (3b) with $B' \to B_s = 1 + i/kr_s$ and $\theta_o' \to \theta_s = \cos^{-1}(z_s/r_s)$. The scattered pressure term may be written as

$$p_{sc}(\underset{\sim}{r}) \approx \frac{ikp_o}{\pi}\iint\limits_S dS_o \frac{e^{ik(|\underset{\sim}{r} - \underset{\sim}{r_o}| + |\underset{\sim}{r_o} - \underset{\sim}{r_s}|)}}{|\underset{\sim}{r} - \underset{\sim}{r_o}||\underset{\sim}{r_o} - \underset{\sim}{r_s}|}$$

$$\times \frac{B' B_s' \cos\theta' \cos\theta_s' (\eta - \eta_A)}{(1 + \eta B' \cos\theta')(1 + \eta_A B_s' \cos\theta_s')} \tag{5}$$

In order to obtain a closed-form expression for the pressure at some distance from the scattering area it is expedient to expand the factors in equation (5) which involve the distances $|\underset{\sim}{r} - \underset{\sim}{r_o}|$ and $|\underset{\sim}{r_o} - \underset{\sim}{r_s}|$ as power series in x_o and y_o. The expansions of such factors multiplying the exponential in equation (5) may be truncated so as to yield a desired accuracy which depends on ratios such as L/r and W/r. However, in the exponent the criterion governing truncation of the expansion involves the Fresnel wave parameters, which have the form r/kL^2.

Retaining second-order terms in x_o, y_o in the exponent in equation (5) yields approximations for the scattered pressure in which diffraction effects are readily discernible. In addition, this treatment allows one to investigate the transition from the Fraunhofer diffraction regime (large Fresnel parameter - equivalent to the Morse-Ingard treatment [4]) to the Fresnel diffraction (small Fresnel parameter) range and beyond to the ray theory limit. An outline of the present expansion of equation (5) is given in Appendix A. The scattered pressure is approximated by

$$p_{sc}(\underset{\sim}{r}) \approx \frac{kLW\, e^{ik(r + r_s)}}{4\pi r r_s} P_{sc}\, I(\alpha_1, \alpha_2, \beta_1, \beta_2, \gamma) \qquad (6)$$

with the abbreviations

$$P_{sc} = ip_o \frac{B\, B_s \cos\theta \cos\theta_s}{(1 + \eta B \cos\theta)(1 + \eta_A B_s \cos\theta_s)} \qquad (7)$$

and

$$I = \int_{-1}^{1} dX\, e^{-i(\alpha_1 X - \beta_1 X^2)} \int_{-1}^{1} dY\, e^{-i[(\alpha_2 + \gamma X)Y - \beta_2 Y^2]}$$

$$X(1 + MX + NY + QX^2 + RY^2 + SXY)(\eta - \eta_A) \qquad (8)$$

and, finally

$$\alpha_{\substack{1\\2}} = \left(\sin\theta \begin{smallmatrix}\cos\\ \sin\end{smallmatrix}\,\phi + \sin\theta_s \begin{smallmatrix}\cos\\ \sin\end{smallmatrix}\,\phi_s\right)\frac{k}{2}\begin{pmatrix}L\\ W\end{pmatrix} \tag{9a}$$

$$\begin{aligned}\beta_{\substack{1\\2}} = {} & \Big[r_s\Big(1 - \sin^2\theta \begin{smallmatrix}\cos^2\\ \sin^2\end{smallmatrix}\,\phi\Big) \\ & + r\Big(1 - \sin^2\theta_s \begin{smallmatrix}\cos^2\\ \sin^2\end{smallmatrix}\,\phi_s\Big)\Big]\frac{k}{8rr_s}\begin{pmatrix}L^2\\ W^2\end{pmatrix}\end{aligned} \tag{9b}$$

$$\gamma = \left(r_s \sin^2\theta \sin 2\phi + r \sin^2\theta_s \sin 2\phi_s\right)\frac{kLW}{8rr_s} \tag{9c}$$

The parameters α_1 and α_2 involve projections of the scattering area's dimensions (normalized by wavelength) on the lines from source and receiver for the center of the area. The parameters β_1, β_2 and γ are similarly projected inverses of Fresnel wave parameters. These parameters characterize the diffraction effects in the approximation for the scattered pressure. The coefficients M, N, Q, R and S in equation (8), in addition to providing correction terms depending on the size of the scattering area relative to source and receiver distances from the patch, are functions of the other geometrical and impedance parameters. The coefficients M and N are linearly dependent on quantities such as $\sin\theta$, $\sin\phi$ and L/r or W/r. Q, R and S are quadratic in these quantities. Explicit expression for these coefficients are given in Appendix A.

II. PATCH WITH CONSTANT IMPEDANCE

For cases in which the impedance of the scattering area is constant, the integrals in equation (8) could be evaluated by completion of squares in the exponents followed by application of standard integration formula, but for one complication - the inner integral (e.g., the integration with respect to Y in equation (8) results in several terms involving Fresnel integrals [5] whose arguments have the form, in this case,

$$\beta_2^{1/2}\left(\frac{\alpha_2 + \gamma X}{2\beta_2} \pm 1\right) \qquad (10)$$

The presence of the second integration variable precludes exact analytical evaluation of the remaining integration. However, reference to equations (9) indicates that the X-dependent and unity terms in the arguments are of order (L/r) compared to the α_2 terms. In addition it can be seen that both α_2 and γ vanish in the important case of specular reflection ($\theta = \theta_s$, $\phi = 0$, $\phi_s = \pi$). For these reasons, and in view of the behavior of the Fresnel integrals in the small- and large-argument limits [5], it seems a reasonable approximation to neglect the X-dependent terms but to retain the unity terms in the arguments exemplified by equation (10).

If this approximation is accepted and the resulting expression simplified by neglecting terms which are of order $(kr)^{-1}$, (L^2/r^2) or smaller, the integral in equation (8) may be approximated as

$$I \simeq \frac{\pi}{2(\beta_1\beta_2)^{1/2}} \left\{ \mu^{-1/2} e^{-i\Phi_1} \Delta F(\beta_2, \alpha_2/2\beta_2) \left[A_1 \Delta F(\mu\beta_1, \nu\alpha_1/2\mu\beta_1) \right.\right.$$

$$\left. + \frac{i\,B_1}{(2\pi\mu\beta_1)^{1/2}} \left(e^{i\Phi_{2+}} - e^{i\Phi_{2-}} \right) \right]$$

$$- \frac{iB_2\, e^{i\beta_2}}{(2\pi\beta_2)^{1/2}} \left[e^{-i\Phi_{3+}} \Delta F\left(\beta_1, \frac{\alpha_1 + \gamma}{2\beta_1}\right) \right.$$

$$\left.\left. - e^{-i\Phi_{3-}} \Delta F\left(\beta_1, \frac{\alpha_1 + \gamma}{2\beta_1}\right) \right] \right\} \qquad (11)$$

with

$$\mu = 1 - \gamma^2/4\beta_1\beta_2 \quad , \quad \nu = 1 + \alpha_2\gamma/2\alpha_1\beta_2 \qquad (12a)$$

$$\Phi_1 = \frac{(\nu\alpha_1)^2}{4\mu\beta_1} + \frac{\alpha_2^2}{4\beta_2} \qquad (12b)$$

$$\Phi_{2\pm} = \mu\beta_1 \left(\frac{\nu\alpha_1}{2\mu\beta_1} \pm 1 \right)^2 \qquad (12c)$$

$$\Phi_{3\pm} = \frac{(\alpha_1 \pm \gamma)^2}{4\beta_1} \pm \alpha_2 \tag{12d}$$

and

$$\Delta F(a,b) = F_f[a^{1/2}(b+1)] - F_f[a^{1/2}(b-1)] \tag{13}$$

in which we have employed the abbreviation $F_f(x) = C(x) + iS(x)$, C and S being the well-known Fresnel integrals [5]. The coefficients of the several terms in equation (11) are

$$B_2 = N + \frac{R\alpha_2}{2\beta_2} + \left(S + \frac{R\gamma}{2\beta_2}\right)\frac{\alpha_1}{2\beta_1} \tag{14a}$$

$$B_1 = M + \frac{N\gamma + S\alpha_2}{2\beta_2} + \frac{R\gamma\alpha_2}{2\beta_2^2} \tag{14b}$$

$$A_1 = 1 + \frac{N\alpha_2}{2\beta_2} + \frac{R\alpha_2^2}{4\beta_2^2} + \frac{\nu\alpha_1}{2\mu\beta_1} B_1$$

$$+ \left(Q + \frac{S\gamma}{2\beta_2} + \frac{R\gamma^2}{4\beta_2^2}\right)\left(\frac{\nu\alpha_1}{2\mu\beta_1}\right)^2 \tag{14c}$$

A_1 contains terms of order unity. The terms in equation (11) which involve B_1 and B_2 are of order $(kr)^{-1/2}$. General expressions for M, N, Q, R and S are given in equations (A8).

One may check that equation (11) reduces to an extension of the result reported by Morse and Ingard [4] by noting that in the limit as β_1, ρ_2 and γ become very small the function $\Delta F(a,b)$ [equation (13)], with arguments such as those in equation (11), may be approximated [6] as

$$\Delta F(a,b) \approx \left(\frac{2}{\pi a}\right)^{1/2} b^{-1} e^{iab^2} \sin(2ab) \qquad (15)$$

Upon substituting this expression in equation (11), the first term reduces to a form similar to equation (8.3.5) of reference 4. The second term in equation (11) vanishes in this limit, while the third term is of order $(\beta^{1/2})$ and hence negligible.

III. TWO LIMITING CASES

Although considerable simplification in the above expressions for the scattered pressure may be achieved in several interesting special geometrical configurations - forward scattering ($\varphi = \phi_s - \pi$) and specular reflection ($\phi = \phi_s - \pi$ and $\theta = \theta_s$) - only two special or limiting cases will be considered in detail here for brevity. The first, which is relevant to the experiments reported in Section IV, concerns reflection in the special case in which the source and receiver are in the plane bisecting perpendicularly the scattering area, i.e., $\phi_s = \pi$. [The case in which the source and receiver are in a plane parallel to the x - z plane of Figure 1 can be treated by an obvious modification of the limits of integration in equation (8).] The second case for which a compact expression for the scattered pressure can be obtained concerns scattering by a strip (taken here as lying along the y-axis of Figure 1).

An explicit expression for the scattered pressure can be readily obtained in the special case of specular reflection with $\phi_s = \pi$:

$$p_{spec} \doteq ip_o \frac{e^{ik(r+r_s)}}{(r+r_s)} \frac{B\, B_s \cos\theta_s\, (\eta-\eta_A)}{(1+\eta B \cos\theta_s)(1+\eta_A B_s \cos\theta_s)}$$

$$\times\; 4F_f(\beta_1^{1/2})F_f(\beta_2^{1/2}) \tag{16}$$

where the factors B and B_s are defined after equation (4). In this case the parameters β_1 and β_2 become

$$\beta_{\substack{1\\2}} = \frac{k(r + r_s)}{8rr_s} \begin{Bmatrix} L^2 \cos^2\theta_s \\ W^2 \end{Bmatrix} \tag{17}$$

The reduction of equation (16) to the form obtained by Leizer [7] for a rigid rectangle is readily apparent if one takes the limit of equation (16) as the normalized impedance η_A becomes very large.

An expression for the scattering by a strip of width L may be obtained from equations (11)-(14) by considering the limit as α_2, β_2, and γ become very large. It is also convenient to take advantage of the y-translational invariance of the geometry by setting $\phi_s = \pi$. In the case of scattering in the specular plane, the scattered pressure term reduces to

$$p_{spec,strip} \doteq \frac{e^{i[k(r+r_s)+1/4\pi]}}{2rr_s(\beta_1\beta_2^1)^{1/2}} \, kL \, P_{sc}\left(e^{-i\phi_1} \, \Delta F\left(\beta_1, \frac{\alpha_1}{2\beta_1}\right)\right.$$

$$\times \left[1 + \frac{\alpha_1}{2\beta_1}\left(M + \frac{\alpha_1}{2\beta_1}Q\right) + \frac{iQ}{2\beta_1}\right] + \frac{i}{(2\pi\beta_1)^{1/2}}\left\{e^{i\phi_{2+}}\left[M + Q\left(\frac{\alpha_1}{2\beta_1} - 1\right)\right]\right.$$

$$\left.\left. - e^{i\phi_{2-}}\left[M + Q\left(\frac{\alpha_1}{2\beta_1} + 1\right)\right]\right\}\right) \tag{18}$$

in which the parameter β_2 of equation (9b) has been modified to

$$\beta_2^1 = \frac{k}{2rr_s}(r + r_s) \tag{19}$$

to produce a form consistent with the direct computation from equation (A4) et seq. with the y_o-limits set to infinity. The coefficients M and Q in this case are:

$$M = \left[\frac{L}{2r}\,\frac{(2 + \eta B\cos\theta)\sin\theta}{(1 + \eta B\cos\theta)}\right] + \left[\text{same}\right]_s \tag{20a}$$

$$Q = \frac{L^2}{4r^2}\left[\frac{\sin^2\theta}{(1+\eta\ B\cos\theta)^2} - 1/2\ \frac{(2+\eta\ B\cos\theta)(1-3\sin^2\theta)}{(1+\eta\ B\cos\theta)}\right]$$

$$+ \frac{L^2}{4r_s^2}\,[\text{same}]_s + \frac{L^2 \sin\theta \sin\theta_s}{rr_s(1+\eta\ B\cos\theta)(1+\eta_A\ B_s\cos\theta_s)}$$

$$[2+\eta B\cos\theta+\eta_A B_s\cos\theta_s+1/2\eta\eta_A BB_s\cos\theta\cos\theta_s]$$

For $\theta = \theta_s$ (specular reflection), equation (18) reduces to

$$p_{refl,strip} \approx \frac{e^{i[k(r+r_s)\ +\ 1/4\pi]}}{(r+r_s)\cos\theta_s}\, 2\, P_{sc}\, F_f(\beta_1^{1/2}) \qquad (21)$$

with β_1 given by equation (17).

IV. EXPERIMENTS ON REFLECTION

In the experimental phase of this investigation, measurements of sound pressure level were made in the specular reflection direction above rectangular scattering areas composed, in one instance, from 4' x 8' (1.22m x 2.44m) sheets of 3/4-inch (0.019 m) plywood laid on the floor of the Anechoic Noise Facility at the NASA Langley Research Center; in a second set of measurements the plywood was overlaid with one-inch (0.025 m) glass-fiber panels. In each case, pure tones were projected from a source small compared with the acoustic wavelength. The source and receiver (a 1/2-inch microphone) were arranged so that the specular plane bisected the scattering area. Incidence angles of 70° and 80° were used. Normal impedances of samples of the plywood and glass-fiber plus plywood were obtained from impedance tube measurements.

The measured impedances were employed in computations based on equation (16); the "background" specific impedance was assumed as unity. The measured impedances for two selected frequencies are presented in Table I. Comparisons of the experimentally obtained sound pressure levels with those computed from equations (1), (3) and (16) are presented in Tables II-IX. Because the primary interest in this study was the variation of the reflected sound with size of the scattering area, all measurements have been normalized to the experimental result for the largest rectangle.

As may be seen from Tables II-IX, the agreement between experimental and theoretical results is by no means uniformly good. Two possible causes of the discrepancies are suggested: First, the assumption that the impedance of the grill-work floor which surrounded the scattering areas can be taken as that of air is suspect. Second, there is the possibility of a distributed-reaction effect in the measurements. The former question could be resolved by further measurements of sound pressures above the bare floor of the anechoic chamber. The second possible problem could be rectified by the inclusion of a distributed impedance in the development following equations (3).

V. CONCLUSION

A theory has been presented for the scattering of sound by rectangular patches characterized by uniform (local-reaction) acoustic impedances. The theory explicitly includes diffraction effects absent from previous analyses. Comparison between this theory and a set of laboratory experiments reveals discrepancies which may be reduced by changes in the measurement procedure or in the analytical model.

ACKNOWLEDGEMENT

This work was supported by the Acoustics and Noise Reduction Division of NASA Langley Research Center under grant NSG 1047.

REFERENCES

1. W. J. Hadden, Jr., E. L. Turner, Jr., and E. D. Kindred, "Effect of Ground Impedance on Sound Propagation from a Source near the Surface," J. Acoust. Soc. Am. 57, S13 (1975).

2. U. Ingard, "On the Reflection of a Spherical Sound Wave from an Infinite Plane," J. Acoust. Soc. Am. 23, 329-333.

3. A. R. Wenzel, "Propagation of Waves along an Impedance Boundary," J. Acoust. Soc. Am. 55, 946-963 (1974).

4. P. M. Morse and U. Ingard, Theoretical Acoustics (McGraw-Hill, New York, 1968), p. 442 ff.

5. I. S. Gradshteyn and I. M. Ryzhik, Table of Integrals, Series, and Products (Academic Press, New York, 1965), pp. 930-932.

6. I. S. Gradshteyn and I. M. Ryzhik, Table of Integrals, Series, and Products (Academic Press, New York, 1965), p. 932, Eqs. 8.255 1. and 2.

7. I. G. Leizer, "Applicability of the Methods of Geometrical Acoustics for the Calculation of Sound Reflection from Plane Surfaces," Sov. Phys. Acoustics 12, 180-184 (1966).

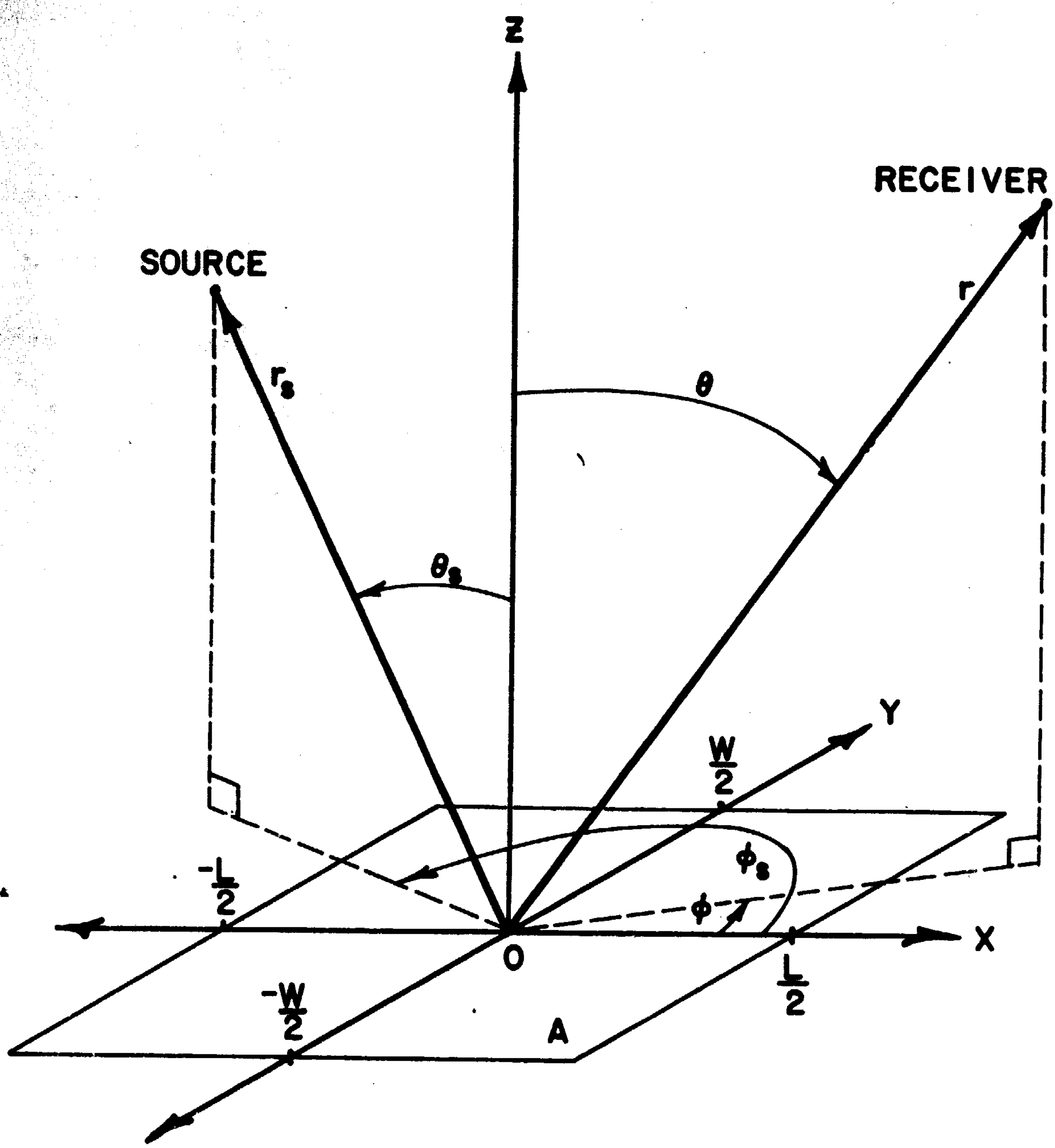

Fig. 1. Sketch of the source-patch-receiver configuration used in the analysis of scattering of sound by a rectangular patch in which the acoustic impedance differs from that in the rest of the plane including the patch.

Table I. Measured Specific Acoustic Impedances of Scattering Areas

Frequency	Plywood	Glass-Fiber over Plywood
1600 Hz	41.89 + i56.69	0.08 - i1.03
3200 Hz	2.33 + i22.62	0.10 + i0.17

Table II. Relative SPL above Rectangular Areas of Plywood with Receiver Distance 2.7 m and Incidence Angle 80°.

Scatterer Dimensions (m)	f = 1600 Hz		f = 3200 Hz	
	Theory	Experiment	Theory	Experiment
6.6 x 5.8	0 db	0 db	0 db	0 db
4.4 x 2.9	3.2	2.8	6.1	-2.8
2.9 x 2.9	1.9	2.0	2.5	-1.6
2.9 x 1.5	-0.6	3.0	3.1	-3.3
1.5 x 1.5	-2.4	3.4	-7.4	-4.3

Table III. Relative SPL above Rectangular Areas of Plywood with Receiver Distance 2.7 m and Incidence Angle 70°.

Scatterer Dimensions (m)	f = 1600 Hz		f = 3200 Hz	
	Theory	Experiment	Theory	Experiment
6.6 x 5.8	0 db	0 db	0 db	0 db
4.4 x 2.9	0	-1.0	0	0
2.9 x 2.9	0.7	-0.8	0	0
1.5 x 1.5	7.0	0.8	0.9	3.4

Table IV. Relative SPL above Rectangular Areas of Plywood with Receiver Distance 2.6 m and Incidence Angle 80°.

Scatterer Dimensions (m)	f = 1600 Hz		f = 3200 Hz	
	Theory	Experiment	Theory	Experiment
6.6 x 5.8	0 db	0 db	0 db	0 db
4.4 x 2.9	2.3	3.0	6.5	-0.5
2.9 x 1.5	-1.6	8.0	3.1	8.5
1.5 x 1.5	-3.4	3.0	-9.1	6.0

Table V. Relative SPL above Rectangular Areas of Plywood with Receiver Distance 2.4 m and Incidence Angle 80°.

Scatterer Dimensions (m)	f = 1600 Hz		f = 3200 Hz	
	Theory	Experiment	Theory	Experiment
4.4 x 2.9	0 db	0 db	0 db	0 db
2.9 x 2.9	0.6	-0.1	1.4	-7.9
2.9 x 1.5	-0.2	3.0	1.0	-10.2
1.5 x 1.5	-2.8	0.6	2.3	2.0

Table VI. Relative SPL above Rectangular Areas of Glass Fiber over Plywood with Receiver Distance 2.7 m and Incidence Angle 80°.

Scatterer Dimensions (m)	f = 1600 Hz		f = 3200 Hz	
	Theory	Experiment	Theory	Experiment
6.6 x 5.8	0 db	0 db	0 db	0 db
4.4 x 2.9	-0.3	-2.6	0.2	1.0
2.9 x 2.9	-1.4	-1.6	0.1	0
1.5 x 1.5	-2.6	0.4	0.1	-3.4

Table VII. Relative SPL above Rectangular Areas of Glass Fiber over Plywood with Receiver Distance 2.7 m and Incidence Angle 70°.

Scatterer Dimensions (m)	f = 1600 Hz		f = 3200 Hz	
	Theory	Experiment	Theory	Experiment
6.6 x 5.8	0 db	0 db	0 db	0 db
4.4 x 2.9	-0.6	-1.0	0.1	-3.0
2.9 x 2.9	0	-1.2	0.1	-4.7
1.5 x 1.5	-1.0	-2.8	-0.4	-5.4

Table VIII. Relative SPL above Rectangular Areas of Glass Fiber over Plywood with Receiver Distance 2.6 m and Incidence Angle 80°.

Scatterer Dimensions (m)	f = 1600 Hz		f = 3200 Hz	
	Theory	Experiment	Theory	Experiment
6.6 x 5.8	0 db	0 db	0 db	0 db
4.4 x 2.9	-1.1	-10.0	0.6	-13.8
2.9 x 2.9	-1.9	-2.5	0.4	-21.8
1.5 x 1.5	-0.8	-7.5	0.2	-3.4

Table IX. Relative SPL above Rectangular Areas of Glass Fiber over Plywood with Receiver Distance 2.6 m and Incidence Angle 70°.

Scatterer Dimensions (m)	f = 1600 Hz		f = 3200 Hz	
	Theory	Experiment	Theory	Experiment
6.6 x 5.8	0 db	0 db	0 db	0 db
4.4 x 2.9	-0.6	5.5	0.1	-0.9
2.9 x 2.9	-0.9	5.5	0.2	-0.8
1.5 x 1.5	-0.6	6.0	-0.4	3.0

Appendix A

Approximations for the Incident Pressure and the Green's Function

It is desired to obtain an approximation for the integrand of equation (5) in which the source and receiver distances from the center of the scattering area are used as reference quantities, correction terms being incorporated in the exponent in the integrand to include diffraction effects and in the remaining factors in the integrand to indicate additional dependences on the size of scattering region.

In order to accomplish this, it is expedient to expand the factors in equation (5) which involve the distances $|\underset{\sim}{r} - \underset{\sim}{r_o}|$ and and $|\underset{\sim}{r_o} - \underset{\sim}{r_s}|$ as power series in x_o and y_o, yielding (to second order),

$$|\underset{\sim}{r} - \underset{\sim}{r_o}| \approx r(1 - \psi/r + V/r^2) \qquad \text{(A1)}$$

$$|\underset{\sim}{r} - \underset{\sim}{r_o}|^{-1} \approx r^{-1}(1 + \psi/r - Tr^2) \qquad \text{(A2)}$$

with

$$\psi(\theta,\phi) = \sin\theta\ (x_o \cos\phi + y_o \sin\phi) \qquad \text{(A3a)}$$

$$V(\theta,\phi) = \frac{x_o^2}{2}(1 - \sin^2\theta \cos^2\phi) + \frac{y_o^2}{2}(1 - \sin^2\theta \sin^2\phi)$$

$$- \frac{1}{2} x_o y_o \sin^2\theta \sin 2\phi \qquad \text{(A3b)}$$

$$T(\theta,\phi) = \frac{x_o^2}{2}(1 - 3\sin^2\theta \cos^2\phi) + \frac{y_o^2}{2}(1 - 3\sin^2\theta \sin^2\phi)$$

$$- \frac{3}{2} x_o y_o \sin^2\theta \sin 2\phi \qquad \text{(A3c)}$$

Applying these approximations throughout equation (5) and factoring out the constants results in an integral of the form

$$\int dS_o \, e^{-ikF(x_o,y_o)} G(x_o,y_o) \qquad \text{(A4)}$$

in which the abbreviations are

$$F = \psi + \psi_s - (V/r + V_s/r_s) \qquad \text{(A5a)}$$

$$G = 1 + \left[\bar{E}\left(\frac{\psi}{r} - \frac{T}{r^2}\right) + \left(\frac{\psi}{r}\right)^2 (1 - E\bar{B})^2\right]$$

$$+ \left[(\text{same})\right]_s + \frac{2\psi\psi_s}{rr_s}\left(\bar{E} + \bar{E}_s - 2 + \frac{1}{2} EE_s\bar{B}\bar{B}_s\right) \qquad \text{(A5b)}$$

and

$$\overline{B} = 1 + i(krB)^{-1} \quad ; \quad E = \frac{\eta B \cos\theta}{1 + \eta B \cos\theta} \quad ;$$

$$\overline{E} = 1 + \frac{\overline{B}}{1 + \eta\ B \cos\theta} \qquad \text{(A5c)}$$

Upon collecting like powers of x_o, y_o and introducing the change of variables $X = 2x_o/L$, $Y = 2y_o/W$ the expressions for F and G become:

$$F = -(\beta_1 X^2 + \beta_2 Y^2) + (\alpha_2 + \gamma X)Y + \alpha_1 X \qquad \text{(A6)}$$

$$G = (1 + MX + NY + QX^2 + RY^2 + SXY)(\eta - \eta_A) \qquad \text{(A7)}$$

with

$$M = \left(\frac{L}{r}\frac{\overline{E}}{2} \sin\theta \cos\phi\right) + (\text{same})_s$$

$$N = \left(\frac{W}{r}\frac{\overline{E}}{2} \sin\theta \sin\phi\right) + (\text{same})_s$$

$$Q = \left\{\frac{L^2}{r^2}\left[\frac{(1-E\overline{B})^2}{4} \sin^2\theta \cos^2\phi - \frac{E}{8}(1-3\sin^2\theta \cos^2\phi)\right]\right\}$$

$$+ \left\{\text{same}\right\}_s + \frac{L^2}{rr_s}\left(\overline{E}+\overline{E}_s-2+\frac{1}{2}EE_s\overline{B}\overline{B}_s\right) \sin\theta \sin\theta_s \cos\phi \cos\phi_s$$

C-2

$$R = \left\{\frac{W^2}{r^2}\left[(1-E\bar{B})^2 \sin^2\theta \sin^2\phi - \frac{\bar{E}}{8}(1-3\sin^2\theta \sin^2\phi)\right]\right\}$$

$$+ \left\{\text{same}\right\}_s + \frac{L^2}{rr_s}\left(\bar{E}+\bar{E}_s-2+\frac{1}{2}EE_s\overline{BB_s}\right)\sin\theta \sin\theta_s \quad \sin\phi \sin\phi_s$$

$$S = \left\{\frac{LW}{r^2}\sin^2\theta \sin 2\phi\left[\frac{3}{8}\bar{E}+\frac{(1-E\bar{B})}{4}\right]\right\} \quad + \quad \left\{\text{same}\right\}_s$$

$$+ \frac{LW}{2rr_s}\left(\bar{E}+\bar{E}_s - 2 + \frac{1}{2}EE_s\overline{BB_s}\right)\sin\theta \sin\theta_s \quad \sin(\phi+\phi_s)$$

and

$$\alpha_{\substack{1\\2}} = \frac{1}{2}k\left(\frac{L}{W}\right)\left(\sin\theta \ {\cos \atop \sin}\phi + \sin\theta_s \ {\cos \atop \sin}\phi_s\right)$$

$$\beta_{\substack{1\\2}} = \frac{k}{8rr_s}\left(\frac{L^2}{W^2}\right)\left[r_s\left(1 - \sin^2\theta \ {\cos^2 \atop \sin^2}\phi\right)\right.$$

$$\left. + r\left(1 - \sin^2\theta_s \ {\cos^2 \atop \sin^2}\phi_s\right)\right] \tag{A9}$$

$$\gamma = \frac{kLW}{8rr_s}\left(r_s \sin^2\theta \sin 2\phi + r \sin^2\theta_s \sin 2\phi_s\right)$$

These expressions are to be used in equations (6)-(8).

Chapter 5

PLANE WAVE DIFFRACTION BY A WEDGE WITH FINITE IMPEDANGE

This chapter consists of a paper by Allan D. Pierce and W. James Hadden Jr. which appeared in the Journal of the Acoustical Society of America, volume 63, pages 17-27.

Plane wave diffraction by a wedge with finite impedance

Allan D. Pierce and W. James Hadden, Jr.

School of Mechanical Engineering, Georgia Institute of Technology, Atlanta, Georgia 30332
(Received 8 September 1976; revised 30 July 1977)

A theory is presented for the diffraction of acoustic waves by barriers with finite acoustical impedance, the shape of the barriers being such that, insofar as diffraction into the shadow zone is concerned, they may be idealized as semi-infinite wedges. The analytical development is based on the known exact solution for plane wave diffraction by a finite impedance wedge, versions of which have been previously given in the literature by Williams [Proc. R. Soc. London Ser. A **252**, 376–393 (1959)], by Senior [Commun. Pure Appl. Math. **12**, 337–372 (1959); Proc. R. Soc. London Ser. A: **213**, 436–458 (1952)], and by Maliuzhinets [Sov. Phys. Acoust. **1**, 152–174, 240–248 (1955)]. This solution is described in detail and the asymptotic limit is derived in a form which demonstrates the satisfaction of the reciprocity principle. Practical implementation is discussed, both through numerical examples and through the presentation of graphs of quantities which will be helpful in barrier design.

PACS numbers: 43.20.Fn, 43.20.Bi

INTRODUCTION

While the diffraction of sound around obstacles is a classic problem in wave theory, dating back to Poincare[1,2] and Sommerfeld,[3] the design or assessment of proposed designs of barriers to reduce noise levels in areas adjacent to community noise sources is currently a topic of considerable interest in applied acoustics.[4–7] Ideally, such designs should be based on a comprehensive and accurate theory of sound diffraction around barriers. In practice, however, the inherent complexities associated with the development of such a theory have necessitated the introduction of a variety of approximations and idealizations. Because of the remanent analytical difficulties, it is difficult to assess the applicability of such approximations and idealizations to actual or proposed barriers. In one of the most severe idealizations, the barrier is assumed to be perfectly rigid. Within the context of this idealization, it is probably fair to state that the current status of the available theories and computation procedures is relatively satisfactory.[4] Diffraction around rigid barriers with planar surfaces can be considered using results derived from theories based on the ideal models of thin screens,[5,6] wedges,[8,9] and trapezoidal (three-sided) barriers.[7,8,10]

The rigid-barrier theories, however, give information only on the effects of barrier size, shape, and geometry on diffraction; they give no insight into the effect of the surface properties on sound levels in the shadow zone. Conceivably, the latter should be an important consideration in barrier design. It is well known, for example, that the finite impedance of the ground may drastically alter the sound levels received near the ground from a source also located near the ground (i.e., the so-called excess ground attenuation effect[11,12] caused by the interference of direct and phase-shifted ground reflected waves).

As regards available theories on the effect of surface impedance on sound diffraction by barriers, the only one specifically devoted to acoustic diffraction of which we are aware is that of Jonasson[13] who gives an approximate theory of sound diffraction by a wedge of finite impedance. This theory, however, applies at best only to highly obtuse wedges, i.e., where the exterior angle β is only slightly greater than 180°. Moreover, it suffers from a lack of rigorous basis and is cumbersome to apply: a crucial set of variables is presented only pictorially. Furthermore, a completely separate construction must be performed and several variables reinterpreted in order to show that the reciprocity principle[14] is satisfied (the point source solution should be invariant on interchange of source and receiver locations). It is accordingly suspect, notwithstanding its good agreement with a limited amount of field data.

There is, however, in the electromagnetic wave propagation literature, an exact solution for diffraction of plane waves by wedges of finite conductivity. Versions of this theory have been independently given by Williams,[15–17] Senior,[18,19] and by Maliuzhinets.[20,21] (Of the three, we have found Williams's account[15] to be the most readable, although it suffers from a number of minor misprints and algebraic errors.) The purpose of the present paper is to extend and apply this theory to problems of acoustic wave diffraction by wedges of finite impedance.

I. STATEMENT OF PROBLEM AND SUMMARY OF RESULTS

In this section we first describe the mathematical model on which our analysis is founded. Immediately following this statement of the problem, we present a concise summary of formulas for the estimation of the acoustic pressure diffracted around a wedge with finite acoustic impedance. This statement of results prior to their derivation is intended to facilitate the application of the results and to give an indication of the objective of the theoretical development in the following sections.

A. The model

We consider sources of such an extent and/or distance from the barrier's tip that the incident pressure waves may be approximated as plane waves. The geometrical arrangement is depicted in Fig. 1; the z axis of a cy-

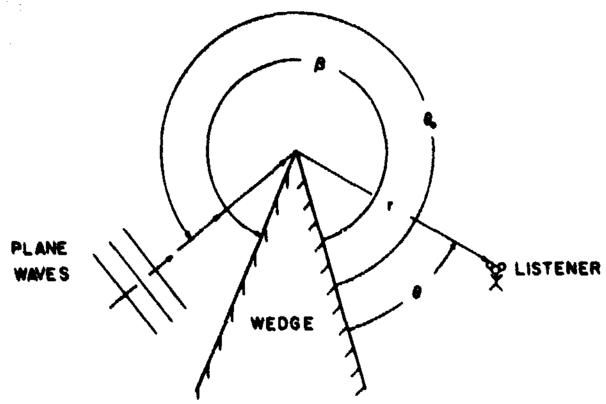

FIG. 1. Diffraction of incident plane wave by wedge of finite impedance. Listener coordinates are r, θ, z. The wave is incident from the θ_0 direction, wave-front normals make an angle γ with the wedge edge (z axis).

lindrical coordinate system is taken along the apex of the wedge; the surfaces of the wedge are the planes $\theta = 0$ and $\theta = \beta$, where β is the exterior angle of the wedge ($\beta > \pi$). We consider plane waves [with time dependence ($e^{-i\omega t}$) suppressed throughout the analysis] incident from the direction θ_0 and at an angle γ with respect to the z axis. On the surfaces $\theta = 0$ and $\theta = \beta$, the acoustic impedance is given in terms of a dimensionless quantity η as

$$Z = \rho_0 c \eta \ , \tag{1}$$

where $\rho_0 c$ is the characteristic impedance of air. This description of the problem is amplified in Sec. II; it should suffice however, in the explanation of the nature of the results.

B. Estimated insertion loss

For purposes of barrier selection or design, it is desirable to have an estimate of the effectiveness of a barrier in reducing sound levels at a given location. Ease of computation is certainly desirable. The model should be a reasonable idealization of practical cases. These conditions are fulfilled for the case of plane waves diffracted by a *nearly* rigid wedge with exterior angle $\beta (> \pi)$ for larger observer distances r from the wedge tip, viz., such that the condition $kr \sin\gamma \gg 1$ holds (where $k = \omega/c$), and for angles θ considerably less than $\theta_0 - \pi$ (i.e., listener well inside the shadow zone).

The quantity of interest is the insertion loss

$$\mathrm{IL} = 20 \log_{10}(|P_{\text{no bar.}}|/|P_{\text{with bar.}}|) \tag{2}$$

which, in the case of a rigid barrier, is well described by the formula[9]

$$\mathrm{IL} = 10 \log_{10}(kr \sin\gamma) - 20 \log_{10}[M_\nu^{-1}(\theta - \theta_0) + M_\nu^{-1}(\theta + \theta_0)] \tag{3}$$

in which we have used

$$M_\nu(\theta) = \frac{\cos(\nu\pi) - \cos(\nu\theta)}{\nu \sin(\nu\pi)} \tag{4}$$

and $\nu = \pi/\beta$. The principal result of this paper is that for a hard (but not rigid) wedge, there is an additional term in the insertion loss estimate, given by

$$\Delta\mathrm{IL} = -10 \log_{10}\{|1 + |S_\beta(\theta, \theta_0)/(\eta \sin\gamma)||^2\} \tag{5}$$

in which one must use

$$S_\beta(\theta, \theta_0) = 2[M_\nu(\theta + \theta_0) + M_\nu(\theta - \theta_0)]^{-1} - \bar{Q}_\beta(-\theta) - \bar{Q}_\beta(-\theta_0) \tag{6}$$

with $\bar{Q}_\beta(-\theta)$ obtained from Fig. 2 or Fig. 3. Further discussion of the function $\bar{Q}_\beta(-\theta)$ is presented in Appendix D. Several numerical examples, in which the computations may be performed using modern desk calculators, are discussed in Sec. VII. The analytical steps which intervene between Pts. A and B of this section are discussed in the following sections.

II. FORMAL SOLUTION FOR DIFFRACTION OF OBLIQUELY INCIDENT PLANE WAVES

In the present section, the formal solution is summarized for the diffraction of obliquely incident plane waves by a wedge of finite acoustic impedance. This is essentially the same as those solutions given previously in the literature by Williams,[15] by Senior,[19] and by Maliuzhinets,[20] although with considerable changes in nomenclature. Consistent with the discussion in Sec. I.A, the incident plane wave is taken in the form

$$p_{\text{inc}} = \exp[-ikr \sin\gamma \cos(\theta - \theta_0)] \exp(ikz \cos\gamma) \ . \tag{7}$$

Here θ_0 denotes the angular coordinate of the direction from which the incident wave is coming, γ (taken between 0 and $\frac{1}{2}\pi$) represents the angle which incident wave-front normals make with the z axis; k is ω/c. One may note that the z-translational symmetry of the problem implies that the resulting solution for the acoustic pressure should have the same z-dependent factor as in (7) above. The dependence on θ and r is governed by the reduced wave equation

$$\left[\frac{\partial^2}{\partial r^2} + \frac{1}{r}\frac{\partial}{\partial r} + \frac{1}{r^2}\frac{\partial^2}{\partial \theta^2} + k^2 \sin^2\gamma\right] p = 0 \ . \tag{8}$$

Boundary conditions at the wedge faces are that the ratio of pressure amplitude to inward normal fluid velocity component amplitude be $\rho_0 c \eta$, where η, the specific (dimensionless) normal incidence impedance, should have a real part greater than zero for an absorbing wedge. (Typically its imaginary part is positive, although not necessarily.) Thus one has

$$\partial p/\partial\theta \pm (ikr/\eta) p = 0 \ , \text{ at } \theta = 0 \text{ and } \theta = \beta \ , \tag{9}$$

where the upper and lower signs correspond to $\theta = 0$ and β, respectively.

An alternate parameter describing the wedge impedance which proves to be especially convenient is that of the (complex) angle α, defined such that

$$\cos\alpha = (\eta \sin\gamma)^{-1} \tag{10}$$

and such that $-\frac{1}{2}\pi < \alpha_R < \frac{1}{2}\pi$, $\alpha_I > 0$ given $\eta_R > 0$ and $\sin\gamma$ positive. The sign of α_R is determined from $\mathrm{sgn}(\alpha_R) = \mathrm{sgn}(\eta_I)$. For a rigid wedge, $\eta \to +\infty$, $\alpha \propto \frac{1}{2}\pi$. For a perfectly soft wedge, $\eta \to 0$, $\alpha \to i\infty$.

The solution for the boundary value problem as posed above may be taken in the form of a contour integral

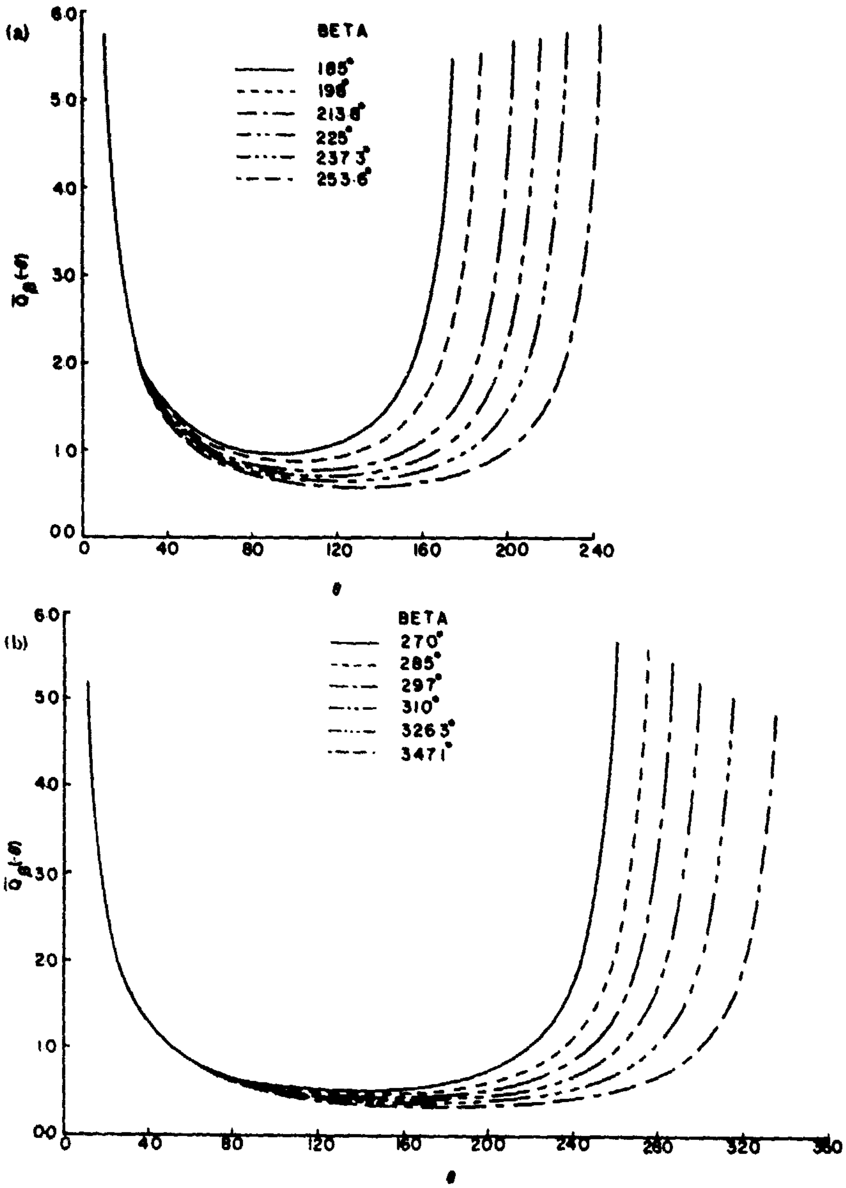

FIG. 2. (a) The function $\bar{Q}_\beta(-\theta)$ for selected values of the parameter β. Note that $\bar{Q}$ is undefined for $\theta > \beta$. (b) The function $\bar{Q}_\beta(-\theta)$ for selected values of the parameter β.

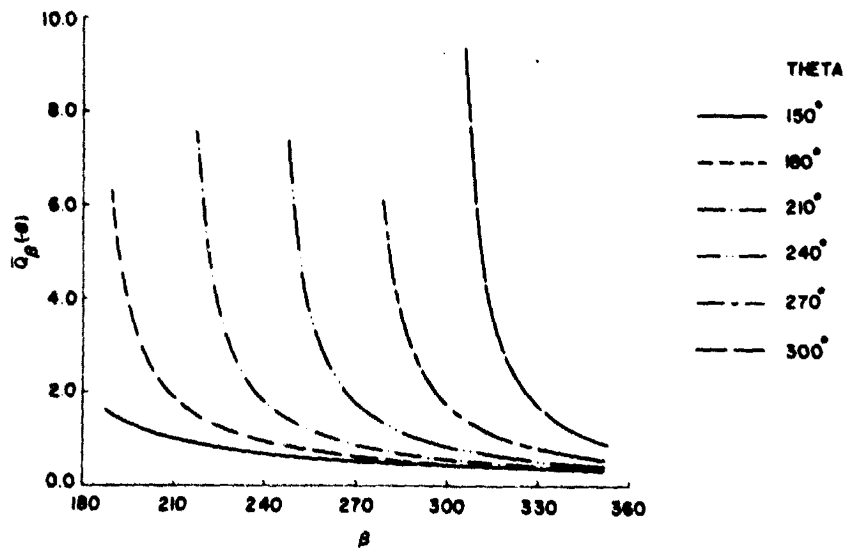

FIG. 3. The function $\bar{Q}_\beta(-\theta)$ plotted versus β for selected values of θ.

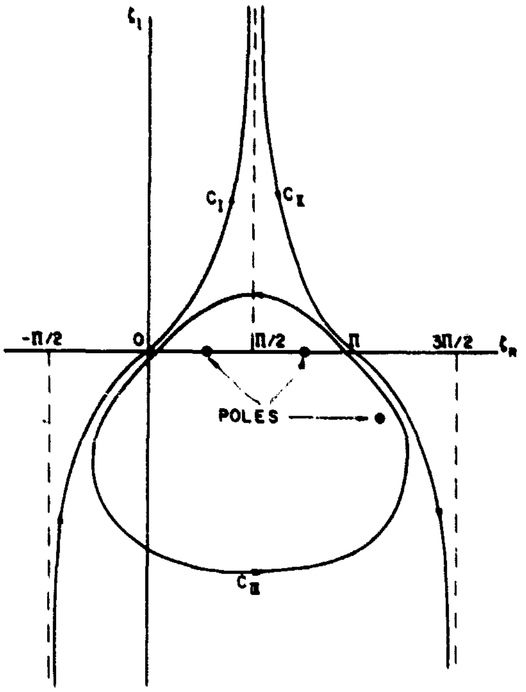

FIG. 4. Integration contours in the complex ζ plane for evaluation of the acoustic field caused by a plane wave incident on a wedge of finite impedance.

$$p = \exp(ikz\cos\gamma)\,\frac{1}{2\pi i}\int_{C_\zeta}\exp(-ikr\sin\gamma\cos\zeta)\times f(\zeta,\theta,\theta_0,\alpha)\,d\zeta\,, \qquad (11)$$

where the contour C_ζ for the ζ integration may be taken (see Fig. 4) as $C_I + C_{II} + C_{III}$ where C_I is the path of steepest descents passing through the saddle point at $\zeta = 0$ of the exponential factor in the integrand, going from $\zeta = -\frac{1}{2}\pi - i\infty$ to $\zeta = \frac{1}{2}\pi + i\infty$. Similarly, C_{II} is the path of steepest descents going from $\zeta = \frac{1}{2}\pi + i\infty$ to $\zeta = \frac{3}{2}\pi - i\infty$ through the saddle point at $\zeta = \pi$. The contour C_{III} encircles in the counterclockwise sense all poles of $f(\zeta,\theta,\theta_0,\alpha)$ which lie in the ζ plane between C_I and C_{II}. Since f (described below) is an odd function of ζ, the integral on contour C_I vanishes identically, so only contours C_{II} and C_{III} are of interest.

The function $f(\zeta,\theta,\theta_0,\alpha)$ is of a relatively complicated form and given by

$$f = S(-\zeta-\theta,\theta_0,\alpha)\,h(\zeta+\theta,\theta_0,\alpha) - S(\zeta-\theta,\theta_0,\alpha)\,h(\zeta-\theta,\theta_0,\alpha) \qquad (12)$$

with

$$h(\zeta,\theta_0,\alpha) = \frac{(\nu/2)\sin(\nu\theta_0)\Psi_\nu(\zeta,\frac{1}{2}\pi-\alpha-\beta)}{\Psi_\nu(\theta_0,\zeta)\,\Psi_\nu(\theta_0,\frac{1}{2}\pi-\alpha-\beta)}\,. \qquad (13)$$

Here we have abbreviated

$$\Psi_\nu(a,b) = \sin[(\tfrac{1}{2}\nu)(a+b)]\sin[(\tfrac{1}{2}\nu)(a-b)] = \tfrac{1}{2}[\cos(\nu b)-\cos(\nu a)]\,, \qquad (14)$$

$$\nu = \pi/\beta\,. \qquad (15)$$

(Note that h is an even function of ζ.) The function S is defined by

$$S(\zeta,\theta_0,\alpha) = H_\beta(\zeta,\alpha)/H_\beta(-\theta_0,\alpha)\,, \qquad (16)$$

where the function $H_\beta(\zeta,\alpha)$ is defined in terms of a function $F_\beta(\zeta)$ (here termed *Williams' F function* in recognition of the fact that it is the same as used by Williams[15]):

$$H_\beta(\zeta,\alpha) = \frac{F_\beta(\zeta+\beta-\pi+\alpha)\,F_\beta(\zeta+\beta+\pi-\alpha)}{F_\beta(\zeta+2\beta+\alpha)\,F_\beta(\zeta+2\beta-\alpha)}\,. \qquad (17)$$

The analytic properties of the functions $F_\beta(\zeta)$ and $H_\beta(\zeta,\alpha)$ are discussed extensively in Appendix A. For angles β of the form

$$\beta = p\pi/2q$$

with p an odd integer and p, q relative primes, the function $F_\beta(\zeta)$ is given by

$$F_\beta(\zeta) = \prod_{n=1}^{(p-1)/2}\sin\{\tfrac{1}{2}\nu[\zeta+\tfrac{1}{2}\pi(4n-1)-2\beta]\}\Big/\prod_{m=0}^{q-1}\sin\{\tfrac{1}{2}[\zeta-\tfrac{1}{2}\pi-2\beta(m+1)]\}\,. \qquad (18)$$

Expressions for $F_\beta(\zeta)$ can be obtained for other values of β, but at the expense of considerably more computational effort.[15]

That Eq. (11) is indeed the appropriate solution can be ascertained by explicitly substituting it into Eqs. (8) and (9) followed by some integrations by parts. The fact that f is the sum of a function of $\zeta-\theta$ and a function of $\zeta+\theta$ is sufficient to insure that the partial differential equation be satisfied. The boundary conditions are satisfied by virtue of the manner in which $H_\beta(\zeta,\alpha)$ is defined in terms of Williams' F functions and of the fact that the h's in Eq. (13) are periodic in ζ with period 2β. The explicit form of the function h was chosen in conformance with notions of radiation conditions; i.e., that at large r the solution must consist of waves (other than the incident wave) which proceed outwards from the wedge and which do not grow exponentially with r. This requires in particular that f not have any poles between C_I and C_{II} for which the imaginary part of $\cos\zeta$ is positive. Since the function $H_\beta(\zeta-\theta,\alpha)$ does not necessarily have this property, $h(\zeta-\theta,\theta_0,\alpha)$ was designed to have a zero which just canceled the "forbidden" pole of $H_\beta(\zeta-\theta,\alpha)$. Also, in order that the solution reproduce the assumed incident wave, it was required that f have poles at $\zeta = \theta-\theta_0$ and at $\zeta = \theta_0-\theta$ one of which is enclosed by C_{III} when geometry indicates the incident wave is present. Finally, the function was required to have residues of appropriate values at these poles such that the C_{III} integration would give a term in the evaluation of (11) equal to (7) when geometry indicated the presence of the incident wave. It has been verified[22] that this formulation is consistent with notions of reciprocity.

The limiting cases of rigid and soft wedges may be obtained by examining the limiting forms of the functions $H_\beta(\zeta,\alpha)$, $S(\zeta,\theta_0,\alpha)$, and $h(\zeta,\theta_0,\alpha)$. In the limit of a rigid wedge ($\alpha \to \frac{1}{2}\pi$), the limiting form of $f(\zeta,\theta,\theta_0,\alpha)$, Eq. (12) is

$$f(\zeta,\theta,\theta_0,\tfrac{1}{2}\pi) = Q_\nu(\zeta,\theta-\theta_0) + Q_\nu(\zeta,\theta+\theta_0) \qquad (19)$$

with

$$Q_\nu(\zeta,\theta)=\nu\sin(\nu\zeta)/[\cos(\nu\theta)-\cos(\nu\zeta)] .$$

Equation (19) corresponds exactly to the function used in Eq. (1) of a previous paper[9] by one of the authors. In the limit of an acoustically soft wedge ($\alpha\to i\infty$), the function f becomes

$$f(\zeta,\theta,\theta_0,i\infty)=Q_\nu(\zeta,\theta-\theta_0)-Q_\nu(\zeta,\theta+\theta_0) \tag{20}$$

which, again, is the correct limit.

III. ASYMPTOTIC SOLUTION FOR DIFFRACTED WAVE

In the shadow zone, the major contribution at large distances r from the edge comes from the C_{II} portion of the contour integral in Eq. (11). The C_{III} integration simply gives the incident wave, a specularly reflected wave, and possibly a surface wave; the former two of which do not exist in the shadow zone, the third of which generally dies out exponentially with large r. The contribution $p_{\mathrm{Diff},\,II}$ from contour C_{II} at large r may be obtained by application of the saddle-point approximation taking into account the possible proximity of poles and zeros to the saddle point at $\zeta=\pi$.

The poles of $f(\zeta,\theta,\theta_0,\alpha)$ are (i) those corresponding to the incident and specularly reflected waves and (ii) any pole of $H_\beta(\zeta-\theta,\alpha)$ or $H_\beta(-\zeta-\theta,\alpha)$ which is not also a zero of $\Psi_\nu(-\zeta-\theta,\pi/2-\alpha-\beta)$ or $\Psi_\nu(\zeta-\theta,\pi/2-\alpha-\beta)$, respectively. [See Eqs. (12) and (13).] The first category of pole is manifested by the factor $\Psi_\nu(\theta_0,\zeta)$ in the donominator of the definition (13). The second category of poles may be determined with reference to Eqs. (A6); the only ones which could conceivably be close to the $\zeta=\pi$ saddle point are where $\zeta-\theta$ or $-\zeta-\theta$ equals $\frac{3}{2}\pi\pm\alpha$ or $-\frac{3}{2}\pi\pm\alpha\mp\beta$, respectively, or thus where $\zeta=\frac{3}{2}\pi\pm\alpha+\theta$, $\zeta=\frac{3}{2}\pi\pm\alpha+\beta-\theta$. For given θ and α, at most one of these poles will be near the saddle point. Let us assume that the relevant pole is at $\zeta=\pi+P_\alpha$; we then set

$$D_3=\zeta-\pi-P_\alpha . \tag{21}$$

Consequently, if one sets

$$f(\zeta,\theta,\theta_0,\alpha)=\frac{\Phi(\zeta,\theta,\theta_0,\alpha)}{D_1D_2D_3} , \tag{22}$$

where, upon rearranging the product of $\Psi_\nu(\theta_0,\zeta-\theta)$ and $\Psi_\nu(\theta_0,\zeta+\theta)$ into the factors

$$D_1=\cos(\nu\zeta)-\cos\nu(\theta-\theta_0) , \tag{23a}$$

$$D_2=\cos(\nu\zeta)-\cos\nu(\theta+\theta_0) . \tag{23b}$$

The function $\Phi(\zeta,\theta,\theta_0,\alpha)$ so defined will have no poles in the vicinity of $\zeta=\pi$.

The analysis then proceeds, as described in Appendix C, by replacing Φ, D_1, D_2, D_3 by power series expansions to first order in $(\zeta-\pi)$ and integrating the resulting form of Eq. (11) along the line of steepest descents through the saddle point at $\zeta=\pi$. Thus the integral on contour C_{II} in Eq. (11) can be expressed in terms of standard functions occurring in diffraction problems as

$$p_{\mathrm{Diff},\,II}=\exp[ik(z\cos\gamma+r\sin\gamma)](e^{i\pi/4}/\sqrt{2})$$
$$\times[G^{(+)}A_D(\Gamma M_\nu^{(+)})+G^{(-)}A_D(\Gamma M_\nu^{(-)})+G^{(\alpha)}A_D(\Gamma P_\alpha)] . \tag{24}$$

where

$$G^{(+)}=\frac{\bar G(\pi,\theta,\theta_0,\alpha)}{[M_\nu^{(-)}-M_\nu^{(+)}][P_\alpha-M_\nu^{(+)}]} , \tag{25}$$

$$M_\nu^{(-)}=M_\nu(\theta-\theta_0);\ M_\nu^{(+)}=M_\nu(\theta+\theta_0) , \tag{26}$$

with $M_\nu^{(\pm)}$ given by Eq. (4), and

$$\bar G(\zeta,\theta,\theta_0,\alpha)\equiv\Phi(\zeta,\theta,\theta_0,\alpha)\ (\nu\sin\nu\pi)^2 . \tag{27}$$

The other two coefficients of the function $A_D(X)$ in Eq. (24) are obtained by cyclic permutations of the quantities $M_\nu^{(+)}$, $M_\nu^{(-)}$, and P_α. In the argument of $A_D(X)$, we have used

$$\Gamma\equiv[(kr\sin\gamma)/\pi]^{1/2} . \tag{28}$$

The function $A_D(X)$ which appears in Eq. (24) is the diffraction integral defined in the previous paper[9] by

$$A_D(X)=\frac{\sqrt{2}}{2\pi}\int_0^\infty\frac{e^{-s^2}ds}{(\frac{1}{2}\pi)^{1/2}X-e^{-i\pi/4}s} \tag{29}$$

which, when X is real, can be expressed as

$$A_D(X)=\mathrm{sign}(X)[f(|X|)-ig(|X|)] , \tag{30}$$

where $f(X)$ and $g(X)$ are the auxiliary Fresnel functions tabulated on pages 323–324 of the NBS *Handbook of Mathematical Functions.*[23] If X is not real, as would be the case for $X=\Gamma P_\alpha$, the above would be inapplicable, but, instead, one could write

$$A_D(X)=(e^{-i\pi/4}/\sqrt{2})\,w[e^{i\pi/4}(\pi/2)^{1/2}X] \tag{31a}$$

or

$$A_D(X)=-(e^{-i\pi/4}/\sqrt{2})\,w[e^{-i\pi/4}(\pi/2)^{1/2}X^*]^* \tag{31b}$$

which would hold for $\mathrm{Im}(e^{i\pi/4}X)$ positive or negative, respectively. The function $w(z)$ is related to the error function of complex argument and is tabulated on pages 325–328 of the NBS *Handbook*[23] for complex values of z.

The calculation of the function $\bar G(\zeta,\theta,\theta_0,\alpha)$, which is quite tedious, is sketched in Appendix C. The results which are relevant to Eq. (25) are

$$\bar G(\pi,\theta,\theta_0,\alpha)=P_\alpha U(\theta_0,\alpha)\,U(\theta,\alpha)\,D(\theta,\theta_0,\alpha), \tag{32}$$

where

$$U(\theta,\alpha)=\frac{(\frac{1}{2})\sin(\nu\theta)}{H_\beta(-\theta,\alpha)\Psi_\nu(\theta,\frac{1}{2}\pi-\alpha-\beta)} \tag{33}$$

and

$$D(\theta,\theta_0,\alpha)=M_\nu(\theta+\theta_0)+M_\nu(\theta-\theta_0)$$
$$+\frac{\cos(2\nu\alpha)-\cos(\nu\pi)}{\nu\sin\nu\pi} . \tag{34}$$

In the *complete asymptotic limit*, where P_α, $M_\nu^{(+)}$, $M_\nu^{(-)}$ are all finite and Γ is large, $A_D(X)$ can be replaced by $(\pi X)^{-1}$ and a considerable simplification results in Eq. (24). Specifically, one finds

$$p_{\mathrm{Diff},\,II}=\exp[ik(z\cos\gamma+r\sin\gamma)]$$
$$\times(e^{i\pi/4}/\sqrt{2})(\pi\Gamma)^{-1}G(\theta,\theta_0,\alpha), \tag{35}$$

where

$$G(\theta,\theta_0,\alpha)=\tilde{G}(\pi,\theta,\theta_0,\alpha)/P_\alpha M_\nu^{(+)}M_\nu^{(-)}. \tag{36}$$

Note that, with $\tilde{G}(\pi,\theta,\theta_0,\alpha)$ given by Eq. (32), the factor P_α cancels out.

The symmetry of Eq. (36) with respect to θ and θ_0 is obvious from $M_\nu(\theta-\theta_0)=M_\nu(\theta_0-\theta)$. Thus the reciprocity requirement is definitely satisfied. In the limit of a rigid wedge ($\alpha=\frac{1}{2}\pi$) one has $U(\theta,\frac{1}{2}\pi)=-1$ by virtue of Eqs. (14), (17), and (A3), and $D(\theta,\theta_0,\frac{1}{2}\pi)=M_\nu(\theta+\theta_0)+M_\nu(\theta-\theta_0)$. Consequently, one has

$$G(\theta,\theta_0,\tfrac{1}{2}\pi)=\frac{1}{M_\nu(\theta+\theta_0)}+\frac{1}{M_\nu(\theta-\theta_0)} \tag{37}$$

and the result for asymptotic diffraction by a rigid wedge is recovered.

Similarly, in the limit of an acoustically soft wedge, i.e., $\alpha\to i\infty$, $D(\theta,\theta_0,\alpha)$ approaches $\exp(-i2\nu\alpha)/2\nu\sin\nu\pi$, $\Psi_\nu(\theta,\frac{1}{2}\pi-\alpha-\beta)$ approaches $-\frac{1}{4}\exp[i\nu(\pi/2-\alpha)]$, $H_\beta(-\theta,\alpha)$ approaches $\exp[-\frac{1}{2}i(\nu\pi)]$, so $U(\theta_0,\alpha)U(\theta_0,\alpha)\times D(\theta,\theta_0,\alpha)$ approaches $2\sin\nu\theta\sin\theta_0$ divided by $\nu\sin\nu\pi$ or just $M_\nu(\theta+\theta_0)-M_\nu(\theta-\theta_0)$. Consequently, one has

$$G(\theta,\theta_0,i\infty)=\frac{1}{M_\nu(\theta-\theta_0)}-\frac{1}{M_\nu(\theta+\theta_0)} \tag{38}$$

which, again, is the correct limit.

In addition to the above-mentioned contributions from the integration contour C_{11}, a complete description of the pressure field in the shadow zone should include the possibility of a contribution from a surface wave which is refracted from the shadowed face of the wedge. Such a contribution would arise from a pole enclosed by the contour C_{111}. For $\theta<\pi$ and $\theta_0>\pi+\theta$, the only pole of $f(\zeta,\theta,\theta_0,\alpha)$ that could conceivably lie within C_{111} is at $\zeta=\frac{3}{2}\pi-\alpha+\theta$. This pole will lie within the contour only if

$$\tfrac{1}{2}\pi-\alpha_R<\sin^{-1}(\tanh\alpha_I) \tag{39}$$

and since in this case the imaginary part of $\cos(\frac{3}{2}\pi-\alpha+\theta)$ is negative, by (11) the C_{111} contribution from this pole decays exponentially with distance from the surface. Furthermore, reference to Eq. (10) indicates that the inequality (39) is not likely to be satisfied in situations of physical interest. For these reasons we omit an explicit description of the surface wave contribution (which is included in Sec. IV of Ref. 22).

IV. NEARLY RIGID BARRIERS

If the barrier is nearly rigid, for $\eta_I>0$ α is close to $\frac{1}{2}\pi$ and one can take the solution of Eq. (10) as

$$\tfrac{1}{2}\pi-\alpha\simeq(\eta\sin\gamma)^{-1} \tag{40}$$

Thus it would seem appropriate to expand $H_\beta(\zeta,\alpha)$ in a power series in $\frac{1}{2}\pi-\alpha$, keeping up to first-order terms in $\frac{1}{2}\pi-\alpha$. In this event one has, from Eq. (17)

$$H_\beta(\zeta,\alpha)\simeq-\tan[\tfrac{1}{2}\nu\zeta][1+\bar{Q}_\beta(\zeta)(\tfrac{1}{2}\pi-\alpha)], \tag{41}$$

where

$$\bar{Q}_\beta(\zeta)=\frac{\partial}{\partial\zeta}\ln\left[\frac{F_\beta(\zeta+\beta+\frac{1}{2}\pi)F_\beta(\zeta+2\beta+\frac{1}{2}\pi)}{F_\beta(\zeta+\beta-\frac{1}{2}\pi)F_\beta(\zeta+2\beta-\frac{1}{2}\pi)}\right]. \tag{42}$$

Making similar expansions in Eqs. (33) and (34) the function $\tilde{G}(\pi,\theta,\theta_0,\alpha)$ in Eq. (32) may be written as

$$\tilde{G}(\pi,\theta,\theta_0,\alpha)\simeq P_\alpha[M_\nu^{(+)}+M_\nu^{(-)}][1+\bar{S}_\beta(\theta,\theta_0)(\tfrac{1}{2}\pi-\alpha)] \tag{43}$$

and consequently, from Eq. (36),

$$G(\theta,\theta_0,\alpha)\simeq\left[\frac{1}{M_\nu(\theta+\theta_0)}+\frac{1}{M_\nu(\theta-\theta_0)}\right][1+\bar{S}_\beta(\theta,\theta_0)(\tfrac{1}{2}\pi-\alpha)] \tag{44}$$

in which

$$\bar{S}_\beta(\theta,\theta_0)=2[M_\nu(\theta+\theta_0)+M_\nu(\theta-\theta_0)]^{-1}-\bar{Q}_\beta(-\theta)-\bar{Q}_\beta(-\theta_0). \tag{45}$$

For observation angles other than $\theta=0$, the diffracted pressure field may be approximated—by combining Eqs. (24), (25), (40), (43), and (45)—as

$$\begin{aligned}p_{\mathrm{Diffr},\,11}\simeq{}&\exp[ik(z\cos\gamma+r\sin\gamma)](e^{i\pi/4}/\sqrt{2})\\&\times P_\alpha[M_\nu^{(+)}+M_\nu^{(-)}][Y^{(+)}A_D(\Gamma M_\nu^{(+)})\\&+Y^{(-)}A_D(\Gamma M_\nu^{(-)})+Y^{(\alpha)}A_D(\Gamma P_\alpha)],\end{aligned} \tag{46}$$

where

$$Y^{(+)}=\frac{1}{[M_\nu^{(-)}-M_\nu^{(+)}][P_\alpha-M_\nu^{(+)}]} \tag{47}$$

and the other coefficients in Eq. (46) are obtained by cyclic permutation of $M_\nu^{(+)}$, $M_\nu^{(-)}$, and P_α. Similarly, in the complete asymptotic limit, one has

$$\begin{aligned}p_{\mathrm{Diffr},\,11,\mathrm{cal}}\simeq{}&\exp[ik(z\cos\gamma+r\sin\gamma)](e^{i\pi/4}/\sqrt{2})(\pi\Gamma)^{-1}\\&\times\{[M_\nu^{(+)}]^{-1}+[M_\nu^{(-)}]^{-1}\}[1+\bar{S}_\beta(\theta,\theta_0)/\eta\sin\gamma].\end{aligned} \tag{48}$$

From this last expression one may obtain a correction to the insertion loss for a hard barrier (*vis-a-vis* a *rigid* barrier) given by

$$-10\log_{10}|1+S_\beta(\theta,\theta_0)/\eta\sin\gamma|^2\ \mathrm{dB} \tag{49}$$

which is just Eq. (5).

V. PRACTICAL APPLICATIONS

The formulas presented in the preceding sections probably appear more formidable than is actually the case. The first important point is that these results can be used most fruitfully in the computation of barrier insertion loss, as set forth in Eq. (2)

$$\mathrm{IL}_{\mathrm{bar.}}=20\log_{10}(|p_{\mathrm{no\ bar.}}|/|p_{\mathrm{bar.}}|).$$

If, as is generally true, the surface wave contribution may be neglected, Eq. (5) provides an estimate of the change in insertion loss, with respect to a rigid barrier's effect, of a barrier with finite impedance.

The second important consideration concerns the function $\bar{Q}_\beta(-\theta)$ which appears in this correction term. It is shown in Appendix D that for angles β of the form $p\pi/2q$, $\bar{Q}_\beta(-\theta)$ has a form which is amenable to numerical computations; in some cases computations are not so taxing as to require a large computer. In practice, it should be possible to obtain useful estimates of the insertion loss (or sound pressure distribution) using a value of β of the above form. One then has [see Eq. (D4)]

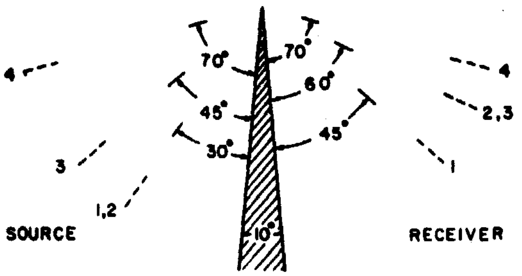

CONFIGURATION	1	2	3	4
ΔIL (dB)	2.3	1.7	1.1	0.5

FIG. 5. The finite-impedance correction to the insertion loss for a wedge with interior angle 10°. The surface admittance was taken as $(1/\eta) = 0.1 - i0.05$. The source-receiver orientations are identified by the configuration numbers: in configuration 1 the incidence direction is at 30° from the adjacent wedge face while the receiver is at 45° from its adjacent wedge face.

$$\bar{Q}_\beta(-\theta) = -\nu\sin(\nu\pi)\sum_{n=1}^{(p-1)/2}\frac{1}{\sin[\nu(\theta-2n\pi)]\sin\{\nu[\theta-(2n-1)\pi]\}}$$
$$+\sum_{m=0}^{q-1}\frac{\sin(\theta+2m\beta)+\sin[\theta+(2m+1)\beta]}{\sin(\theta+2m\beta)\sin[\theta+(2m+1)\beta]} \quad . \qquad (50)$$

For angles θ of the form $\theta = k\pi/2q$, k an integer less than or equal to p, there is a singlular term in each sum in Eq. (50). A straightforward expansion of the two terms reveals that they combine so that $\bar{Q}_\beta(-\theta)$ is in fact regular. Difficulties in numerical computations may be avoided by avoiding such angles.

A more detailed investigation of the cases in which the receiver angle θ is very small or the source angle θ_0 approaches β reveals that $\bar{Q}_\beta(-\theta)$ becomes

$$\bar{Q}_\beta(-\delta) \simeq Q_\beta(-\beta+\delta) \simeq (\sin\delta)^{-1}\,, \quad \delta \ll 1\ . \qquad (51)$$

Since $\bar{Q}_\beta(-\theta)/(\eta\sin\gamma)$ serves as a first-order correction term to the rigid-wedge limit for $H_\beta(-\theta)$ [see Eq. (41)], the behavior of $\bar{Q}_\beta$ exhibited in Eq. (51) indicates that the approximation in Eq. (41) is not useful for situations in which the incidence or receiver directions are at small angles δ with respect to a wedge face. This behavior is a manifestation of the familiar phenomenon of the vanishing effective surface impedance for plane waves at grazing incidence.[24] This is borne out by inspection of Eq. (A5): Substituting in the appropriate values for ζ and α, one has

$$R[\delta, \tfrac{1}{2}\pi-(\eta\sin\gamma)^{-1}] \simeq R[\beta-\delta, \tfrac{1}{2}\pi-(\eta\sin\gamma)^{-1}]$$
$$\simeq \left\{\frac{\tan(\tfrac{1}{2}\nu\delta)-\tan(\nu/2\eta\sin\gamma)}{\tan(\tfrac{1}{2}\nu\delta)+\tan(\nu/2\eta\sin\gamma)}\right\} \qquad (52)$$

for the plane wave reflection coefficient at each face. For a given value of η, the reflection coefficient approaches -1 as δ goes to zero. These considerations indicate that useful estimates of the insertion loss correction can be obtained for $\delta\eta\sin\gamma \gg 1$.

As an alternate aid to applications of these results, we have computed $\bar{Q}_\beta(-\theta)$ for a number of values of β and θ. These are presented in Fig. (2). In addition, these curves are plotted again, with β appearing as the independent variable, θ as a parameter, in Fig. (3). Thus one has the option of using one of the "special" values of β to approximate a desired wedge or of using values for the desired wedge angle for a selection set of angles θ.

As an illustration of the use of these results we have calculated the correction to the insertion loss via Eq. (5) for perpendicular incidence ($\gamma = \frac{1}{2}\pi$) on wedges with exterior angles $\beta = 350°$ and 240° for a surface admittance $\eta^{-1} = 0.1 - i\,0.05$, which is representative of turf at 1000 Hz.[25] Values for the function $\bar{Q}$ were obtained from Figs. 2 and 3. Insertion-loss corrections are presented in Figs. 5 and 6 for several incidence and observation angles.

In the case of the acute-angled wedge, the surface impedance has a small effect—less than 3 dB. For the obtuse-angled wedge, the effect from considering the finite acoustic impedance is on the order of 6 dB when both source and receiver are at fairly small angles with respect to their adjacent sides of the wedge. Thus consideration of the finite impedance seems to be of considerably greater significance for obtuse wedges than for acute ones, especially since in many practical realizations of the obtuse wedge model the sources and receivers are close to the surface.

VI. CONCLUSION

A theoretical analysis has been presented for the diffraction of plane waves by a wedge of arbitrary surface impedance. Particular attention has been given to the pressure field in the shadow zone for large distances from this tip of the wedge. The results presented here make use of simplifications that result for a large number of special wedge angles. In a detailed discussion of

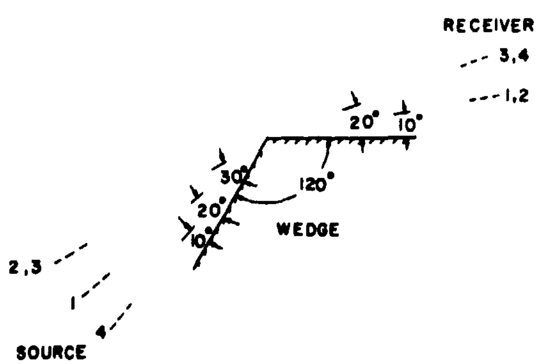

CONFIGURATION	1	2	3	4
ΔIL (dB)	6.1	4.6	1.8	6.9

FIG. 6. The finite-impedance correction to the insertion loss for a wedge with interior angle 120° and surface admittance $(1/\eta) = 0.1 + i0.05$. Source and receiver orientations are labelled as in Fig. 5.

the nearly rigid wedge a correction to the insertion loss of a rigid wedge has been obtained. Numerical computations indicate a significant effect of finite surface impedance for obtuse wedges with source and/or receiver at a fairly small angle with respect to the plane of the wedge face. In addition, the solution presented here should provide a good point of departure for the analysis of diffraction by spherical waves or by broad barriers.

ACKNOWLEDGMENTS

This research was supported in part by grant NSG1047 from the NASA Langley Research Center. It is a pleasure to acknowledge the preparation of the numerical examples by Ms. Robin A. Vidimos and Mr. Philip M. Pencil.

APPENDIX A: DISCUSSION OF THE F AND H FUNCTIONS

The F function $F_\beta(\zeta)$ appearing in Eq. (17) is defined such that it satisfied the two recurrence relations

$$F_\beta(\zeta+2\beta)=F_\beta(\zeta)\tan\left[\tfrac{1}{2}(\zeta-\tfrac{3}{2}\pi)\right] , \tag{A1a}$$

$$F_\beta(\zeta+2\beta)=F_\beta(-\zeta) , \tag{A1b}$$

and such that it is analytic and has no poles or zeros in the strip $0<\zeta_R<2\beta$, the function asymptotically approaching zero as $\zeta_I\to\pm\infty$. Explicit expressions for this function for some particular values of β are given in Appendix B.

Since $F_\beta(\zeta)$ has no zeros or poles in the strip $(0, 2\beta)$ it follows from Eqs. (A1) that its zeros must be at

$$\zeta=\beta\pm(\tfrac{3}{2}\pi+\beta+K) \tag{A2a}$$

while its poles are at

$$\zeta=\beta\pm(\tfrac{1}{2}\pi+\beta+K) , \tag{A2b}$$

where $K=2n\pi+2m\beta\geq 0$, n and m being arbitrary nonnegative integers. (Of course, there is the possibility that a pole location may coincide with a zero location, in which case the function will have neither a pole nor a zero at the point in question.) Examination of the locations of the poles and zeros of the function $\{\sin[(\tfrac{1}{2}\nu)\times(\zeta+\tfrac{1}{2}\pi)]F_\beta(\zeta+\pi)\}^{-1}$, reveals that these are identical to those given above, so one may infer that $F_\beta(\zeta)$ has the property

$$F_\beta(\zeta)F_\beta(\zeta+\pi)=\frac{A_\beta}{\sin[(\tfrac{1}{2}\nu)(\zeta+\tfrac{1}{2}\pi)]} , \tag{A3}$$

where A_β is some number independent of ζ (the precise value of which is immaterial). It then follows from this and Eq. (A2b) that the asymptotic values of $F_\beta(\zeta)$ should be

$$F_\beta(\zeta)\to A_\beta e^{i(\nu/4)\zeta} ,\quad \zeta_I\to\infty \tag{A4a}$$

$$\to iA_\beta e^{-i(\nu/4)\zeta} ,\quad \zeta_I\to-\infty . \tag{A4b}$$

Analogous relations may be deduced for the $H_\beta(\zeta,\alpha)$ function starting from the definition of Eq. (17). It satisfies recurrence relations of the form

$$\frac{H_\beta(\zeta,\alpha)}{H_\beta(-\zeta,\alpha)}=-\left[\frac{\sin(\nu\zeta)-\cos(\nu\alpha)}{\sin(\nu\zeta)+\cos(\nu\alpha)}\right]$$

$$=-\frac{\tan[(\tfrac{1}{2}\nu)(\zeta-\tfrac{1}{2}\pi+\alpha)]}{\tan[(\tfrac{1}{2}\nu)(\zeta+\tfrac{1}{2}\pi-\alpha)]}$$

$$=\frac{H_\beta(-\zeta-\beta,\alpha)}{H_\beta(\zeta-\beta,\alpha)}=-R(\zeta,\alpha) , \tag{A5}$$

where $R(\zeta,\alpha)$ may be interpreted as a plane wave reflection coefficient. The zeros of $H_\beta(\zeta,\alpha)$ are at

$$\zeta=-\beta\pm\alpha\pm(\tfrac{1}{2}\pi+\beta+K) \tag{A6a}$$

and

$$\zeta=\pm(\pi-\alpha)\pm(\tfrac{3}{2}\pi+\beta+K) \tag{A6b}$$

any sign combination being a possibility, while its poles are at

$$\zeta=-\beta\pm\alpha\pm(\tfrac{3}{2}\pi+\beta+K) \tag{A7a}$$

and

$$\zeta=\pm(\pi-\alpha)\pm(\tfrac{1}{2}\pi+\beta+K) \tag{A7b}$$

for, again, $K=2n\pi+2m\beta$, $n\geq 0$, $m\geq 0$. Also, it follows from Eq. (A3) that

$$H_\beta(\zeta,\alpha)H_\beta(\zeta+\pi,\alpha)$$
$$=\frac{\sin\{\tfrac{1}{2}\nu[\tfrac{1}{2}(\zeta+\pi)+\alpha]\}\sin\{\tfrac{1}{2}\nu[\tfrac{1}{2}(\zeta+\pi)-\alpha]\}}{\cos\{\tfrac{1}{2}\nu[\tfrac{1}{2}(\zeta-\pi)+\alpha]\}\cos\{\tfrac{1}{2}\nu[\tfrac{1}{2}(\zeta+3\pi)-\alpha]\}} \tag{A8}$$

APPENDIX B: THE FUNCTION $F_\beta(\zeta)$ FOR PARTICULAR VALUES OF THE WEDGE ANGLE β

The function $F_1(w)$ defined in Eq. (32) of Williams' paper[15] fails to exhibit the proper asymptotic behavior in the limit as $\alpha\to i\infty$, e.g., it does not obey our Eq. (A4). Accordingly, we describe here the construction of our function $F_\beta(\zeta)$ for $\beta=p\pi/2q$, with p an odd integer, q an integer. We shall include two examples for wedge angles of particular physical interest.

We begin by recalling from Eq. (A2a) that the function $F_\beta(\zeta)$ has zeros at the values

$$\zeta-\beta=\pm(\tfrac{3}{2}\pi+\beta+K) \tag{B1}$$

which, for the particular values of β under consideration here, may be written as

$$(2q/\pi)(\zeta-p\pi/2q)=\pm(p+3q+4nq+2mp)\equiv\pm F_z(n,m). \tag{B2}$$

Similarly, $F_\beta(\zeta)$ has poles at (see Eq. (A2b))

$$\zeta-\beta=\pm(\tfrac{1}{2}\pi+\beta+K) \tag{B3}$$

which in turn may be written as

$$(2q/\pi)(\zeta-p\pi/2q)=\pm(p+q+4nq+2mp)\equiv\pm F_p(n,m). \tag{B4}$$

We may use Eqs. (B2) and (B4) to represent the function $F_\beta(\zeta)$ schematically by

$$F_\beta(\zeta)=\prod_{m,n=0}^{\infty}[x-F_z(n,m)][x+F_z(n,m)]\Big/\prod_{m,n=0}^{\infty}[x-F_p(n,m)][x+F_p(n,m)] . \tag{B5}$$

There are several relationships between the pole and zero locations, $F_z(n, m)$ and $F_p(n, m)$, which are important in the development of $F_\beta(\zeta)$. They are

$$F_z(n+\tfrac{1}{2}(p-1),\ m-q)=F_p(n, m), \tag{B6}$$

$$F_p(n,\ m)=F_p(-n+\tfrac{1}{2}(p-1),\ -m-1-q), \text{ and} \tag{B7}$$

$$F_p(n+p,\ m-2q)=F_p(n,\ m)\ . \tag{B8}$$

Substituting Eq. (B6) into Eq. (B5), with appropriate changes of limits, yields

$$F_\beta(\zeta)=\prod_{n=-1/2(p-1)}^{\infty}\ \prod_{m=q}^{\infty}[x-F_p(n,m)][x+F_p(n,m)]\Big/\prod_{n=0}^{\infty}\ \prod_{m=0}^{\infty}[x-F_p(n,m)][x+F_p(n,m)]\,. \tag{B9}$$

After canceling out the common factors, we have

$$F_\beta(\zeta)=\prod_{n=-1/2(p-1)}^{-1}\ \prod_{m=q}^{\infty}[x-F_p(n,m)][x+F_p(n,m)]\Big/\prod_{n=0}^{\infty}\ \prod_{m=0}^{q-1}[x-F_p(n,m)][x+F_p(n,m)]\,. \tag{B10}$$

We next apply Eq. (B7) to the $[x+F_p(n,m)]$ factors in Eq. (B10) and rearrange the factors to obtain

$$F_\beta(\zeta)=\prod_{n=-1/2(p-1)}^{-1}\ \prod_{m=q}^{\infty}[x-F_p(n,m)]\prod_{n=1/2(p+1)}^{p-1}\ \prod_{m=-\infty}^{-(2q+1)}[x-F_p(n,m)]\Big/\prod_{n=0}^{\infty}\ \prod_{m=0}^{q-1}[x-F_p(n,m)]\prod_{n=-\infty}^{1/2(p-1)}\ \prod_{m=-2q}^{-(q+1)}[x-F_p(n,m)] \tag{B11}$$

which becomes, after use of Eq. (B8) and further adjustment of the product limits,

$$F_\beta(\zeta)=\prod_{n=-1/2(p-1)}^{-1}\ \prod_{m=q}^{\infty}[x-F_p(n,m)]\prod_{n=-1/2(p-1)}^{-1}\ \prod_{m=-\infty}^{-1}[x-F_p(n,m)]\Big/\prod_{n=0}^{\infty}\ \prod_{m=0}^{q-1}[x-F_p(n,m)]\prod_{n=-\infty}^{-1/2(p+1)}\ \prod_{m=0}^{q-1}[x-F_p(n,m)]\,. \tag{B12}$$

Note that the numerator of Eq. (B12) may be consolidated to read

$$\text{Num}=\prod_{n=-1/2(p-1)}^{-1}\ \prod_{m=-\infty}^{\infty}[x-F_p(n,m)]\Big/\prod_{n=-1/2(p-1)}^{-1}\ \prod_{m=0}^{q-1}[x-F_p(n,m)]\,. \tag{B13}$$

Similar treatment of the denominator of Eq. (B12) yields a form similar to Eq. (B13), but with the limits, $|n|=\infty$, $0\le m\le q-1$. Thus we have the final schematic representation for $F_\beta(\zeta)$

$$F_\beta(\zeta)=\prod_{n=-1/2(p-1)}^{-1}\ \prod_{m=-\infty}^{\infty}[x-F_p(n,m)]\Big/\prod_{m=0}^{q-1}\ \prod_{n=-\infty}^{\infty}[x-F_p(n,m)]\ . \tag{B14}$$

A specific functional form for $F_\beta(\zeta)$ which satisfies all the requirements of zero and pole locations is

$$F_\beta(\zeta)=\prod_{n=-1/2(p-1)}^{-1}\sin(\pi/2p)[x-p-(4n+1)q]\Big/\prod_{m=0}^{q-1}\sin\frac{\pi}{4q}[x-p-(2m+1)p]\,, \tag{B15}$$

where we have used the definition of $F_p(n,\ m)$, Eq. (A4). Finally, making the substitution, $x=(2q/\pi)(\zeta-p\pi/2q)$, and simplifying, we obtain

$$F_\beta(\zeta)=\prod_{n=1}^{1/2(p-1)}\sin[(q/p)\zeta-\pi+(\pi q/2p)(4n-1)]\Big/\prod_{m=0}^{q-1}\sin[\tfrac{1}{2}\zeta-\tfrac{1}{4}\pi-(p\pi/2q)(m+1)]\,. \tag{B16}$$

We conclude by quoting two examples for particular wedge angles β which are of physical interest. First for the right-angle wedge, $\beta=\frac{3}{2}\pi$, Eq. (B16) yields:

$$F_{3\pi/2}(\zeta)=\frac{-\sqrt{2}\cos(\frac{1}{3}\zeta)}{\sin(\frac{2}{3}\zeta)+\cos(\frac{2}{3}\zeta)}\ . \tag{B17}$$

Secondly, for the oblique wedge, $\beta=5\pi/4$, we find

$$F_{5\pi/4}(\zeta)=\frac{\sqrt{2}[\cos(\frac{4}{5}\zeta)-\cos(\frac{4}{5}\pi)]}{[1+\cos(\frac{4}{5}\zeta)+\sin(\frac{4}{5}\zeta)]}\ . \tag{B18}$$

Other wedge angles may be treated with greater effort. It is noteworthy, however, that the expression we have obtained for $F_\beta(\zeta)$ is considerably simpler than that obtained by Williams. It may be verified readily that Eq. (B16) exhibits the correct asymptotic limits prescribed by Eq. (A4).

APPENDIX C: ASYMPTOTIC APPROXIMATION OF $f(\zeta,\theta,\theta_0,\alpha)$

In obtaining an approximation for the function $f(\zeta,\theta,\theta_0,\alpha)$ in the vicinity of the saddle point at $\zeta=\pi$, the quantities D_1, D_2, D_3 and $\Phi(\zeta,\theta,\theta_0,\alpha)$ in Eqs. (23)–(25) are expanded in powers of $(\zeta-\pi)$ to yield

$$f(\zeta,\theta,\theta_0,\alpha)=\frac{-\tilde{G}(\zeta,\theta,\theta_0,\alpha)}{[P_a-(\zeta-\pi)][M_\nu^{(+)}-(\zeta-\pi)][M_\nu^{(-)}-(\zeta-\pi)]}\,, \tag{C1}$$

where we have used $M_\nu^{(+)}=M_\nu(\theta+\theta_0)$ and $M_\nu^{(-)}=M_\nu(\theta-\theta_0)$, with M_ν given in Eq. (5), while

$$\tilde{G}(\zeta,\theta,\theta_0,\alpha)=\frac{\Phi(\zeta,\theta,\theta_0,\alpha)}{(\nu\sin\nu\pi)^2} \tag{C2}$$

is assumed to be expanded in a power series in $\zeta-\pi$ up to first order in $(\zeta-\pi)$.

As regards the actual integration, one replaces $\cos\zeta$ by $-1+(\frac{1}{2})(\zeta-\pi)^2$ in the exponential factor of Eq. (11) and integrates along the line of steepest descent of the approximate integrand, i.e., along a line going obliquely downwards making an angle of 45° with the real axis and passing through the saddle point at π. The integration variable is charged to s, given by

$$(\zeta-\pi)=(2/kr\sin\gamma)^{1/2}\, s\, e^{-i\pi/4}$$

the s integration now going from $-\infty$ to ∞. The approximate factor for f is also replaced by means of the algebraic identity

$$\frac{w+xs}{(a-s)(b-s)(c-s)}=\frac{1}{(b-a)(c-a)}\left(\frac{w+xa}{a-s}-x\right) \quad \text{(C3)}$$

+ two additional terms obtained by cyclic permutation of a, b, and c.

This yields the asymptotic approximation to the diffracted pressure field, Eq. (24).

It is now necessary to obtain a suitable expression for $\tilde{C}(\zeta,\theta,\theta_0,\alpha)$. By comparing Eqs. (12) and (22) and their associated definitions, one may obtain an explicit representation for Φ

$$\Phi(\zeta,\theta,\theta_0,\alpha)=\frac{2\nu\sin(\nu\theta)D_3}{\Psi_\nu(\pm\zeta-\theta,\frac{1}{2}\pi-\alpha-\beta)H_\beta(-\theta_0,\alpha)}$$

$$\times[\Psi_\nu(\theta_0,\zeta+\theta)\phi_1-\Psi_\nu(\theta_0,\zeta-\theta)\phi_2]\,, \quad \text{(C4)}$$

where

$$\phi_{1_2}\equiv\Psi_\nu(\pm\zeta-\theta,\tfrac{1}{2}\pi-\alpha-\beta)H_\beta(\pm\zeta-\theta,\alpha)\,. \quad \text{(C5)}$$

Now, by using Eqs. (A8) and (14) in Eq. (C5) and performing several trigonometric manipulations, one may obtain

$$\phi_{1_2}=\frac{1}{4}\,\frac{\Psi_{2\nu}(\zeta\mp\theta-\frac{1}{2}\pi,\alpha)}{H_\beta(\pm\zeta-\theta\mp\pi,\alpha)\Psi_\nu(\zeta\mp\theta-\pi,\frac{1}{2}\pi-\alpha-\beta)}\,. \quad \text{(C6)}$$

Then after substituting Eqs. (C6) into Eq. (C4), the result into Eq. (C2), and expanding and recombining the terms

$$\Psi_\nu(\theta_0,\zeta+\theta)\Psi_{2\nu}(\zeta-\theta-\tfrac{1}{2}\pi,\alpha)-\Psi_\nu(\theta_0,\alpha-\theta)\Psi_{2\nu}(\zeta+\theta-\tfrac{1}{2}\pi,\alpha)$$

and using the definition

$$U(\theta,\alpha)\equiv\frac{\frac{1}{2}\sin\nu\theta}{H_\beta(-\theta,\alpha)\Psi_\nu(\theta,\frac{1}{2}\pi-\alpha-\beta)} \quad \text{(C7)}$$

one has finally

$$\tilde{C}(\pi,\theta,\theta_0,\alpha)=P_a U(\theta,\alpha)U(\theta_0,\alpha)D(\theta,\theta_0,\alpha) \quad \text{(C8)}$$

with

$$D(\theta,\theta_0,\alpha)=M_\nu(\theta+\theta_0)+M_\nu(\theta-\theta_0)+\frac{\cos(2\nu\alpha)-\cos(\nu\pi)}{\nu\sin(\nu\pi)} \quad \text{(C9)}$$

which completes the outline of the analysis leading to Eqs. (32)–(34).

APPENDIX D: THE FUNCTION $\bar{Q}_\beta(\zeta)$ FOR PARTICULAR ANGLES β

The function $\bar{Q}_\beta(\zeta)$ is defined in Eq. (42) as

$$\bar{Q}_\beta(\zeta)=\frac{\partial}{\partial\zeta}\ln\left[\frac{F_\beta(\zeta+\beta+\frac{1}{2}\pi)F(\zeta+2\beta+\frac{1}{2}\pi)}{F_\beta(\zeta+\beta-\frac{1}{2}\pi)F(\zeta+2\beta-\frac{1}{2}\pi)}\right]\,. \quad \text{(D1)}$$

It serves as a corection term in the function $H_\beta(\zeta)$ for nearly rigid wedges. Since the function $F_\beta(\zeta)$ takes on a simple form for angles β of the form $p\pi/2q$, it is reasonable to expect that $\bar{Q}_\beta(\zeta)$ might also be cast in a relatively simple form in the same instances.

One begins by noting that from Eq. (B16) one has

$$\ln F_\beta(\zeta)=\sum_{n=1}^{1/2(p-1)}\ln(\sin\{\tfrac{1}{2}\nu[\zeta-2\beta+\tfrac{1}{2}\pi(4n-1)]\})$$

$$-\sum_{m=0}^{q-1}\ln(\sin\{\tfrac{1}{2}[\zeta-\tfrac{1}{2}\pi-2\beta(m+1)]\}) \quad \text{(D2)}$$

and thus

$$\frac{d}{d\zeta}\ln F_\beta(\zeta)=\tfrac{1}{2}\nu\sum_{n=1}^{1/2(p-1)}\cot\{\tfrac{1}{2}\nu[\zeta-2\beta+\tfrac{1}{2}\pi(4n-1)]\}$$

$$-\frac{1}{2}\sum_{m=0}^{q-1}\cot\{\tfrac{1}{2}[\zeta-\tfrac{1}{2}\pi-2\beta(m+1)]\}\,. \quad \text{(D3)}$$

Then upon substitution of Eq. (D3) into Eq. (D1), consolidation of arguments of the several cotangents, and use of the identity

$$\cot\theta_1\pm\cot(\theta_2)\equiv\frac{\sin(\theta_2\pm\theta_1)}{\sin\theta_1\sin\theta_2}$$

followed by the use of trigonometric angle-addition relationships, one may obtain

$$\bar{Q}_\beta(\zeta)=-\nu\sin(\nu\pi)\sum_{n=1}^{1/2(p-1)}\frac{1}{\sin[\nu(\zeta+2n\pi)]\sin\{\nu[\zeta+\pi(2n-1)]\}}$$

$$-\sum_{m=0}^{q-1}\frac{\sin(\zeta-2m\beta)+\sin[\zeta-\beta(2m+1)]}{\sin(\zeta-2m\beta)\sin[\zeta-\beta(2m+1)]}\,. \quad \text{(D4)}$$

It should be pointed out that for $\zeta=-k/2q$, with k a positive integer less than p, there is one singular term in each sum in Eq. (D4). It can be shown, however, that the two singular terms combine in such a way that $\bar{Q}(\zeta)$ is continuous at the apparent singularity. For $\zeta=0$, there is a true singularity in $\bar{Q}_\beta$. In this case one may see from Eq. (41) that this singularity is cancelled by the $\tan(\frac{1}{2}\nu\zeta)$ factor in H_β to give

$$H_\beta(0,\alpha')=\frac{\nu}{2\eta\sin\gamma} \quad \text{(D5)}$$

for $\alpha'=\frac{1}{2}\pi-(\eta\sin\gamma)^{-1}$, which indicates the manner in which the rigid wedge limit of $H_\beta(0,\alpha)$ is approached as the impedance η becomes infinite. Similar behavior may be noted for $\zeta=-\beta$.

[1]H. Poincaré, "Sur la polarisation par diffraction," Acta Math. 16, 297–339 (1892).

[2]H. Poincaré, "Sur la polarisation par diffraction (seconde partie)," Acta Mach. 20, 313–355 (1896).

[3]A. Sommerfeld, "Mathematische Theorie der Diffraction," Math. Ann. 47, 317–374 (1896).

[4]U. J. Kurze, "Noise Reduction by Barriers," J. Acoust. Soc. Am. 55, 504–518 (1974). (A comprehensive up-to-date review article listing 59 Refs.)

[5]E. J. Rathe, "Note on Two Common Problems of Sound Propagation," J. Sound Vib. 10, 472–479 (1969); correction by R. M. Ellis, J. Sound Vib. 11, 503–508 (1970).

[6]Z. Maekawa, "Noise Reduction by Screens," Appl. Acoust. 1, 157–173 (1968).

[7]F. Fujiwara, Y. Ando, and Z. Maekawa, "Attenuation of a Spherical Sound Wave Diffracted by a Thick Plate," Acustica **28**, 341–317 (1973).

[8]P. Ambaud and A. Bergassoli, "Le probleme du dièdre en acoustique," Acustica **27**, 291–298 (1972).

[9]A. D. Pierce, "Diffraction of Sound around Corners and over Wide Barriers," J. Acoust. Soc. Am. **55**, 941–955 (1974).

[10]A. T. Trad and W. Eckhaus, "Sur l'influence de l'épaisseur dans le problème de diffraction de Sommerfield," J. Mec. **5**, 293–307 (1966).

[11]U. Ingard, "On the Reflection of a Spherical Sound Wave from an Infinite Plane," J. Acoust. Soc. Am. **23**, 329–355 (1951).

[12]U. J. Kurze and L. L. Beranek, "Sound Propagation Outdoors," in *Noise and Vibration Control*, edited by L. L. Beranek (McGraw–Hill, New York, 1971), pp. 164–193.

[13]H. G. Jonasson, "Diffraction by Wedges of Finite Acoustic Impedance with Application to Depressed Roads," J. Sound Vib. **25**, 577–585 (1972).

[14]P. M. Morse and H. Feshbach, *Methods of Theoretical Physics* (McGraw–Hill, New York, 1953), Vol. I, pp. 803–808, especially p. 808.

[15]W. E. Williams, "Diffraction of an *E*-polarized Plane Wave by an Imperfectly Conducting Wedge," Proc. R. Soc. London Ser. A **252**, 376–393 (1959).

[16]W. E. Williams, "Diffraction by an Imperfectly Conducting Right-Angled Wedge," Proc. Camb. Philos. Soc. **55**, 195–209 (1959).

[17]W. E. Williams, "Propagation of Electromagnetic Surface Waves along Wedge Surfaces," Q. J. Mech. Appl. Mat. **13**, 277–284 (1960).

[18]T. B. A. Senior, "Diffraction by an Imperfectly Conducting Wedge," Commun. Pure Appl. Math. **12**, 337–372 (1959).

[19]T. B. A. Senior, "Diffraction by a Semi-Infinite Metallic Sheet," Proc. R. Soc. London Ser. A **213**, 436–458 (1952).

[20]G. D. Maliuzhinets, "The Radiation of Sound by the Vibrating Boundaries of an Arbitrary Wedge, Part I," Sov. Phys. Acoust. **1**, 152–174 (1955).

[21]G. D. Maliuzhinets, "Radiation of Sound from Vibrating Faces of an Arbitrary Wedge, Part II," Sov. Phys. Acoust. **1**, 240–248 (1955).

[22]A. D. Pierce and W. J. Hadden, Jr., "Theory of Sound Diffraction around Absorbing Barriers," Proc. Int. Conf. Acoust. Protection of Residential Areas by Barriers, Marseille, France, 1975 (to be published).

[23]W. Gautschi, "Error Function and Fresnel Integrals," in *Handbook of Mathematical Functions*, edited by M. Abramowitz and I. A. Segun (Dover, New York, 1965), pp. 295–329.

[24]P. M. Morse and U. Ingard, *Theoretical Acoustics* (McGraw–Hill, New York, 1968), pp. 259–263.

[25]H. G. Jonasson, "Sound Reduction by Barriers on the Ground," J. Sound Vib. **22**, 113–126 (1972).

Chapter 6

EFFECTS OF AMBIENT FLOW AND DISTRIBUTED SOURCES

Diffraction in the Pressure of Ambient Flow

The model sketched in Fig. 1 may be used to assess the effects of ambient flow on barrier diffraction. The barrier is taken as a thin screen which occupies the region $x < 0$ of the $y = 0$ plane; the edge of the screen lies along the z axis. The source is taken as being localized as a point x_S, y_S, z_S where $y_S < 0$, the listener is at (x_L, y_L, z_L). A uniform ambient flow of velocity U_o is in the +x direction, tangential to the screen and having the same velocity on both sides of the screen. Since the screen is idealized as being arbitrarily thin, there is no discontinuity in U_o at the edge.

The solution for plane wave diffraction in terms of such a model has previously been given by Candel.[1,2] Here, a slightly different approach is used for the case when the incident wave ensues from a point source.

If one limits one's consideration to a single frequency component and uses the device of taking $e^{-i\omega t}$ to describe the

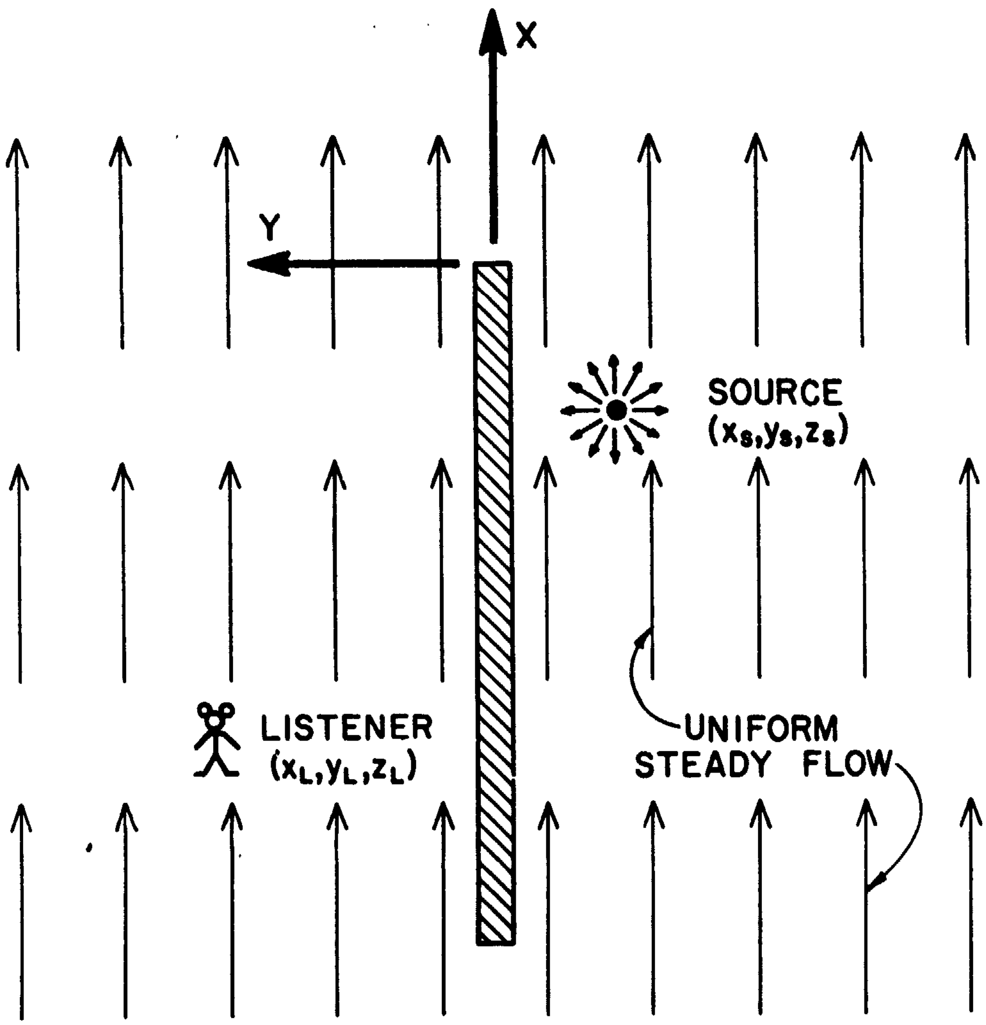

Fig. 1. Geometry used in the study of the effects of ambient flow on sound diffraction. A point source is immersed in a uniform steady flow near a thin screen.

time dependence, then the complex amplitudes of the acoustic field variables satisfy the equations

$$[-i\omega + U_o\partial/\partial x]p/c^2 + \rho_o\nabla\cdot\vec{u} = 0 \tag{1a}$$

$$\rho_o[-i\omega + U_o\partial/\partial x]\vec{u} + \nabla p = 0 \tag{1b}$$

everywhere except in the immediate vicinity of the source. From these one may derive the generalization of the scalar Helmholtz equation which takes ambient flow into account, i.e.,

$$\mathcal{L}_1\{p\} = 0 \tag{2}$$

$$\mathcal{L}_1 = \nabla^2 - c^{-2}[-i\omega + U_o\partial/\partial x]^2 \tag{3}$$

There is a transformation[3] which, for $U_o/c < 1$, will reduce equation (2) to one resembling the scalar Helmholtz equation without ambient flow, i.e.,

$$\mathcal{L}_1 p = e^{-i(M\omega/c)x/\beta^2}\,\mathcal{L}_2\left\{p\, e^{i(M\omega/c)x/\beta^2}\right\} \tag{4}$$

where

$$M = U_o/c \tag{5}$$

is the Mach number, and

$$\beta = [1 - M^2]^{1/2} \tag{6}$$

$$\mathcal{L}_2 = \partial^2/\partial(x/\beta)^2 + \partial^2/\partial y^2 + \partial^2/\partial z^2 + (\omega/\beta)^2/c^2 \tag{7}$$

Consequently, one may conclude that any solution of Eq. (2) corresponding to a given angular frequency ω may be taken as

$$p(x,y,z,\omega) = e^{-i(M\omega/c)x/\beta^2}\,\hat{p}(\hat{x},\hat{y},\hat{z},\hat{\omega}) \tag{8}$$

where

$$\hat{x} = x/\beta \tag{9a}$$

$$\hat{y} = y \tag{9b}$$

$$\hat{z} = z \tag{9c}$$

$$\hat{\omega} = \omega/\beta \tag{9d}$$

and

$$[\partial^2/\partial\hat{x}^2 + \partial^2/\partial\hat{y}^2 + \partial^2/\partial\hat{z}^2 + (\hat{\omega}/c)^2]\hat{p} = 0 \tag{10}$$

The latter is the scalar Helmholtz equation corresponding to no ambient flow.

For the screen diffraction problem, one requires that $u_y = 0$ at $y = 0$ for $x < 0$. Consequently, from Eq. (1b), $\partial p/\partial y$ should also be zero for the same circumstances. However, one sees from Eq. (8) that this requires

$$\partial\hat{p}/\partial\hat{y} = 0 \qquad \hat{y} = 0, \qquad \hat{x} < 0 \tag{11}$$

which is the same boundary condition as one would have in the absence of ambient flow. Also, if the source is at x_S, y_S, z_S, then $\hat{p}$ should correspond to a field generated by a source at $\hat{x}_S, \hat{y}_S, \hat{z}_S$. Consequently, one concludes that the solution of

$$\mathcal{L}_1 p = -4\pi S(x,y,z) \tag{12}$$

subject to the boundary condition mentioned above may be taken as

$$p = \iiint e^{i(M\omega/c)(x_o - x)/\beta^2} S(x_o,y_o,z_o) G(x/\beta,y,z|x_o/\beta,y_o,z_o|\omega/\beta)\, dx_o dy_o dz_o \quad . \tag{13}$$

where $G(x,y,z|x_o,y_o,z_o|\omega)$ is the Green's function for the scalar Helmholtz equation in the absence of ambient flow, satisfying

$$[\nabla^2 + (\omega/c)^2] G(x,y,z|x_o,y_o,z_o|\omega) = -4\pi\delta(\vec{x} - \vec{x}_o) \tag{14}$$

In the case $S(x,y,z)$ is taken as $S_o\delta(\vec{x} - \vec{x}_S)$, the above reduces to

$$p = e^{i(M\omega/c)(x_S - x)/\beta^2} G(x/\beta, y, z | x_S/\beta, y_S, z_S | \omega/\beta) \tag{15}$$

which may be considered as the Green's function for the problem of diffraction of waves by a thin screen in the presence of ambient flow.

Effect of Ambient Flow on Insertion Loss

The Green's function without ambient flow included is described in some length in Chapter 1 of the present report and the fact that it is amenable to numerical computation implies that the problem discussed above is also. Here, for simplicity, we limit our discussion to the circumstances described by Fig. 2. The Green's function in the absence of ambient flow for such circumstances is given by the Fresnel number approximation

$$G = \frac{e^{ikL}}{L} \frac{e^{i\pi/4}}{\sqrt{2}} \left\{ f([2N]^{1/2}) - ig([2N]^{1/2}) \right\} \tag{16a}$$

$$= \frac{e^{ikL}}{L} \left\{ (1/2) - N^{1/2} e^{-i\pi/4} \right\} \qquad N \ll 1 \tag{16b}$$

$$\rightarrow \frac{e^{ikL}}{L} \frac{e^{i\pi/4}}{2\pi N^{1/2}} \qquad N \gg 1 \tag{16c}$$

where N is the Fresnel number given by

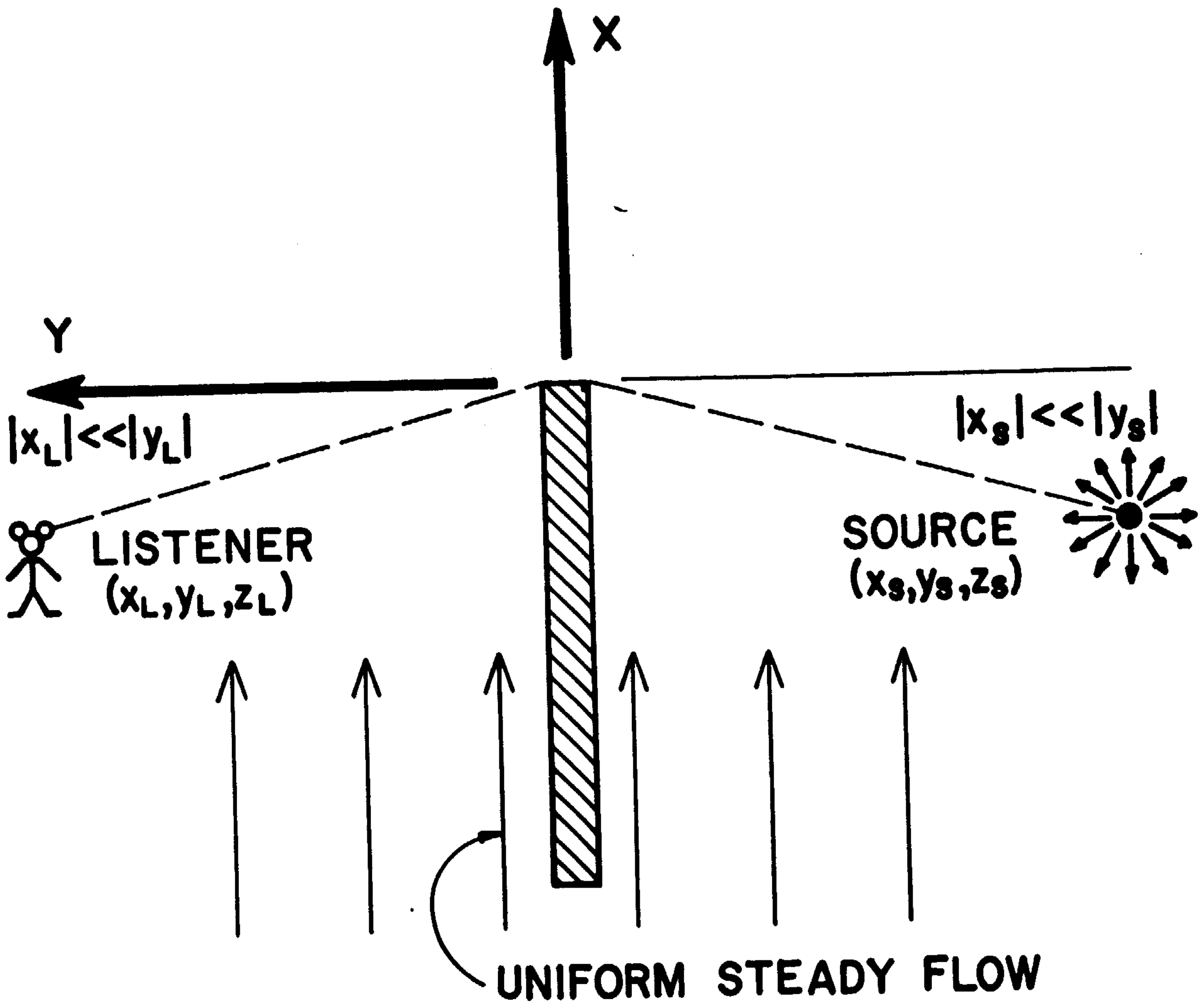

Fig. 2. Sketch of limiting case discussed in the text.

$$N = \frac{L - R}{(\lambda/2)} \tag{17}$$

where $\lambda = 2\pi/k$ and

$$L = [(z_L - z_S)^2 + (r_L + r_S)^2]^{1/2} \tag{18a}$$

$$R = [(x_L - x_S)^2 + (y_L - y_S)^2 + (z_L - z_S)^2]^{1/2} \tag{18b}$$

$$r_L = (x_L^2 + y_L^2)^{1/2}; \quad r_S = (x_S^2 + y_S^2)^{1/2} \tag{18c}$$

The functions f and g are the auxiliary Fresnel functions tabulated in the NBS Handbook of Mathematical Functions.[4] For most purposes, the asymptotic limit (16c) may be considered as realized when $(2N)^{1/2} > 2$ or $N > 2$.

The insertion loss due to the barrier is defined as the loss in decibels of the sound pressure level at the listener location due to the presence of the barrier and, for waves from a point source, is accordingly

$$IL = 10 \log_{10} |G_{NB}/G_B|^2 \tag{19}$$

where G_{NB} and G_B are the Green's function without and with the barrier present, respectively, Thus, in the absence of ambient flow and in the Fresnel number approximation, one has

$$IL = -10 \log_{10}\left\{(1/2)(R/L)^2\left[f^2([2N]^{1/2}) + G^2([2N]^{1/2})\right]\right\} \tag{20}$$

Furthermore, for circumstances allowing the Fresnel number approximation, it is a good approximation also to set the factor $R/L = 1$, so one has

$$IL = -10 \log_{10}\left\{(1/2)\left[f^2([2N]^{1/2}) + g^2([2N]^{1/2})\right]\right\} \tag{21}$$

$$\approx \quad 20 \log_{10}2[1 + (2N)^{1/2}] \qquad N << 1$$

$$\approx \quad 20 \log_{10}2 + [20/\ln 10](2N)^{1/2} \qquad N << 1$$

$$\approx \quad 6 + (12.3)N^{1/2} \quad \text{dB} \qquad N << 1 \tag{22}$$

$$\rightarrow \quad 10 \log_{10}(4\pi^2 N) = 16 + 10 \log_{10} N \qquad N >> 1 \tag{23}$$

which is a monotomically increasing function of Fresnel number only.

According to the analysis of the preceding section the magnitude of a Green's function when ambient flow is present is that of the Green's function when ambient flow is not present providing one lets $x \rightarrow x/\beta$, $\omega \rightarrow \omega/\beta$, $x_S = x_S/\beta$ in the arguments of the latter. (This is true regardless of whether or not the barrier is present.) Consequently, the above approximate expressions for the insertion loss will still apply to the case when there is an ambient flow, providing the Fresnel number is similarly transformed, i.e.,

$$N(x_L, y_L, z_L | x_S, y_S, z_S | \omega)$$

$$\rightarrow \quad N(x_L/\beta, y_L, z_L | x_S/\beta, y_S, z_S | \omega/\beta) \tag{24}$$

In general, the ratio of the transformed and untransformed Fresnel numbers is spatially dependent. However, for the case when $|y_L/x_L| \ll 1$ and $|y_S/x_S| \ll 1$, one has

$$r_L = |y_L + x_L^2/2y_L| \tag{25a}$$

$$r_S = |y_S + x_S^2/2y_s| \tag{25b}$$

$$\begin{aligned} (r_L + r_S)^2 &= (y_L + x_L^2/2y_L - y_S - x_S^2/2y_S)^2 \\ &= (y_L - y_S)^2 - (y_L - y_S)[x_S^2/y_S - x_L^2/y_L] \end{aligned} \tag{26}$$

$$L = \left[(z_L - z_S)^2 + (y_L - y_S)^2\right]^{1/2} - \frac{(y_L - y_S)[x_S^2/y_S - x_L^2/y_L]}{2\left[(z_L - z_S)^2 + (y_L - y_S)^2\right]^{1/2}} \tag{27a}$$

$$R = \left[(z_L - z_S)^2 + (y_L - y_S)^2\right]^{1/2} + \frac{(x_S - x_L)^2}{2\left[(z_L - z_S)^2 + (y_L - y_S)^2\right]^{1/2}} \tag{27b}$$

and, consequently,

$$L - R \approx \frac{-(y_L/y_S)x_S^2 - (y_S/y_L)x_L^2 + 2x_Sx_L}{2\left[(z_L - z_S)^2 + (y_L - y_S)^2\right]^{1/2}} \tag{27c}$$

(Here, it should be recalled that the source and listener are presumed to be on opposite sides of the barrier, so y_L and y_S have opposite signs. Consequently, the above gives $L - R > 0$, as must be the case.)

The above expression for $L - R$ is bilinear in x_S and x_L so with the substitutions $x_S \rightarrow x_S/\beta$, $y_S \rightarrow y_S/\beta$ one has $L - R \rightarrow (L - R)/\beta^2$. Also the substitution $\omega \rightarrow \omega/\beta$ causes $\lambda/2 \rightarrow \beta\lambda/2$. Consequently, in the case described above

$$N \rightarrow N/\beta^3$$

Since $\beta = (1 - M^2)^{1/2}$ is less than 1, the transformed Fresnel number is larger than that corresponding to no flow. The insertion loss with ambient flow present is then given by Eqs. (21,22,23) only with N replaced by N/β^3 so one has in particular

$$IL \approx 6 + (12.3)N^{1/2}/\beta^{3/2} \qquad N<<1 \tag{28a}$$

$$IL \approx 10 \log_{10}(4\pi^2 N/\beta^3) \qquad N>>1 \tag{28b}$$

In summary, the insertion loss is <u>increased</u> when there is an ambient flow, the increase being independent of the direction of the flow. For larger values of the Fresnel number, the effect of ambient flow is to add an additional increment to the insertion loss of

$$\Delta(IL) = 10 \log_{10}[1/(1 - M^2)^{3/2}] \tag{29}$$

If the Mach number is 0.5, for example, the additional insertion loss is 1.9 dB.

Green's Function for Source Near Edge

In Chapter 3, one of the limiting cases examined was that of a thin screen ($\nu = 1/2$) when $rr_S/L^2 \to 0$, $kr_S r/L$ finite. This includes the case shown in Fig. 3 when the listener is many wavelengths from the diffracting edge and when the source is much closer to the edge than is the listener. However, the source is not presumed to be either very close or very far from the edge relative to a wavelength. The Green's function for this case can be constructed easily by the principle of reciprocity from Sommerfeld's known exact solution for the diffraction of an incident plane wave by a thin screen. (This was pointed out to one of the authors by Donald Lansing.) The result, for the case when the listener is in the shadow zone, is that the Green's function is given by

$$G = \frac{e^{ikL}}{L} \frac{e^{i\pi/4}}{\sqrt{2}} \Big[f(X) - ig(X) \Big]_{\zeta = |\theta - \theta_S|}$$

$$+ \left. [f(X) - ig(X)]_{\zeta = \theta + \theta_S} \right| \tag{30}$$

with

$$X = [8rr_S/\lambda L]^{1/2} |\cos(\zeta/2)| \tag{31}$$

The functions $f(X)$ and $g(X)$ are the auxiliary Fresnel functions described in the previous section. This Green's function may also be modified to take into account the presence of ambient flow by use of the transformation described previously.

The fact that the above Green's function covers cases when r_S is very close and not so close to the edge, that it is easily computed, and that it may be easily extended to include ambient flow suggests that it may be useful in studies of the diffraction of engine noise around wings while an airplane is in flight.

Sound from Distributed Sources

In order to illustrate the application of the general theory to sound diffraction from a distributed source (Fig. 4), one may take, for simplicity, all the sources to be along the far side of the screen with $\theta_S = 2\pi$ in each case and to each have $z_S = 0$ (i.e., the sources lie along a line transverse to the edge of the screen). The listener is considered also to have z coordinates equal to 0 and we consider $r \gg r_S$ such that

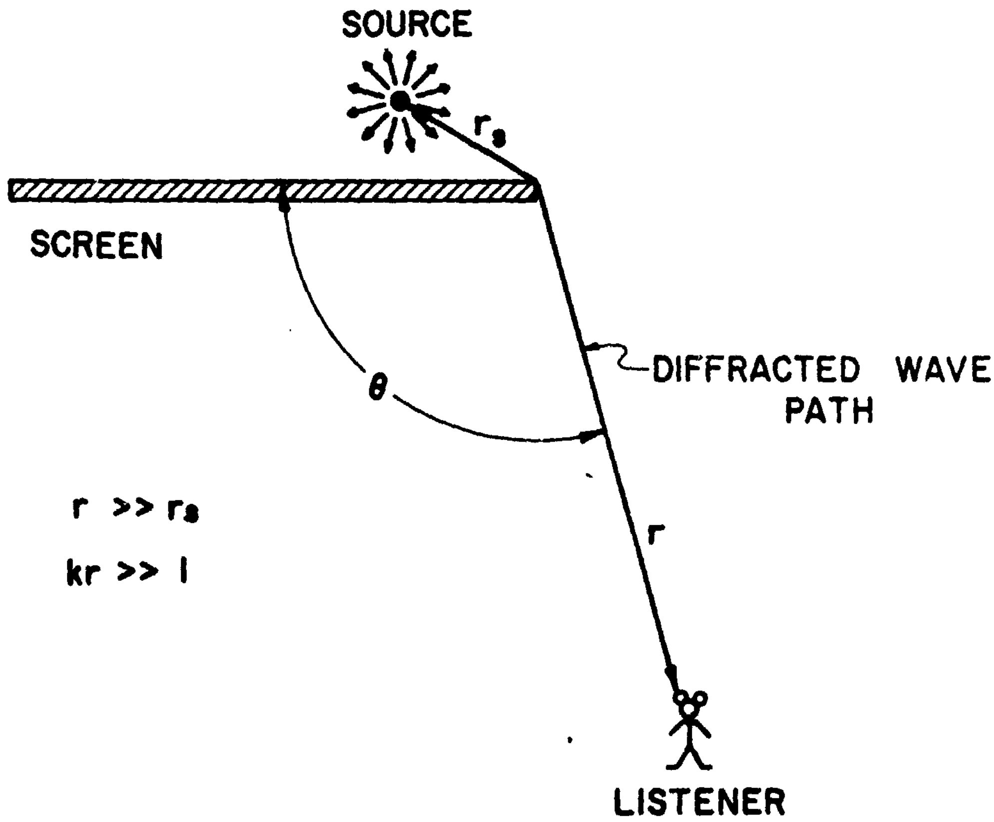

Fig. 3. Limiting case of listener many wavelengths from edge of thin screen.

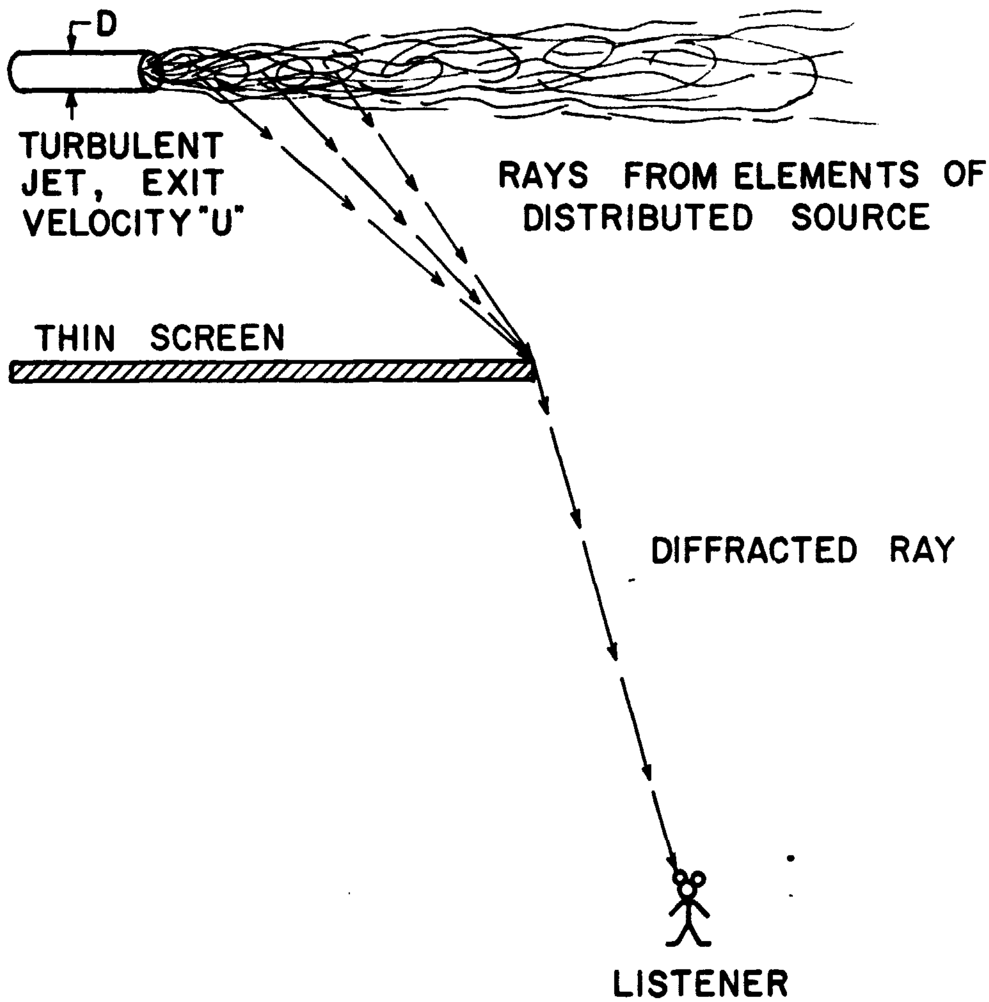

Fig. 4. Sketch of concepts utilized in the analysis of diffraction from a distributed source.

we may approximate L by r except in the exponent where it is taken as $r + r_S$. In this manner, G reduces to

$$G \approx \sqrt{2}\ \frac{e^{i[kr + \pi/4]}}{r} \left\{ f(8r_S/\lambda]^{1/2} \cos[\theta/2]) - ig([8r_S/\lambda]^{1/2} \cos[\theta/2]) \right\} e^{ikr_S} \tag{32}$$

If the source strength per unit length is taken as $\hat{s}(r_S)$ for a given frequency component, then the corresponding complex pressure amplitude in the far field is given by superposition as

$$p \approx \sqrt{2}\ \frac{e^{i[kr + \pi/4]}}{r} \int_0^\infty [f - ig]\hat{s}(r_S)\ e^{ikr_S}\ dr_S \tag{33}$$

Here, for simplicity, we assume the source does not extend beyond the "trailing" edge, so all of the received sound is diffracted.

For simplicity, we also assume the spatial extent of the source is somewhat less than a wavelength of the radiated sound such that we may approximate f, g and e^{ikr_S} by appropriate truncated power series expansions. If we do so, we have

$$p \approx 2\ \frac{e^{ikr}}{r} \int_0^\infty \left[1/2 - (4r_S/\lambda)^{1/2} \cos(\theta/2) e^{-i\pi/4}\right]$$

$$\cdot\ \hat{s}(r_S)[1 + ikr_S - (1/2)k^2 r_S^2]\ dr_S \tag{34}$$

One of the interesting aspects of the above is that the <u>diffraction could enhance the received sound at low frequencies</u>. Suppose, for example, that the source were a quadrupole (e.g., as for jet noise) such that

$$\int \hat{s}(r_S)dr_S = \int r_S \hat{s}(r_S)dr_S = 0 \tag{35}$$

Then the expression for p would reduce to

$$p \approx -(1/4)k^2 \frac{e^{ikr}}{r} \int r_S^2 \hat{s}(r_S)dr_S$$

$$- 4/(2\pi)^{1/2} k^{1/2} \frac{e^{ikr}}{r} \cos(\theta/2)e^{-i\pi/4} \int r_S^{1/2}\ \hat{s}(r_S)dr_S \tag{36}$$

The first term is weakened at low frequencies by the presence of the k^2 factor while the second has a factor of $k^{1/2}$ which may be larger when the frequency is low. The first term, incidentally, is just the sound field expected in the absence of the screen. [Time limitations, unfortunately, have precluded a more thorough investigation of the question of whether diffraction could actually enhance the sound of a distributed source which tends to radiate as a quadrupole in the absence of a barrier.]

REFERENCES

1. S. M. Candel, "Diffraction of a Plane Wave by a Half Plane in a Subsonic and Supersonic Medium," J. Acoust. Soc. Amer. 54, 1008-1016 (1973).

2. S. M. Candel, Analytical Studies of Some Acoustical Problems of Jet Engines, Ph.D. Thesis, California Institute of Technology (1972).

3. D. I. Blokhintzev, Acoustics of a Nonhomogeneous Moving Medium (English translation of 1946 text), National Advisory Committee on Aeronautics, Report NACA TM 1399, pp. 74-85.

4. W. Gautschi, "Error Function and Fresnel Integrals," in Handbook of Mathematical Functions, edited by M. Abramowitz and I. A. Stegun (Dover, New York, 1965), pp. 295-329.